

LOCAL SCOUR CHARACTERISTICS AROUND SEMI-CIRCULAR END  
BRIDGE ABUTMENTS WITH AND WITHOUT COLLARS

A THESIS SUBMITTED TO  
THE GRADUATE SCHOOL OF NATURAL AND APPLIED SCIENCES  
OF  
MIDDLE EAST TECHNICAL UNIVERSITY

BY

FATİME TEKİN

IN PARTIAL FULFILLMENT OF THE REQUIREMENTS  
FOR  
THE DEGREE OF MASTER OF SCIENCE  
IN  
CIVIL ENGINEERING

JUNE 2012

Approval of the thesis:

**LOCAL SCOUR CHARACTERISTICS AROUND SEMI-CIRCULAR END  
BRIDGE ABUTMENTS WITH AND WITHOUT COLLARS**

submitted by **FATİME TEKİN** in partial fulfillment of the requirements for the degree of **Master of Science in Civil Engineering Department, Middle East Technical University** by,

Prof. Dr. Canan Özgen  
Dean, Graduate School of **Natural and Applied Sciences** \_\_\_\_\_

Prof. Dr. Güney Özcebe  
Head of Department, **Civil Engineering** \_\_\_\_\_

Assist. Prof. Dr. Mete Köken  
Supervisor, **Civil Engineering Department, METU** \_\_\_\_\_

**Examining Committee Members:**

Prof. Dr. Mustafa Göğüş  
Civil Engineering Dept., METU \_\_\_\_\_

Assist. Prof. Dr. Mete Köken  
Civil Engineering Dept., METU \_\_\_\_\_

Prof. Dr. Nuray Tokyay  
Civil Engineering Dept., METU \_\_\_\_\_

Assoc. Prof. Dr. Ayşe Burcu Altan Sakarya  
Civil Engineering Dept., METU \_\_\_\_\_

Assoc. Prof. Dr. M. Ali Kökpınar  
Technical Research and Quality Control Dept., DSI \_\_\_\_\_

**Date:** \_\_\_\_\_ 22.06.2012

**I hereby declare that all information in this document has been obtained and presented in accordance with academic rules and ethical conduct. I also declare that, as required by these rules and conduct, I have fully cited and referenced all material and results that are not original to this work.**

Name, Last name: Fatime TEKİN

Signature:

## **ABSTRACT**

### **LOCAL SCOUR CHARACTERISTICS AROUND SEMI-CIRCULAR END BRIDGE ABUTMENTS WITH AND WITHOUT COLLARS**

Tekin, Fatime

M.Sc., Department of Civil Engineering

Supervisor: Assist. Prof. Dr. Mete Köken

June 2012, 123 Pages

The major damage to bridges occurs due to scour of the bed materials around piers and abutments during severe floods. This study involves the experimental investigations of the various scour patterns forming around abutment models tested with and without collars as scour countermeasures. The experiments were conducted in a rectangular channel under clear-water scour conditions.

In the first part of this study, 34 experiments were conducted with semi-circular end abutment models with and without a collar for a period of 3 hours. Collars of various sizes were placed at different elevations on the abutment models, and the scour reduction efficiencies of collars were investigated for the different flow depths. Based on the results of the experimental studies, the optimum locations of collars on the abutments, which result in minimum scour depth around the abutments, are obtained at the bed level and below the bed level depending on the flow intensity values.



In the second part of this study, the effects of flow depth and abutment length on the temporal development of local scour at bridge abutments were studied. 20 experiments were performed without collars for a time period of 8 hours. It was observed that at the upstream of the abutment, the depth of the local scour increases rapidly within the first three hours of the experiment for the different flow depths.

Keywords: Scour, Semi-Circular End Bridge Abutments, Scour Countermeasures, Collar, Temporal Development

## ÖZ

### **KORUYUCU PLAKALI VE PLAKASIZ YARI DAİRESEL KÖPRÜ KENAR AYAKLARI ETRAFINDA OLUŞAN YEREL OYULMALARIN KARAKTERİSTİKLERİ**

Tekin, Fatime

Yüksek Lisans, İnşaat Mühendisliği Bölümü

Tez Yöneticisi: Yrd. Doç. Dr. Mete Köken

Haziran 2012, 123 Sayfa

Şiddetli taşkınlar sırasında köprü orta ve kenar ayakları etrafında meydana gelen oyulmadan ötürü büyük hasarlar meydana gelmektedir. Bu çalışmada, köprü kenar ayakları etrafında oluşan oyulmalar ve bu oyulma derinliklerinin azaltılması için yerleştirilen plakaların etkisi deneysel olarak incelenmiştir. Deneyler dikdörtgen bir kanalda temiz su oyulması koşulu altında yapılmıştır.

Bu çalışmanın ilk kısmında koruyucu plakalı ve plakasız yarı dairesel köprü kenar ayakları ile 3'er saatlik periyotlarla 34 adet deney yapılmıştır. Değişik boyutlarda plakalar köprü kenar ayakları etrafında farklı kotlarda yerleştirilmiş ve farklı su derinliklerinde plakaların oyulma derinliğini azaltıcı etkisi gözlemlenmiştir. Deneyler sonucunda, kenar ayaklar etrafında oyulma derinliğini en aza indirgeyen plakaların seviyesi akım yoğunluklarına bağlı olarak yatak seviyesinde ve yatak seviyesinin altında gözlenmiştir.

Çalışmanın ikinci kısmında ise, köprü kenar ayakları etrafında oluşan yerel oyulmanın, akım derinliğinin ve kenar ayak boyunun fonksiyonu olarak zamanla değişimi incelenmiştir. Bu kapsamda, plakasız köprü kenar ayaklarında 8'er saatlik periyotlarla 20 adet deney yapılmıştır. Farklı akım derinliklerinde yapılan deneyler sonucunda, ilk üç saat içerisinde kenar ayağın membasında hızlı bir oyulma paterni gözlenmiştir.

Anahtar Kelimeler: Oyulma, Yarı Dairesel Köprü Kenar Ayakları, Oyulma Önleyici Tedbirler, Plakalar, Zamana Bağlı Değişim

TO MY FAMILY

## ACKNOWLEDGEMENTS

This study was suggested and has been completed under the supervision of Assist. Prof. Dr. Mete Köken in the Hydromechanics Laboratory at Middle East Technical University (METU) in Ankara, Turkey.

I would like to express my sincere appreciation and deep sense of graditude to my supervisor Assist. Prof. Dr. Mete Köken for his invaluable guidance, advice and encouragement throughout this study. My sincere acknowledgement also goes to Prof. Dr. Mustafa Göğüş for his invaluable and helpful suggestions and guidance in this study.

I wish to also express my graditude and thanks to Süeyla Daşkın, Burhan Yıldız and Hydromechanics Laboratory staff for their invaluable help and support during the experimental part of the study.

I would also like to express my profound graditude to Su-Yapı Engineering and Consulting Inc. for their support and patience throughout this study.

Lastly, I thankfully acknowledge to my family members for their love, understanding and support throughout my whole life. Specially, I wish to express my sincerest thankfulness to my mother and husband for their understanding, encouragement and invaluable support all the time.

## TABLE OF CONTENTS

|  |      |
|--|------|
| ABSTRACT .....   | iv   |
| ÖZ .....   | vi   |
| DEDICATION.....  | viii |
| ACKNOWLEDGEMENTS .....                                       | ix   |
| TABLE OF CONTENTS.....                                       | x    |
| LIST OF TABLES.....  | xiii |
| LIST OF FIGURES .....  | xiv  |
| LIST OF SYMBOLS .....  | xix  |
| CHAPTERS   |      |
| 1. INTRODUCTION .....  | 1    |
| 1.1 BACKGROUND.....  | 1    |
| 1.2 OBJECTIVES .....   | 2    |
| 1.3 SCOPE .....  | 3    |
| 1.4 SYNOPSIS OF THE THESIS .....                             | 3    |
| 2. LITERATURE REVIEW.....                                    | 4    |
| 2.1 INTRODUCTION.....  | 4    |
| 2.2 SCOUR .....  | 4    |
| 2.2.1 Definition of Scour .....                              | 4    |
| 2.2.2 Types of Scour .....                                   | 5    |
| 2.3 BRIDGE ABUTMENT SCOUR MECHANISM .....                    | 7    |
| 2.4 PARAMETERS INFLUENCING LOCAL SCOUR AT<br>ABUTMENTS ..... | 10   |
| 2.4.1 The Effect of Flow Intensity .....                     | 12   |
| 2.4.2 The Effect of Flow Depth .....                         | 13   |
| 2.4.3 The Effect of Abutment Length .....                    | 14   |
| 2.4.4 The Effect of Abutment Shape .....                     | 15   |

|   |    |
|---|----|
| 2.4.5 The Effect of Abutment Skewness .....   | 16 |
| 2.4.6 The Effect of Sediment Size .....   | 16 |
| 2.4.7 The Effect of Sediment Gradation .....  | 17 |
| 2.5 TEMPORAL DEVELOPMENT OF SCOUR .....   | 18 |
| 2.6 BRIDGE ABUTMENT SCOUR COUNTERMEASURES .....   | 19 |
| 2.6.1 Local Scour Countermeasures at Bridge Abutments .....   | 20 |
| 2.6.2 Bridge Abutment Collar as a Scour Countermeasure .....  | 22 |
| 2.7 CONCLUSION .....  | 25 |
| 3. EXPERIMENTAL SETUP AND METHODOLOGY .....   | 27 |
| 3.1 INTRODUCTION.....   | 27 |
| 3.2 FLUME .....   | 27 |
| 3.3 ABUTMENT MODEL .....  | 30 |
| 3.4 SEDIMENT CHARACTERISTICS .....  | 34 |
| 3.5 FLOW CHARACTERISTICS .....  | 35 |
| 3.6 MEASUREMENTS AND INSTRUMENTATION .....  | 35 |
| 4. EFFECT OF FLOW DEPTH ON LOCAL SCOUR AT BRIDGE<br>ABUTMENTS.....                                  | 40 |
| 4.1 GENERAL .....   | 40 |
| 4.2 DIMENSIONAL ANALYSIS .....  | 40 |
| 4.3 DISCUSSION OF RESULTS .....   | 43 |
| 4.3.1 Application of Collars around the Bridge Abutment<br>Models .....                             | 43 |
| 4.3.1.1 The Abutment of $L_a=15$ cm at the Flow Depth<br>of $y=17.4$ cm (Experiments R1~R6) .....   | 45 |
| 4.3.1.2 The Abutment of $L_a=15$ cm at the Flow Depth<br>of $y=15.2$ cm (Experiments R7~R12) .....  | 46 |
| 4.3.1.3 The Abutment of $L_a=35$ cm at the Flow Depth<br>of $y=17.4$ cm (Experiments R13~R21) ..... | 47 |
| 4.3.1.4 The Abutment of $L_a=35$ cm at the Flow Depth<br>of $y=15.2$ cm (Experiments R22~R30) ..... | 49 |

|   |     |
|---|-----|
| 4.3.2 Comparison of Scour for Various Collar Applications ..... | 51  |
| 4.3.3 Comparison of Scour Hole for Different Flow Depths .....  | 68  |
| 5. TIME DEVELOPMENT OF LOCAL SCOUR AT BRIDGE                    |     |
| ABUTMENTS .....   | 76  |
| 5.1 GENERAL .....   | 76  |
| 5.2 DISCUSSION OF RESULTS .....                                 | 76  |
| 5.2.1 Time Development of Scour Hole at Short Abutment          |     |
| ( $L_a=15$ cm) .....  | 77  |
| 5.2.1.1 Time Development of Scour at the Flow Depth             |     |
| of $y=13.5$ cm .....  | 77  |
| 5.2.1.2 Time Development of Scour at the Flow Depth             |     |
| of $y=17.4$ cm .....  | 86  |
| 5.2.2 Time Development of Scour Hole at Long Abutment           |     |
| ( $L_a=35$ cm) .....  | 94  |
| 5.2.2.1 Time Development of Scour at the Flow Depth             |     |
| of $y=13.5$ cm .....  | 94  |
| 5.2.2.2 Time Development of Scour at the Flow Depth             |     |
| of $y=17.4$ cm .....  | 103 |
| 6. CONCLUSIONS AND RECOMMENDATIONS .....                        | 111 |
| 6.1 CONCLUSIONS .....   | 111 |
| 6.2 RECOMMENDATIONS .....                                       | 112 |
| REFERENCES .....  | 114 |



## LIST OF TABLES

### TABLES

|  |    |
|--|----|
| Table 2.1 Comparison between armoring and flow-altering scour countermeasures<br>(Deng and Cai, 2010) .....  | 22 |
| Table 3.1 Experimental arrangements of abutments and collars.....  | 36 |
| Table 4.1 Experimental data for $Q=0.0678 \text{ m}^3/\text{s}$ and $B_a=10 \text{ cm}$ at flow intensities<br>of $U/U_c=0.70$ ( $y=17.4 \text{ cm}$ ) and $U/U_c=0.80$ ( $y=15.2 \text{ cm}$ )..... | 44 |
| Table 4.2 List of the experiments where the secondary scour hole is observed ...   | 50 |
| Table 4.3 Optimum design parameters of the abutment-collar arrangements .....  | 56 |
| Table 4.4 Optimum design parameters of the abutment-collar arrangements in<br>Daşkın's study (2011).....   | 56 |

## LIST OF FIGURES

### FIGURES

|   |    |
|---|----|
| Figure 2.1 Bridge scour (Deng and Cai, 2010) .....  | 6  |
| Figure 2.2 Schematic diagram of flow field at an abutment (after Kwan, 1988).....                 | 9  |
| Figure 2.3 Influence of abutment length on scour depth (Kayatürk, 2005).....                      | 15 |
| Figure 3.1 General view of the flume .....  | 28 |
| Figure 3.2 Schematic layout of the experimental setup.....  | 29 |
| Figure 3.3 Schematic illustration of the abutment model .....                                     | 30 |
| Figure 3.4 Abutment $L_a=35$ cm with collar $B_c=7.5$ cm at $Z_c/y=0.00$ ,<br>$y=15.2$ cm .....   | 31 |
| Figure 3.5 Abutment $L_a=35$ cm with collar $B_c=5.0$ cm at $Z_c/y=-0.25$ ,<br>$y=17.4$ cm .....  | 32 |
| Figure 3.6 Abutment $L_a=35$ cm with collar $B_c=10.0$ cm at $Z_c/y=-0.50$ ,<br>$y=17.4$ cm ..... | 32 |
| Figure 3.7 Abutment $L_a=15$ cm with collar $B_c=10.0$ cm at $Z_c/y=0.00$ ,<br>$y=17.4$ cm .....  | 33 |
| Figure 3.8 Abutment $L_a=15$ cm with collar $B_c=7.5$ cm at $Z_c/y=-0.25$ ,<br>$y=15.2$ cm .....  | 33 |

|  |    |
|--|----|
| Figure 3.9 Abutment $L_a=15$ cm with collar $B_c=5.0$ cm at $Z_c/y=0.00$ ,<br>$y=15.2$ cm .....  | 34 |
| Figure 3.10 Seatek Ultrasonic Ranging System .....   | 38 |
| Figure 3.11 Acoustic device used in the experiments.....   | 39 |
| Figure 4.1 Schematic illustration of the collar-abutment arrangement.....  | 41 |
| Figure 4.2 Effect of collar size and elevation on the maximum scour depth around<br>the abutments of $L_a=15$ cm and $L_a=35$ cm ( $Q=0.0678$ m <sup>3</sup> /s, $y=15.2$ cm<br>and $y=17.4$ cm, $d_{50}=1.5$ mm) .....  | 52 |
| Figure 4.3 Effect of collar size and elevation on the maximum scour depth around<br>the abutments of various lengths ( $Q=0.0678$ m <sup>3</sup> /s, $y=13.5$ cm,<br>$d_{50}=1.5$ mm) (Daşkın, 2011) .....   | 53 |
| Figure 4.4 Variation of $[(d_s)_{\max,c}/y]_{\text{opt}}$ with $\theta$ ( $Q=0.0678$ m <sup>3</sup> /s, $y=17.4$ cm, $F_r=0.48$ ,<br>$U/U_c=0.70$ , $d_{50}=1.50$ mm, $t=3$ hours) ( $Q=0.0678$ m <sup>3</sup> /s, $y=15.2$ cm,<br>$F_r=0.24$ , $U/U_c=0.80$ , $d_{50}=1.50$ mm, $t=3$ hours)..... | 58 |
| Figure 4.5 Variation of $[(d_s)_{\max,c}/y]_{\text{opt}}$ with $\theta$ ( $Q=0.0678$ m <sup>3</sup> /s, $y=13.5$ cm, $F_r=0.29$ ,<br>$U/U_c=0.90$ , $d_{50}=1.50$ mm, $t=3$ hours) (Daşkın, 2011) .....  | 59 |
| Figure 4.6 Variation of $[(d_s)_{\max,c}/y]_{\text{opt}}$ with $\sqrt{\theta(L_a/B_c)}$ .....  | 61 |
| Figure 4.7 Variation of $[Z_c/y]_{\text{opt}}$ with $L_a/B_c$ .....  | 63 |
| Figure 4.8 Variation of $[Z_c/y]_{\text{opt}}$ with $L_a/B_c$ .....  | 64 |

|  |    |
|--|----|
| Figure 4.9 Variation of $[\%Reduction]_{opt}$ with $L_a/B_c$ .....   | 67 |
| Figure 4.10 3-D views of the scour and deposition patterns around the abutment<br>model of $L_a=35$ cm: a) at flow depth of $y=17.4$ cm; b) at flow depth of<br>$y=13.5$ cm..... | 69 |
| Figure 4.11 Schematic illustration of the sections taken around the abutment model<br>of $L_a=35$ cm.....  | 70 |
| Figure 4.12 Section I: a) at flow depth of $y=17.4$ cm; b) at flow depth of $y=13.5$ cm<br>.....   | 71 |
| Figure 4.13 Section II: a) at flow depth of $y=17.4$ cm; b) at flow depth of $y=13.5$ cm<br>.....  | 73 |
| Figure 4.14 Section III: a) at flow depth of $y=17.4$ cm; b) at flow depth of $y=13.5$ cm<br>.....   | 74 |
| Figure 4.15 Section IV: a) at flow depth of $y=17.4$ cm; b) at flow depth of $y=13.5$ cm<br>.....  | 75 |
| Figure 5.1 Schematic illustration of the sections taken around the abutment model of<br>$L_a=15$ cm for the flow depth of $y=13.5$ cm.....                                       | 78 |
| Figure 5.2 Time development of local scour around the abutment model of $L_a=15$ cm<br>at section 1 .....  | 81 |
| Figure 5.3 Time development of local scour around the abutment model of $L_a=15$ cm<br>at section 2 .....  | 82 |

|  |    |
|--|----|
| Figure 5.4 Time development of local scour around the abutment model of $L_a=15$ cm<br>at section 3 .....                                  | 83 |
| Figure 5.5 Time development of local scour around the abutment model of $L_a=15$ cm<br>at section 4 .....                                  | 84 |
| Figure 5.6 Time development of local scour around the abutment model of $L_a=15$ cm<br>at section 5 .....                                  | 85 |
| Figure 5.7 Schematic illustration of the sections taken around the abutment model of<br>$L_a=15$ cm for the flow depth of $y=17.4$ cm..... | 86 |
| Figure 5.8 Time development of local scour around the abutment model of $L_a=15$ cm<br>at section 1 .....                                  | 89 |
| Figure 5.9 Time development of local scour around the abutment model of $L_a=15$ cm<br>at section 2 .....                                  | 90 |
| Figure 5.10 Time development of local scour around the abutment model of<br>$L_a=15$ cm at section 3 .....                                 | 91 |
| Figure 5.11 Time development of local scour around the abutment model of<br>$L_a=15$ cm at section 4 .....                                 | 92 |
| Figure 5.12 Time development of local scour around the abutment model of<br>$L_a=15$ cm at section 5 .....                                 | 93 |
| Figure 5.13 Schematic illustration of the sections taken around the abutment model<br>of $L_a=35$ cm at the flow depth of $y=13.5$ cm..... | 94 |

|   |     |
|---|-----|
| Figure 5.14 Time development of local scour around the abutment model of<br>$L_a=35$ cm at section 1 .....                                  | 98  |
| Figure 5.15 Time development of local scour around the abutment model of<br>$L_a=35$ cm at section 2 .....                                  | 99  |
| Figure 5.16 Time development of local scour around the abutment model of<br>$L_a=35$ cm at section 3 .....                                  | 100 |
| Figure 5.17 Time development of local scour around the abutment model of<br>$L_a=35$ cm at section 4 .....                                  | 101 |
| Figure 5.18 Time development of local scour around the abutment model of<br>$L_a=35$ cm at section 5 .....                                  | 102 |
| Figure 5.19 Schematic illustration of the sections taken around the abutment model<br>of $L_a=35$ cm at the flow depth of $y=17.4$ cm ..... | 103 |
| Figure 5.20 Time development of local scour around the abutment model of<br>$L_a=35$ cm at section 1 .....                                  | 106 |
| Figure 5.21 Time development of local scour around the abutment model of<br>$L_a=35$ cm at section 2 .....                                  | 107 |
| Figure 5.22 Time development of local scour around the abutment model of<br>$L_a=35$ cm at section 3 .....                                  | 108 |
| Figure 5.23 Time development of local scour around the abutment model of<br>$L_a=35$ cm at section 4 .....                                  | 109 |
| Figure 5.24 Time development of local scour around the abutment model of<br>$L_a=35$ cm at section 5 .....                                  | 110 |

## LIST OF SYMBOLS

|                        |  |
|------------------------|--|
| $A_{\text{total}}$     | Total area of the abutment with collar                                     |
| $A_{\text{abutment}}$  | Abutment area on the horizontal plane                                      |
| $B$                    | Channel width  |
| $B_a$                  | Abutment width   |
| $B_c$                  | Collar width around the abutment   |
| $B_t$                  | Total width of the abutment width and collar width on the horizontal plane |
| $C$                    | Cohesiveness   |
| $C_u$                  | Uniformity coefficient   |
| $d_s$                  | Local scour depth at the abutment at any time                              |
| $(d_s)_{\text{max}}$   | Maximum scour depth at the abutment at the end of the given time duration  |
| $(d_s)_{\text{max,c}}$ | Maximum scour depth at the abutment with collar                            |
| $d_{50}$               | Median size of sediment  |
| $d_{84}$               | Sediment size for which 84 % of the sediment finer                         |
| $d_{60}$               | Sediment size for which 60 % of the sediment finer                         |
| $d_{16}$               | Sediment size for which 16 % of the sediment finer                         |
| $d_{10}$               | Sediment size for which 10 % of the sediment finer                         |
| $Fr$                   | Froude number of flow  |
| $Fr_c$                 | Critical Froude number at the threshold of grain motion                    |
| $g$                    | Gravitational acceleration   |
| $K_a$                  | Shape factor of abutment   |
| $K_G$                  | Approach channel geometry factor   |
| $L_a$                  | Projecting length of abutment, perpendicular to the flow                   |
| $L_c$                  | Projecting length of collar, perpendicular to the flow                     |
| $R^2$                  | Correlation coefficient  |
| $Re^*$                 | Particle Reynolds number   |

|            |   |
|------------|---|
| $Q$        | Discharge of the flow   |
| $S_0$      | Slope of the channel  |
| $S_e$      | Energy slope of flow  |
| $S_p$      | Particle shape factor   |
| $S_s$      | Specific gravity  |
| $T_c$      | Collar thickness  |
| $t$        | Time  |
| $U$        | Mean approach flow velocity   |
| $U_c$      | The value of the $U$ at the threshold of grain motion                                       |
| $U_*$      | Shear velocity of the approach flow   |
| $U_{*c}$   | The value of the $U_*$ at the threshold of grain motion                                     |
| $y$        | Normal flow depth   |
| $y_c$      | Critical flow depth at the threshold of grain motion  |
| $w$        | Sediment fall velocity  |
| $Z_c$      | Collar level on the abutment with reference to bed level                                    |
| $\theta$   | Ratio of total area of the abutment and collar to the abutment area on the horizontal plane |
| $\alpha_a$ | Abutment skewness   |
| $\alpha_c$ | Shild's entrainment factor, dimensionless critical shear factor                             |
| $\sigma_g$ | Standard deviation of particle-size distribution  |
| $\varphi$  | Angle of repose   |
| $\rho$     | Fluid density   |
| $\rho_s$   | Sediment density  |
| $\mu$      | Dynamic viscosity of fluid  |
| $\tau_0$   | Bed shear stress  |
| $\tau_c$   | Critical shear stress for sediment particles to move  |



## **CHAPTER 1**

### **INTRODUCTION**

#### **1.1 BACKGROUND**

“The main concern of the engineer when considering the safety of an existing bridge, is to ensure that it will not collapse. This requirement is generally met by providing maintenance and repair to keep and, where necessary, restore structural adequacy to a level implied by good practice as manifest through standards and codes of practice for bridge design and assessment” (Menzies, 1997). Ettema (2000) states that “The history of bridge hydraulics is replete with incidents of failed bridges whose design did not adequately account for the capacity of alluvial rivers to erode, or scour, channel beds and banks. Images of undermined piers, undercut abutments, and washed out bridge approaches have haunted bridge engineers since antiquity” (Melville and Coleman, 2000).

The bridges constructed in alluvial rivers cause a contraction in the waterway at the bridge site which leads to significant scour. As the scour continuously progresses in close proximity to piers and abutments, it undermines the foundations of the structure leading to possible failure (Khawairakpam and Mazumdar, 2009). Although scour action may occur at any time, this dynamic phenomenon is especially strong during floods which leads to the sudden failure of structures without prior warning (Deng and Cai, 2010). In spite of the significant investment in bridge scour research, failure of bridges due to scour at their foundations is a common occurrence.

It is believed that this is due to the inadequacies in both design criteria adopted for older bridges and also the present state of knowledge about some aspects of bridge hydraulics and scouring mechanism (Melville and Coleman, 2000).

Bridge failure or collapse has been an important social and economical fallout. For example, Melville (1992) and Cardoso and Bettess (1999) reported the data on the problem of scour in the United States and in New Zealand by demonstrating that bridge repair is an important part of the public expenditures. Failure of bridges due to scour at bridge foundations during flood events has been widely documented (Parola et al., 1998, Morris and Pagan-Ortiz, 1999, Richardson and Davis, 2001). Also, Melville and Coleman (2000) reported important case studies associated with the bridge-scour damages having occurred in New Zealand providing the costs of repairing or rebuilding different bridge structures.

Therefore, local scour at piers and abutments has been studied over several decades, mainly through experimental or semi empirical approaches. Although most of bridge failures are due to abutment scour, researches on pier scour received more attention. Flow field as well as resulting scour pattern around bridge abutments is still not well documented despite its high importance (Abou-Seida et al., 2009). In spite of the considerable effort attained in this three-dimensional complicated phenomenon, further understanding of the abutment scour process is still needed to develop improved ways of protecting bridges against the ravages of scour.

## **1.2 OBJECTIVES**

The principle objective of this study is to investigate the effects of flow depth and collars, attached to the semi-circular end abutment models at different elevations, on the development of local scour around bridge abutments. Also, this study includes the assesment of the effects of flow depth and abutment length on the temporal development of local scour at bridge abutments.

### **1.3 SCOPE**

The study reported herein is based on the experiments performed in the Hydromechanics Laboratory at Middle East Technical University, METU, using a physical hydraulic model. The study was confined to almost uniform cohesionless sand bed material under clear-water scour conditions.

### **1.4 SYNOPSIS OF THE THESIS**

In Chapter 2, a comprehensive review of the scour phenomena, the temporal development of scour, various countermeasures against scour at bridge abutments as well as the literature related to the use of collars as a scour countermeasure are covered. Chapter 3 gives a description of the experimental equipment, instrumentation and procedure. The results of the experimental investigations related to the investigation of the effects of flow depth and the use of collars are presented and compared with the previous studies of Kayatürk (2005), Doğan (2008) and Daşkın (2011) in Chapter 4. In Chapter 5, the results of the experiments performed to investigate the effects of the flow depth and abutment length on the time development of local scour at bridge abutments are discussed. Finally, the principal conclusions drawn from the results of the experiments and recommendations for future studies are given in Chapter 6.

## **CHAPTER 2**

### **LITERATURE REVIEW**

#### **2.1 INTRODUCTION**

Bridge abutments commonly border swift, turbulent flow through bridged waterways, and therefore risk of failure occurs due to scour (Ettema et al., 2010). Because of the bridge failures due to scour at their foundations, many researchers have conducted various studies on local scour at bridge abutments over the past few decades. There have been intensive studies to explore the causes of scouring and to develop mitigation countermeasures for bridge abutment scour in the literature. This chapter presents a review of the scour phenomena at bridge abutments, parameters affecting local scour, the temporal development of scour as well as various countermeasures against scour at abutments. Application of collars around bridge abutments as a scour countermeasure is also reviewed.

#### **2.2 SCOUR**

##### **2.2.1 Definition of Scour**

Scour is defined as a natural phenomenon caused by the erosive action of the flowing water in rivers and streams (Breusers et al., 1977). Cheremisinoff et al. (1987) defined scour as the lowering of the river bed level by water erosions exposing the foundations of riverine structures such as bridges. The amount of this lowering of the

river bed level after the commencement of the scour is termed as the scour depth or depth of scour (Melville and Coleman, 2000). Moreover, Richardson and Davis (2001) has noted that scour occurs as a result of the erosive action of flowing water, excavating and carrying away material from the bed and banks of streams and also from the vicinity of piers and abutments of bridges. The construction of bridge piers and abutments in alluvial channels causes a contraction in the waterway leading to significant scour at the bridge site. As the development of scour continues at the bridge foundations, it can result in failure of the bridge structure, loss of life and property (Khawairakpam and Mazumdar, 2009).

### **2.2.2 Types of Scour**

The types of scour that affect the performance and safety of bridges are typically referred to as general scour, contraction scour, and local scour (Melville and Coleman, 2000).

*General Scour* – This type of scour is the lowering of the streambed across the stream caused by natural changes in the catchment or by human activities. General scour develops irrespective of the existence of the bridge structure and can occur as either short-term or long-term scour. These two types are distinguished by the time taken for the development of scour. Short-term general scour develops during a single flood event or several closely-spaced floods. In contrast to short-term general scour, long-term general scour has a considerably longer time scale, normally of the order of several years or longer, and includes progressive degradation of the river bed and lateral bank erosion.

*Contraction Scour* – This type of scour is directly attributable to the existence of the bridge structure. Contraction scour occurs as a result of the constriction of the flow due to the bridge or its road approaches encroaching onto the floodplain of a river.

The flow at a bridge usually converges as it approaches the bridge, and contracts further within the bridge opening, accelerating to the narrowest section. This accelerated flow induces scour at the contracted section and referred to as contraction scour.

*Local Scour* – This type of scour involves removal of sediment from around bridge piers and abutments. Local scour is caused by the interference of the piers and abutments with the flow and is characterised by the formation of scour holes at the vicinity of bridge piers or abutments (see Figure 2.1).

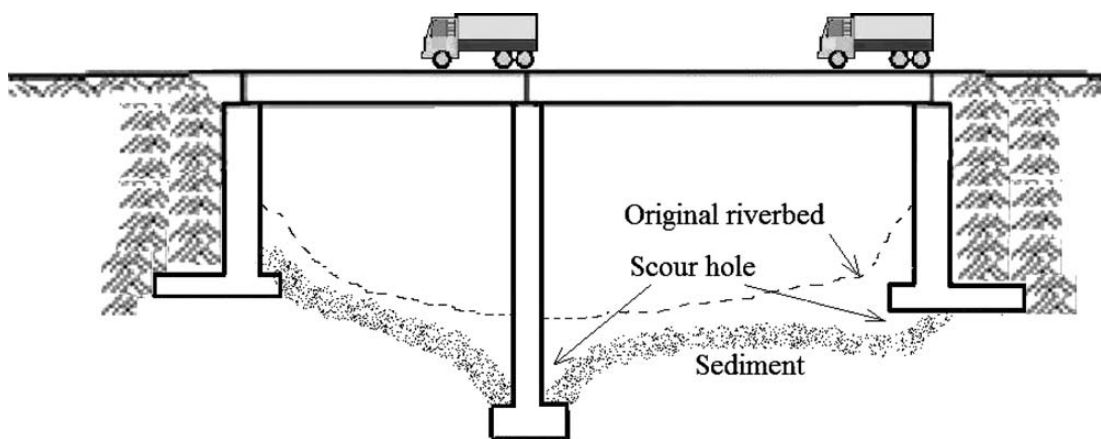


Figure 2.1 Bridge scour (Deng and Cai, 2010)

According to the mode of sediment transport from the vicinity of bridge piers and abutments by the approaching flow, local scour is classified by Chabert & Engeldinger (1956) as clear-water scour and live-bed scour. Clear-water scour occurs where there is no sediment transport into the scour hole by the approaching flow. On the contrary, live-bed scour occurs where there is continuous transport of bed material to the scour hole by the approaching flow (Barbhuiya and Dey, 2004). The maximum local scour depth for the clear-water scour case is obtained when the flow can no longer remove the bed material from the scour hole. On the other hand, when

live-bed scour occurs, the equilibrium scour depth is obtained when the time-averaged transport of bed material into the scour hole equals to that of removed from it (Melville and Coleman, 2000).

### **2.3 BRIDGE ABUTMENT SCOUR MECHANISM**

Bridge foundations cause significant changes in the flow pattern when introduced into a channel flow. Local scour occurs around the bridge piers and abutments when the local flow field near the bridge foundations is strong enough to remove bed material. In the process of local scour, the obstruction to the flow caused by the bridge foundations is of primary importance (Melville and Coleman, 2000). Local scour mechanism and the flow pattern around the piers and abutments are complex phenomena resulting from the strong interaction of the three-dimensional turbulent flow field around the bridge foundations and the erodible bed material (Laursen, 1962, Melville, 1997). An abutment as an obstruction to the main channel flow results in a three-dimensional vortex flow system. This vortex flow system causes the evolution and development of the local scour hole in the vicinity of the abutment (Dey and Barbhuiya, 2005). According to Lim (1997), “the flow accelerates and separates at the upstream face of the abutment as it moves past the bridge abutment, creating a vortex trail that moves downstream in a direction approximately perpendicular to the structure. The result is that the bed erodes locally around the bridge abutment creating local scour hole”.

Abou-Seida and others (2009) reported that when the flow approaches the abutment, the streamlines contract causing the flow to accelerate and therefore to increase the local shear stresses. The turbulent shear stress is greater than the critical shear stress for the bed material at the upstream corner of the abutment which causes initiation of motion.

After the initiation of scour and flow separation at the upstream side of the abutment, the flow is pushed to the downward direction into a strong spiraling flow that leads to the development of the primary vortex. Kwan (1988) and Kwan and Melville (1994) identified this primary vortex, which is similar to the horseshoe vortex at piers, along with the downflow as the principal cause of local scour at bridge abutments (Barbhuiya and Dey, 2004). Moreover, Dey and Barbhuiya (2005) reported that at the upstream face of the abutment the approaching flow becomes stationary. Since the velocity of the approaching flow is maximum at the free surface and decreases to zero at the bed level, the stagnation pressure decreases in the same direction which results in a flow being driven downward at the upstream face of the abutment, termed downflow. The downflow acts as a vertical jet that erodes sediment from the bed (Lim, 1997). According to Kwan and Melville (1994), the primary vortex and the downflow are confined mainly to the scour hole beneath the original bed level. As the strength of the primary vortex and downward flow increase, more sediment particles are eroded and removed from around the abutment which leads to increase in the size and depth of the scour hole (Abou-Seida et al., 2009).

The flow field at an abutment is shown schematically in Figure 2.2. As illustrated in the figure, Kwan and Melville (1994) identified a secondary vortex, with counter-rotational direction to that of the primary vortex, occurring next to the primary vortex. The secondary vortex is considered to have restricting effect on the scouring capacity of the primary vortex (Barbhuiya and Dey, 2004).



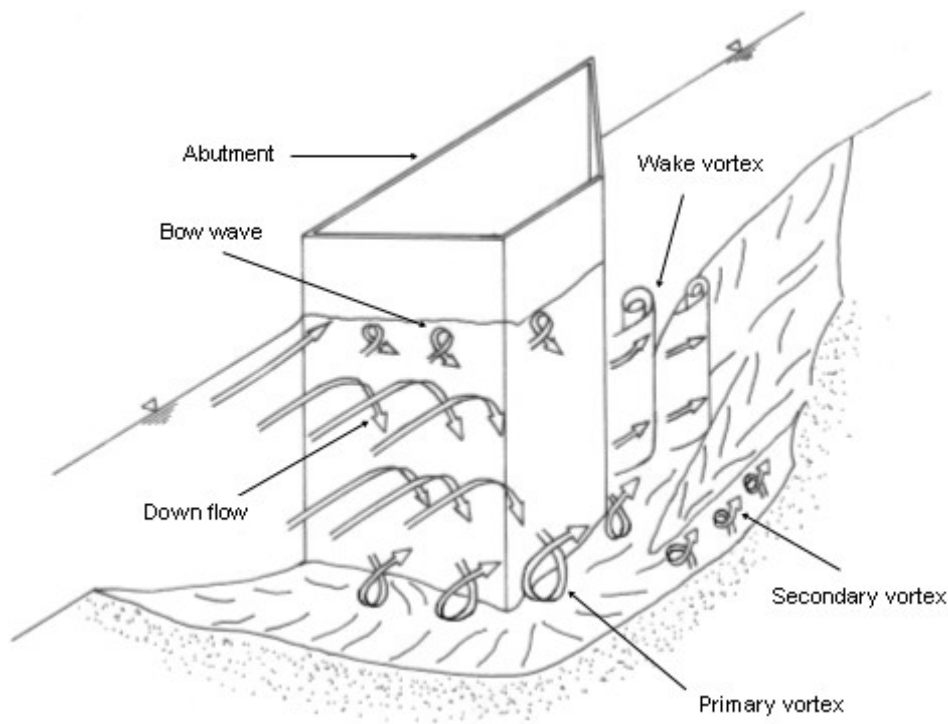


Figure 2.2 Schematic diagram of flow field at an abutment (after Kwan, 1988)

According to Barbhuiya and Dey (2004), at the downstream of the abutment, wake vortices are created due to the separation of flow at upstream and downstream of the abutment corners. The flow separation creates unstable shear layers that roll up to form eddy structures, termed wake vortices. The wake vortices, drifted to downstream due to the mean flow, act like small tornadoes and lift up sediments from the bed. The strength of these wake vortices are rather smaller than that of the primary vortex (Barbhuiya and Dey, 2004).

The three-dimensional turbulent flow field in a scour hole at a semi-circular end abutment was investigated by Dey and Barbhuiya (2005) under clear-water scour conditions using an acoustic Doppler velocimeter. According to the results of experimental investigations, Dey and Barbhuiya (2005) reported that the main characteristic features of the flow at a semi-circular end abutment are a relatively large primary vortex flow associated with the downflow and skewed velocity distributions.

The approaching flow separates at the upstream edge of the scour hole, as a line of separation forming a vortex flow inside the scour hole, which acts like a separation zone. The downflow, developed due to the downward negative stagnation pressure gradient of the approaching flow velocity along the upstream face of the abutment, is pushed up by the vortex. It was also observed that the approaching flow curves down into the scour hole and rolls to form a vortex flow, called primary vortex, which migrates downstream by the side of the abutment (Dey and Barbhuiya, 2005).

The unsteady dynamics of the flow field around vertical wall abutments were studied by Köken and Constantinescu (2008a, 2008b) using Large Eddy Simulation (LES) both for flat bed and equilibrium scour bed conditions at a Reynolds number of 18000. It was noticed that due to the adverse pressure gradients induced by the abutment, the approaching flow separates close to the abutment and horseshoe vortices are formed. If the bed material is loose, the horseshoe vortex system has a significant role in the formation of the scour hole around the abutments at all stages of the scouring process. It is found that primary horseshoe vortex shows aperiodic bimodal oscillations, which increase the turbulence along the core of the primary vortex. This mechanism further increases the bed shear stress along the trajectory of the primary vortex. Köken and Constantinescu (2009, 2011) made a similar investigation at a much larger Reynolds number ( $\sim 2.5 \times 10^5$ ) which is closer to the practical values observed in natural rivers. They identified the differences observed in the turbulent structures around vertical wall abutments.

## **2.4 PARAMETERS INFLUENCING LOCAL SCOUR AT ABUTMENTS**

The parameters affecting the magnitude of the local scour depth at abutments are given by Richardson and Davis (2001) as: the approach flow velocity, flow depth, projected length of the abutment into the flow, size and gradation of the bed material, angle of attack of the approach flow to the abutment, abutment shape, bed configuration, and ice formation or debris jams.

According to Barbhuiya and Dey (2004), the parameters listed above and the related factors involved in the scour phenomenon at bridge abutments can be grouped as below:

1. Approaching flow parameters: Flow depth, mean flow velocity, shear velocity, roughness.
2. Fluid parameters: Density, viscosity, gravitational acceleration and temperature.
3. Bed material parameters: Grain size distribution, median size, mass density, cohesiveness and angle of repose.
4. Abutment parameters: Size, shape, orientation with respect to main flow (i.e. angle of attack) and surface condition.
5. Channel geometry parameters: Width, slope and cross-sectional shape.
6. Time of scouring can be included as an additional parameter for the development of the scour hole.

Moreover, Li et al. (2006) specified the parameters that affect the local scour depth at abutments and using these parameters the local scour depth ( $d_s$ ) at a bridge abutment is presented as a function of them as:

$$d_s = f[\rho, \mu, y, U, S_e, g, B, S_0, K_G, d_{50}, S_s, \sigma_g, w, S_p, \phi, C, \alpha_c, Re^*, L_a, \alpha_a, K_a, t] \quad (2.1)$$

where  $\rho$  = fluid density,  $\mu$  = dynamic viscosity of the fluid,  $y$  = normal flow depth,  $U$  = mean approach flow velocity,  $S_e$  = energy slope of flow,  $g$  = gravitational acceleration,  $B$  = channel width,  $S_0$  = slope of the channel,  $K_G$  = geometry of the channel,  $d_{50}$  = median particle grain size,  $S_s$  = specific gravity,  $\sigma_g$  = geometric standard deviation of sediment size distribution,  $w$  = fall velocity of sediment,  $S_p$  =

particle shape factor,  $\phi$  = angle of repose,  $C$  = cohesiveness,  $\alpha_c$  = dimensionless critical shear stress,  $Re^*$  = particle Reynolds number,  $L_a$  = abutment length,  $\alpha_a$  = abutment skewness,  $K_a$  = abutment shape, and  $t$  = scouring time.

Neglecting some of these parameters under certain cases, Li et al. (2006) proposed the following nondimensional parameters as the most important variables influencing the scour at bridge abutments:

$$d_s/L = f(U/U_c, L_a/d_{50}, L_a/y, \sigma_g, K_a, K_G, \alpha_a, t) \quad (2.2)$$

where  $U_c$  is the critical velocity for the initiation of sediment motion and  $U/U_c$  represents the flow intensity.

Bridge abutment scour is a complicated phenomenon which includes the interaction of the parameters mentioned above. In order to develop scour countermeasures for bridge abutments, it is necessary to know the effects of these variables to this complicated process. Therefore, a discussion of these parameters and their effects is presented below.

#### **2.4.1 The Effect of Flow Intensity**

Melville and Chiew (1999) defined flow intensity as the ratio of the shear velocity ( $U^*$ ) to the critical shear velocity ( $U_{*c}$ ) or the ratio of the mean approach flow velocity ( $U$ ) to the critical mean velocity ( $U_c$ ). The shear velocity ratio  $U^*/U_{*c}$  is a good measure of the strength of the downflow and the scouring potential of the vortex structures at bridge abutments; however, due to the difficulties of measuring the shear velocity under live-bed scour conditions, the velocity ratio  $U/U_c$  can be used as a measure of the flow intensity (Li et al., 2006).

Dongol (1994) observed that the local scour depth increases almost linearly with flow velocity or shear velocity until the flow velocity reaches the threshold condition. Under clear-water scour conditions, the maximum local scour depth occurs when  $U/U_c = 1$ , and the corresponding maximum scour depth is termed as the threshold peak (Barbhuiya and Dey, 2004). The local scour depth in uniform sediments decreases after the velocity exceeds the threshold velocity and then increases to a second peak not exceeding the threshold peak and termed as live-bed peak (Melville and Coleman, 2000). The same trend was observed by Chabert and Engeldinger (1956), Gill (1972), Ettema (1980), Raudkivi and Ettema (1983), Chiew (1984), Baker (1986) and Dongol (1994). Therefore, it can be concluded that under clear-water scour conditions, the maximum local scour depth in uniform sediments occurs at the threshold condition as obtained in the studies of Laursen and Toch (1956), Shen and Schneider (1969), Shen (1971) and Breusers et al. (1977).

#### **2.4.2 The Effect of Flow Depth**

The results of the laboratory investigations of Gill (1972), Wong (1982), Tey (1984) and Kandasamy (1989) show that for constant value of the shear velocity ratio  $U^*/U_{*c}$ , the maximum scour depth increases with increase in approaching flow depth (Barbhuiya and Dey, 2004). Moreover, Li et al. (2006) reported that based on the abutment scour data obtained by Wong (1982), Tey (1984), Kwan (1988), Kandasamy (1989), and Dongol (1994), the scour depth at abutment increases with increase in approach flow depth at a decreasing rate towards a limiting value beyond which the effect of flow depth is negligible.

According to Barbhuiya and Dey (2004), for live-bed scour conditions, the equilibrium scour depth increases significantly with increase in the flow depth for smaller flow depths; on the contrary, equilibrium scour depth is independent of the flow depth for higher flow depths.

### 2.4.3 The Effect of Abutment Length

The influence of abutment length on the scour depth has been studied by many investigators (e.g. Garde et al. (1961), Laursen (1962), Gill (1972), Zaghoul and McCorquodale (1975), Rajaratnam and Nwachukwu (1983), Cunha (1975), Wong (1982), Tey (1984), Kandasamy (1989), Melville (1992), Dongol (1994)). In order to evaluate the effect of abutment length on the scour depth, various dimensionless parameters have been used including ratio of abutment length to flow depth  $L_a / y$ , contraction ratio, and opening ratio, as the inverse of contraction ratio (Li et al., 2006). The study by Husain et al. (1998) is noteworthy in that the scour depth increased with the decrease of the contraction ratio,  $\alpha = (B - L_a) / B$ , when other variables were kept constant; and similar trends were obtained by Garde et al. (1961), and Liu et al. (1961) for various  $\alpha$  values studied as the contraction ratio parameter.

Li et al. (2006) reported that based on the study of Dongol (1994) related to the effect of abutment length on scour, the obtained data was plotted together with data by Tey (1984) and Kandasamy (1989) for wing wall abutments and Kwan (1984) for semi-circular end abutments. It was observed that the rate of increase of scour depth with abutment length is insignificant for  $L_a / y \geq 60$ , and scour depth virtually remains constant when  $L_a / y \geq 100$ .

Kayatürk (2005) studied the effect of abutment length on local scour at bridge abutments under clear-water scour conditions and based on the experimental data, it was observed that for a given Froude number, the maximum scour depth increases with the increase in the length of the abutment.

Figure 2.3 shows the relationship of the dimensionless maximum scour depth,  $(d_s)_{\max}/y$ , with dimensionless abutment length,  $L_a/B$ , for three different Froude numbers (Kayatürk, 2005). In this figure, Froude number of 0.34 represents the threshold condition of the sediment motion in the flume channel ( $Fr_c$ ).

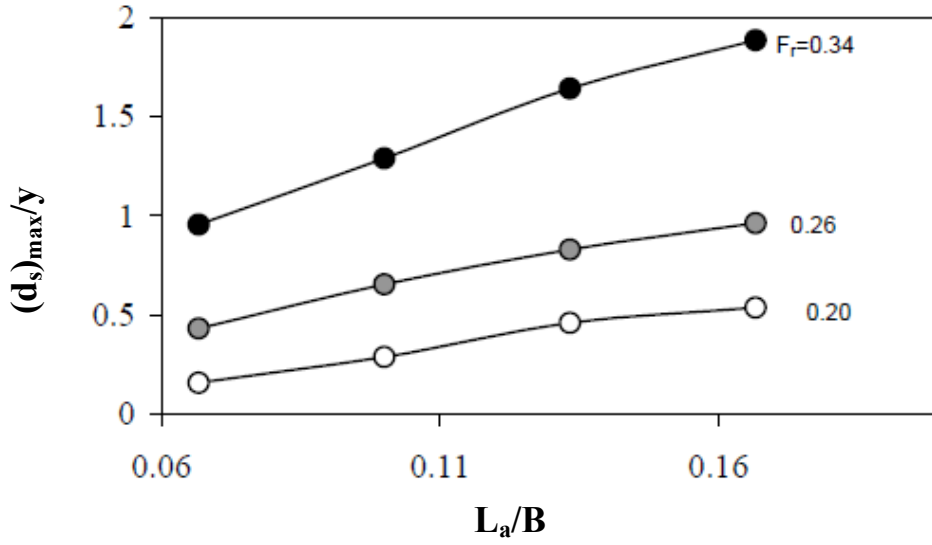


Figure 2.3 Influence of abutment length on scour depth (Kayatürk, 2005)

#### 2.4.4 The Effect of Abutment Shape

The local scour depth at abutments depends on the shape of the abutment. The most common bridge abutment shapes are vertical-wall, wing-wall, spill-through and semi-circular ended abutments. The effect of abutment shape on the local scour at abutments has been reported by many researchers (e.g. Laursen and Toch (1956), Liu et al. (1961), Garde et al. (1961), Wong (1982), Melville (1992) and Dongol (1994)). Barbhuiya and Dey (2004) reported that semi-circular ended, spill-through and wing-wall abutments as streamlined bodies produce low strength turbulent vortices, whereas vertical-wall abutments as blunt obstructions to the flow can produce strong turbulent vortices. Therefore, a deeper local scour depth is observed at a blunt obstruction as concluded by the other investigators studied the local scour depth at the vertical-wall abutments in comparison with spill-through and wing-wall abutments.

The effect of the shape of the abutments is accounted for by using a shape factor  $K_s$ , proposed by Melville (1992) for design purposes (Li et al., 2006). Moreover,

Barbhuiya and Dey (2004) reported that according to Melville (1992), when the abutment length becomes longer, the importance of abutment shape diminishes and therefore it has been recommended that for  $L_a/y \geq 10$ ,  $K_s^*$  is used as an adjusted shape factor which varies linearly with the abutment shape factor,  $K_s$  at  $L_a/y = 10$ , and is unity at  $L_a/y = 25$ .

#### **2.4.5 The Effect of Abutment Skewness**

The effect of the angle of approaching flow with respect to the abutment alignment, also referred to as the angle of attack, plays an important role on scour depth at bridge abutments (Barbhuiya and Dey, 2004). The effect of abutment alignment has been studied by Ahmad (1953), Laursen (1958), Garde et al. (1961), Sastry (1962), Field (1971), Zaghoul (1983), Kwan (1984), Kandasamy (1985) and Melville (1992). Li et al. (2006) reported that the results of the experimental investigations related to the effect of angle of attack,  $\alpha_a$  on local scour at abutments show that for both clear-water and live-bed scour conditions, the local scour depth increases with an increase in  $\alpha_a$  for  $\alpha_a \leq 90^\circ$ .

#### **2.4.6 The Effect of Sediment Size**

The sediment characteristics are determined from the particle size distribution curves and median sediment diameter  $d_{50}$  is the most commonly used parameter to identify the size of the bed sediment particles (Barbhuiya and Dey, 2004).

Dongol (1994) studied the effect of sediment size on scour development and classified the sediment coarseness into four groups according to the ratio of the abutment length  $L_a$ , to the median sediment size  $d_{50}$  as: (1)  $L_a / d_{50} > 100$ : fine sediment; (2)  $100 > L_a / d_{50} > 40$ : intermediate sediment; (3)  $40 > L_a / d_{50} > 10$ : coarse sediment; (4)  $10 > L_a / d_{50}$ : very coarse sediment (Li et al., 2006).



Barbhuiya and Dey (2004) reported that according to Ahmad (1953), Laursen and Toch (1956) and Izzard and Bradley (1958), the maximum scour depth is independent of the sediment size. However, Blench (1957), Garde et al. (1961) and Gill (1972) claimed that sediment size has an influence on the maximum scour depth.

Li et al. (2006) mentioned that when considering the effects of sediment size on scour, it is important to distinguish between clear-water and live-bed scour. Laursen (1960) pointed out that the maximum scour depth is affected by sediment size under clear-water scour condition rather than under live-bed scour condition (Barbhuiya and Dey, 2004). Moreover, under clear-water scour conditions Doğan (2008) studied the effect of the sediment grain size on the performance of abutment collars and found that the change in sediment size did not affect the optimum location of the collar at the abutment when compared with the previous study conducted by different sediment size.

Barbhuiya and Dey (2004) also reported that according to Ahmad (1953), Izzard and Bradley (1958), Garde et al. (1961) and Gill (1972), the rate of scour changes with different bed sediments and for fine sediments the rate of scour is faster than coarser sediments.

#### **2.4.7 The Effect of Sediment Gradation**

The gradation of sediments is mostly specified using the geometric standard deviation of the sand size,  $\sigma_g = (d_{84}/d_{16})^{1/2}$ . Breusers and Raudkivi (1991) has noted that the limit value of the geometric standard deviation is 1.35, beyond which the bed material can be considered to be nonuniform as in the case of natural river bed materials. Doğan (2008) reported that the coefficient of uniformity,  $C_u = d_{60} / d_{10}$  is also a parameter to characterize the uniformity of the bed sediments. The sediment material can be identified as uniform if the value of  $C_u$  is less than 3.0.

Barbhuiya and Dey (2004) reported that according to Ahmad (1953) and Ramu (1964), the equilibrium scour depth depends on the sediment gradation. Li et al. (2006) reported that the effect of sediment gradation on scour depth at abutments depends on the scour condition i.e. whether it is clear-water scour or live-bed scour. Ettema (1980), Wong (1982), Melville (1992) and Dongol (1994) found that under similar flow conditions and for the sediment with the same  $d_{50}$  value, less scour development is observed in nonuniform sediments than in uniform sediments. They also observed that scour depth decreases progressively with the increase in sediment gradation  $\sigma_g$ .

Dongol (1994) conducted experiments to study the effect of sediment gradation on scour depth at two different flow depths. It is observed that the effect of sediment gradation on scour depth is more prominent at lower flow velocities (Li et al., 2006).

## **2.5 TEMPORAL DEVELOPMENT OF SCOUR**

The determination of the maximum local scour depth at bridge abutments is an important aspect to the engineers in terms of the design criteria of the bridge foundations against scour formation. Therefore, the temporal variation of scour depth and the time required for the scour to reach the equilibrium state play a significant role in obtaining the maximum scour depth (Li et al., 2006). Most of the methods related to the investigation of the scour phenomena deal with the scour depth using design discharges for steady flow conditions; however, during flood events the flow in a river is unsteady. In general, for a design discharge, the time required for scour to reach the equilibrium conditions is much greater than the actual flood time (Kumcu et al., 2007). Therefore, in order to estimate the maximum scour depth under flood flows, temporal evolution of the scour process becomes significant and various experimental investigations have conducted by Cunha (1975), Wong (1982), Tey (1984), Cardoso and Bettess (1999), Ballio and Orsi (2000), Oliveto and Hager (2002), Coleman et al. (2003), and Dey and Barbhuiya (2005).

Equilibrium scour depth occurs when the scour depth does not change appreciably with time. Equilibrium state can be defined as the asymptotic state of scour attained when the scouring rate becomes insignificant. An equilibrium is reached progressively between the erosive capability of flow and the resistance to motion of the bed materials through erosion of the flow boundary (Alabi, 2006).

Li et al. (2006) reported that the local scour depth increases progressively with time and then the equilibrium state is reached. In the development of local scour, three phases have been identified as the initial, the principal, and the equilibrium phases by various researchers including Gill (1972), Wong (1982), Tey (1984), Kwan (1984), Ettema (1980), Kandasamy (1985) and Dongol (1994).

Cardoso and Bettess (1999) conducted experimental investigations on development of local scour at abutments located in compound channels and they identified two phases of development as the principle phase and the equilibrium phase, besides in some cases an initial phase can be distinguished, also (Coleman et al., 2003).

Dey and Barbhuiya (2004) reported that for uniform sediments, time variation of scour depth is a family of parallel lines for different sediment sizes and abutment lengths. On the other hand, time variation of scour depth for nonuniform sediments reduces with increase in nonuniformity of the sediment size distributions. Barbhuiya and Dey (2004) also reported that equilibrium scour depth at an abutment is attained asymptotically as a general consensus.

## **2.6 BRIDGE ABUTMENT SCOUR COUNTERMEASURES**

The scour mechanism has the potential to threaten the structural integrity of bridges that leads to the collapse of the structure when the foundation of the bridges is undermined (Masjedi et al., 2010). There have been many studies performed over the years to develop countermeasures against scour at bridge piers and abutments.

In this section of the literature review, a review of countermeasures for preventing local scour at bridge abutments are presented.

### **2.6.1 Local Scour Countermeasures at Bridge Abutments**

A wide variety of countermeasures have been studied to mitigate abutment scour and the criteria required for the selection of the proper countermeasure method have been investigated by various researchers. Richardson and Davis (2001) defined countermeasures as “features that make a bridge less vulnerable to damage or failure from scour or stream instability”.

They also stated that an action plan should be developed for the scour critical bridges, and depending on the risk factor, it might include development of a monitoring program or immediate installation of countermeasures against failure due to scour or stream instability.

FHWA Hydraulic Engineering Circular No. 23 (HEC 23) “Bridge Scour and Stream Instability Countermeasures - Experience, Selection, and Design Guidance” (2001) and NCHRP Report 587 “Countermeasures to Protect Bridge Abutments from Scour” (2007) present various countermeasures against scour. The main issues that comprise the essential considerations underlying the criteria for selecting a countermeasure include technical effectiveness, constructibility, durability and maintainability, aesthetics, environmental impact and cost (NCHRP, Report 587, 2007).

Scour countermeasures have been categorized into three main groups based on their functionality with respect to scour and stream instability as:

- Hydraulic countermeasures,
- Structural countermeasures,
- Monitoring.

Hydraulic countermeasures can be further grouped into armoring countermeasures and flow-altering countermeasures including river training structures (Li et al., 2006). Li et al. (2006) also reported that countermeasures for local scour at bridge abutments consists of flow-altering countermeasures that move local scour away from the abutment and armoring countermeasures which provides resistance to erosion.

The armoring of the flow boundaries subjected to erosion is the most common form of scour countermeasure at bridge abutments (NCHRP, Report 587, 2007). Deng and Cai (2010) reported that the basic principle of armoring countermeasure is the addition of another layer resisting to the hydraulic shear stress which provides protection against scouring of the more erodible materials underneath. Riprap is the most commonly used form of armoring countermeasure, and other forms of armoring include cable-tied blocks, geobags, tied mats, tetrapods and soil reinforcement, etc. (NCHRP, Report 587, 2007).

The basic aim of flow-altering countermeasures, on the contrary, includes modifying the flow field at an abutment to reduce the scour capacity of the local flow field around abutments (NCHRP, Report 587, 2007). Flow-altering countermeasures are composed of spur dikes, guidebanks, submerged vanes, parallel walls and collars, etc. A comparison between the two types of scour countermeasures with respect to the working principle, advantages and disadvantages are presented in Table 2.1.

Table 2.1 Comparison between armoring and flow-altering scour countermeasures (Deng and Cai, 2010)

|                          | <b>Armoring countermeasures</b>  | <b>Flow-altering countermeasures</b>   |
|--------------------------|--|--|
| <b><i>Principle</i></b>  | Protect the bed materials underneath the armoring layer from being scoured away  | Alter the flow alignment or break up vortices and therefore reduce the scour effect  |
| <b><i>Advantages</i></b> | Most commonly used type; easy to use; works well in most situations  | Different designs can be selected for different site conditions to achieve satisfactory results                                |
| <b><i>Problems</i></b>   | Winnowing of sands through the armor; difficult to keep the armor in place; constrict the channel and cause additional contraction scour | Special design may be needed for particular site conditions; significant cost and construction of new structures may be needed |

Lagasse et al. (2001) provided the design specifications for many of these scour mitigation techniques, management and inspection strategies for scour critical bridges in Hydraulic Engineering Circular No. 23. Also, a comprehensive review of different scour countermeasures and the criteria to be considered when selecting a scour countermeasure are given in NCHRP, Report 587 (2007).

### **2.6.2 Bridge Abutment Collar as a Scour Countermeasure**

Among flow-altering countermeasures for local scour at bridge foundations, collars are the horizontal protective plates attached to bridge piers and abutments to provide protection against local scour formation in the vicinity of the bridge foundations. Collars block the direct impact of downflow, which results the reduction of local scour depth by reducing the strength of downflow and the horseshoe vortex below the collar.

The effectiveness of collars in scour reduction was investigated by Laursen and Toch (1956), Chabert and Engeldinger (1956), Tanaka and Yano (1967), Ettema (1980), Dargahi (1990), Chiew (1992), Fotherby and Jones (1993), Kapoor and Keana (1994), Kumar et al. (1999), Singh et al. (2001), Mashahir and Zarrati (2002), Borghei et al. (2004), Kayatürk (2005), Alabi (2006), Doğan (2008) and Daşkın (2011).

Kayatürk (2005) studied the effect of collars on the reduction of local scour around bridge abutments. Collars of different sizes, attached to the abutments at various elevations, were tested as scour countermeasures under clear-water scour conditions. It was found that the efficiency of collars in preventing scour is a function of its size and elevation relative to the bed level. The scour depth decreases as the size of the collar increases. Kayatürk (2005) also investigated the temporal development of local scour around the abutment with and without collars of different sizes. The experimental results show that the local scour depth decreases as the elevation of the collars decrease below the bed level.

It was also observed that collars are very effective in reducing the rate of temporal development of scouring. According to Kayatürk (2005), a 63-69 % reduction in the scour depth was achieved at the end of 6-hours test duration and based on the results of tests having 12-hours test duration, up to 73 % reduction was observed. The use of partial collars was also proposed in the doctoral study of Kayatürk (2005) as an economical alternative to provide maximum scour reduction.

Li et al. (2006) conducted laboratory experiments with collars attached around the vertical-face wing-wall abutment as a countermeasure against abutment scour. Collars of different lengths and widths were tested at three different elevations under clear-water conditions to obtain the best configuration for collars and to observe the effect of collars on temporal development of local scour. It was observed that collars were able to protect the bridge abutment from local scour by isolating the turbulent flow and vortex systems from the bed material around the abutment.

Based on the experimental results, it was concluded that the collar should be lower than the bed level in order to keep the secondary vortex above the collar, and thus preventing the sediment material from scouring action of the secondary vortex. Besides, it was reported that the maximum scour reduction was obtained when the collar was placed at an elevation of  $0.08 y$  below the mean bed sediment level where  $y$  is the main channel flow depth. According to the results of this study, the minimum collar width that eliminates the local scour was obtained as  $0.23 L$ , where  $L$  is the abutment length perpendicular to the direction of flow. Li et al. (2006) also observed that collars retarded the formation of the scour hole which constitutes another advantage of the use of collars as scour countermeasures at bridge abutments.

Doğan (2008) experimentally studied the effect of collars on the development of local scour at the base of the abutments under clear-water scour conditions. Collars of different sizes were attached around the vertical abutments, and the elevations of the collars were changed systematically to investigate the scour reduction efficiency of collars. The experiments were conducted with abutments that were rectangular in plan section using almost uniform cohesionless bed material of  $d_{50}=0.90$  mm.

In this study, since one of the objectives is to compare the results obtained from Kayatürk's (2005) study, the experiments were carried out with almost the similar parameters used in the previous experimental study except the grain size of the sand material. The effect of the sediment grain size on the scour reduction performance of abutment collars was also investigated. It was observed that the change of the sediment size did not significantly influence the optimum location of the collar at the abutment that gives the maximum scour reduction. Based on the results of the experiments, it was concluded that the scour depth decreases with the increase in the size of the collar. However, the scour reduction performance of a collar reduced with the increase in the abutment length. It was also reported that the experimental results was similar with the results of Kayatürk's (2005) study. According to the results, regardless of the flow depth, the scour reduction efficiency of the collar increases with decreasing  $L_a/B_c$ , and as  $L_a/B_c$  increases, the collar depths shifted in the downward direction from the bed level.



Daşkın (2011) carried out a series of experiments having 3-hours test duration to investigate the effect of collars on local scour around the abutments as a scour countermeasure. The experiments were conducted with and without collars of various sizes placed around the semi-circular end abutments at different elevations under clear-water scour conditions. According to the results of the experiments, collars were found to be an effective scour countermeasure for semi-circular end abutments. When the size of the collar increases, the scour depth decreases which is similar with the results obtained in the previous studies of Kayatürk's (2005) and Doğan's (2008).

Based on the results of this study, it was observed that the scour reduction efficiency of a collar increases as  $L_a/B_c$  value decreases. It was also noticed that almost the similar trends were observed with the previous two studies, regardless of the abutment shape and test duration, in terms of the optimum locations of the collars which yield the maximum scour reduction around the abutment as a function of  $L_a/B_c$ .

In summary, according to the results of the experimental investigations related to the use of collar as a countermeasure for local scour at bridge abutments, it can be concluded that collars are found to be effective at preventing local scour around the abutments. The use of collars not only reduces the scour depth, but also retards the rate of temporal development of the scour hole.

## **2.7 CONCLUSION**

In this chapter, a comprehensive review of the scour phenomena, effects of the parameters on local scour and various mitigation countermeasures developed for bridge abutment scour is presented.

Local scour at bridge abutments is a dynamic phenomenon that depends on many parameters. Although there are numerous investigations to explore this complex mechanism at bridge piers and abutments, further studies are still required especially in the area of the use of collars as a countermeasure for local scour at bridge abutments to prevent failure of the bridges and reduce the scour in an effective manner. Therefore, it is important to perform more studies on collars to investigate their efficiency on scour reduction performance and on the temporal development of scour around the abutments.

## **CHAPTER 3**

### **EXPERIMENTAL SETUP AND METHODOLOGY**

#### **3.1 INTRODUCTION**

In this chapter, the experimental equipment and procedure, including the flume, the abutment model, the flow and sediment characteristics, and instrumentation are described. The experiments of this study were performed in the Hydromechanics Laboratory at Middle East Technical University, METU, in Ankara.

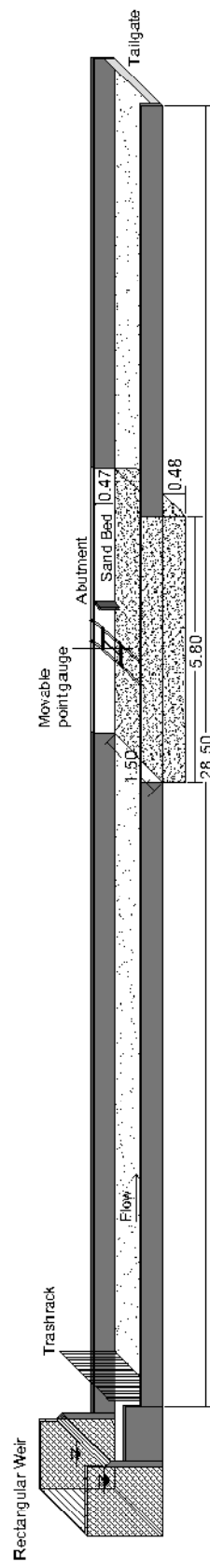
#### **3.2 FLUME**

The experiments were conducted in the 28.5 m long, 1.5 m wide, and 0.47 m deep glass-sided rectangular laboratory flume. The flume channel had a constant slope,  $S_0$ , of 0.001 with a 5.8 m long, 1.5 m wide, and 0.48 m deep recessed section that is filled with sediment. To get the fully developed turbulent flow, the sand bed recess and the center of the abutment model were located 13.75 m and 17.65 m downstream of the flume inlet, respectively. The recirculating flow for the flume was supplied from a constant-head water tank by a pump. At the downstream end of the flume, the flow was directed from the collecting tank to the laboratory return channel and then pumped to the water tank for the circulating flow system. Figure 3.1 and Figure 3.2 show a photograph of the flume and the schematic layout of the experimental setup, respectively. A tailgate was located at the downstream end of the flume to adjust the flow depths.

The flume channel bed was made of concrete, and roughened with the sediment particles having the same size as that were used in the recessed section by glueing these particles over the bed throughout the entire section in the flow direction except the working section. The discharge in the flume was measured with a sharp-crested rectangular weir having a width of 1.5 m and a height of 0.30 m mounted at the upstream section of the flume. Bricks and sheet-iron strainer were located at the upstream end of the flume to facilitate the development of the turbulent boundary layer on the channel bed. In order to have the fully developed turbulent flow, the screen provides friction to ensure the existence of the developed flow and serves for the elimination of turbulent eddies and surface waves at the entrance of the flume channel.



Figure 3.1 General view of the flume



Note : Dimensions are given in meter.

Figure 3.2 Schematic layout of the experimental setup

### 3.3 ABUTMENT MODEL

All the abutment models used for the experiments had semi-circular ends and were made of plexiglass. The width of the abutment models were kept constant in accordance with the earlier studies (Kayatürk 2005, Doğan 2008, Daşkın 2011). According to the studies of Oliveto and Hager (2002) and Kayatürk (2005), the effect of the streamwise abutment length,  $B_a$ , on the development of the scour hole is small and can be neglected. Therefore, the semi-circular end abutment models having a constant value of  $B_a=10$  cm were used in the experiments. Two different abutment lengths of  $L_a=15$  cm, and  $L_a=35$  cm were used and three different collar widths of  $B_c= 5.0, 7.5,$  and  $10.0$  cm were tested with each abutment in this study. The collar plates used in the experiments were made from plexiglass and have a thickness of 3 mm. In order to evaluate the efficiency of collars as a scour countermeasure for bridge abutments; the widths,  $B_c$ , and elevations,  $Z_c$ , of the collars attached to the abutments, as scour reducing paramaters, were changed in each experiment. Figure 3.3 shows a schematic illustration of an abutment model with all the related parameters used in this study.

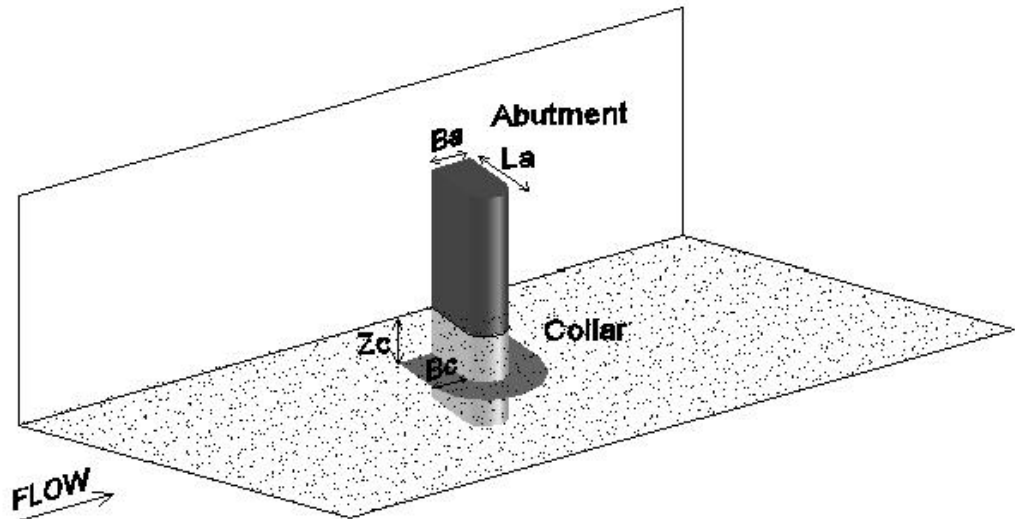


Figure 3.3 Schematic illustration of the abutment model

For each experimental run, the abutment model was embedded at the same location in the sediment recess of the flume, and attached to the glass sidewall of the flume channel which enables visual observation of the flow and development of scour forming around the abutment model. In Figures 3.4 to 3.8 some photographs of the abutment-collar arrangements tested in the experiments are shown below.



Figure 3.4 Abutment  $L_a=35$  cm with collar  $B_c=7.5$  cm at  $Z_c/y=0.00$ ,  $y=15.2$  cm



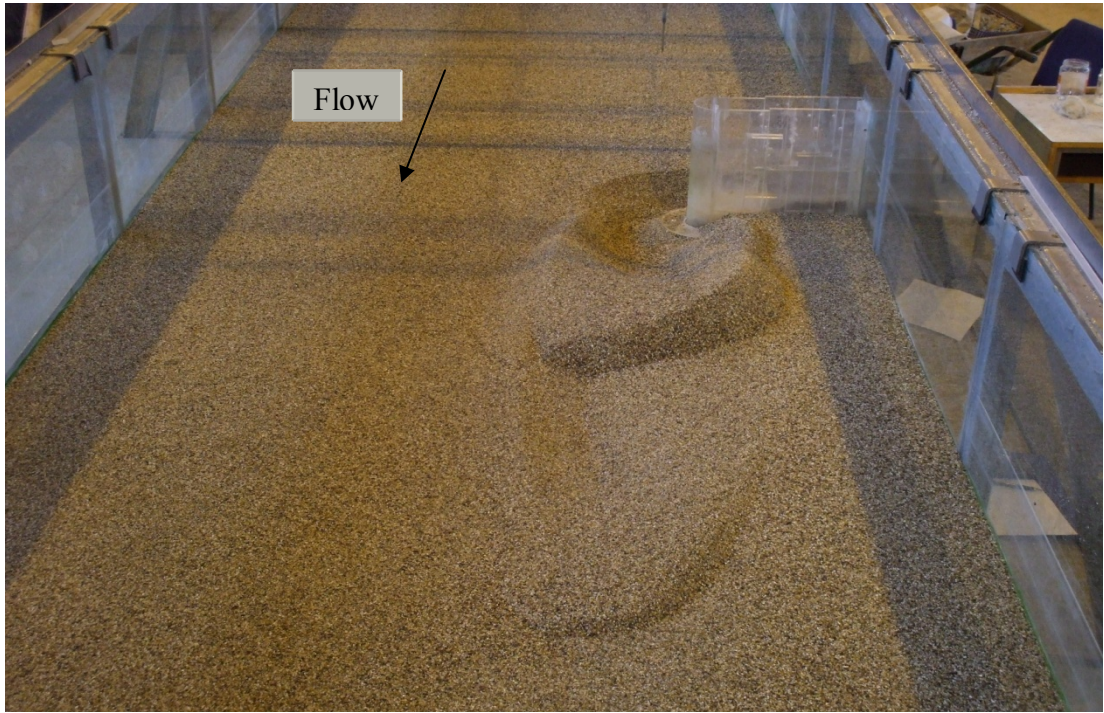


Figure 3.5 Abutment  $L_a=35$  cm with collar  $B_c=5.0$  cm at  $Z_c/y=-0.25$ ,  $y=17.4$  cm



Figure 3.6 Abutment  $L_a=35$  cm with collar  $B_c=10.0$  cm at  $Z_c/y=-0.50$ ,  $y=17.4$  cm



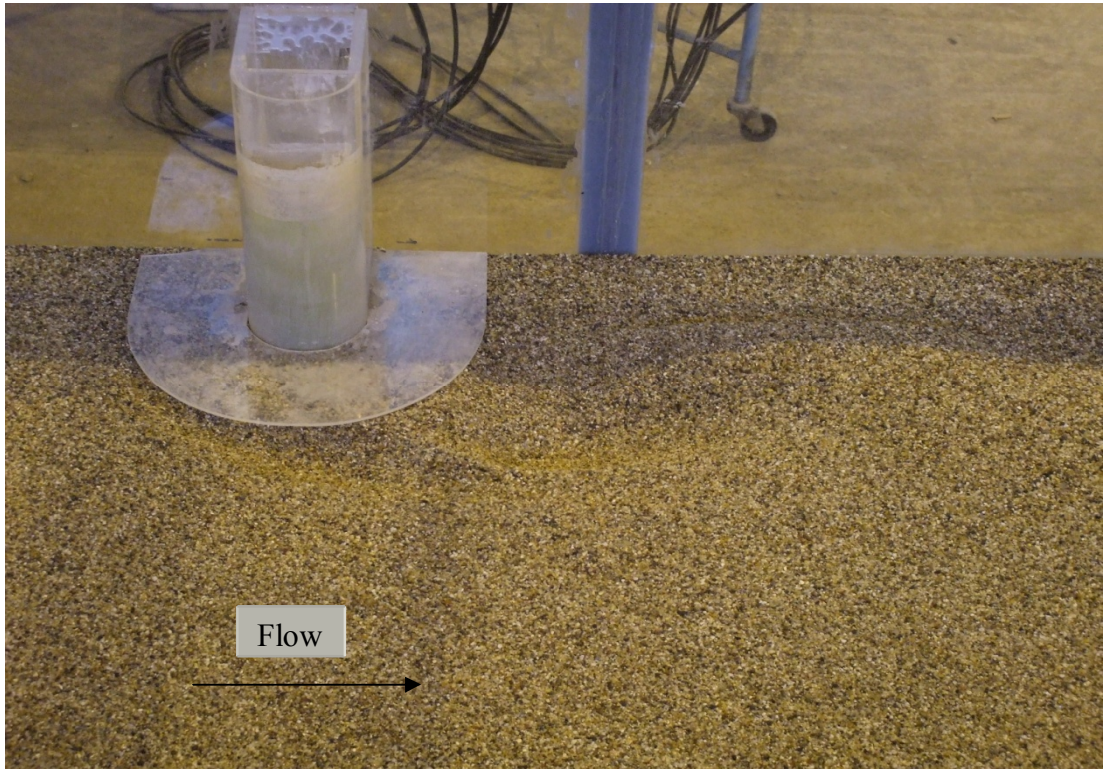


Figure 3.7 Abutment  $L_a=15$  cm with collar  $B_c=10.0$  cm at  $Z_c/y=0.00$ ,  $y=17.4$  cm



Figure 3.8 Abutment  $L_a=15$  cm with collar  $B_c=7.5$  cm at  $Z_c/y=-0.25$ ,  $y=15.2$  cm





Figure 3.9 Abutment  $L_a=15$  cm with collar  $B_c=5.0$  cm at  $Z_c/y=0.00$ ,  $y=15.2$  cm

### 3.4 SEDIMENT CHARACTERISTICS

The recessed section of the flume was filled with erodible sand bed material having a median grain size of  $d_{50}=1.50$  mm with a geometric standard deviation of the sediment size distribution ratio of  $\sigma_g=1.29$  and uniformity coefficient of  $C_u=1.7$ . Having these properties the bed material can be considered to be approximately uniform. According to the studies of Dongol (1994), the effect of sediment size become insignificant for large values of  $L_a/d_{50}$ , and in this study the values of  $L_a/d_{50}$  are 100 and about 233 for the abutment lengths of  $L_a=15$  cm and  $L_a=35$  cm, respectively. For a constant protrusion length of an abutment, the scour depth increases rapidly with sediment size to a peak at  $L_a/d_{50} > 50$  and then decreases (Ettama 1980, Gill 1970, Wong 1982, Kwan 1987, Kandasamy 1989). According to

this criterion, the effect of sediment size has negligible effect on the scour depth in this study.

### **3.5 FLOW CHARACTERISTICS**

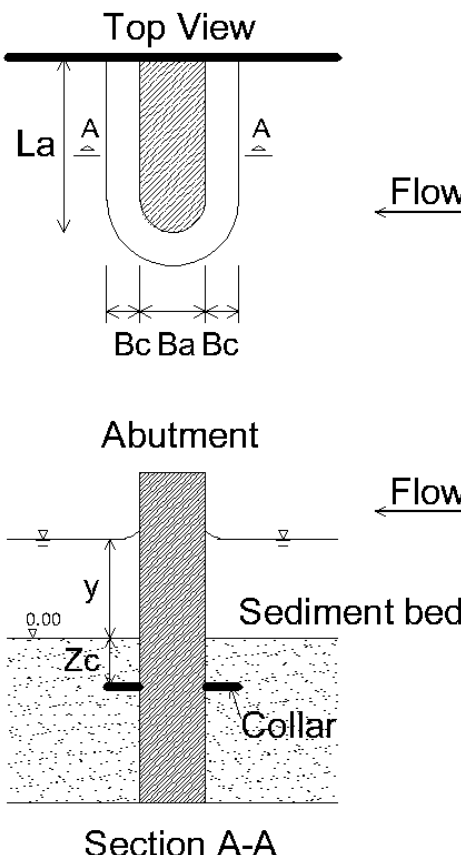
All experiments were conducted under clear-water flow conditions satisfying the velocity ratio of  $U/U_c < 1$ , where  $U$  is the average approaching flow velocity and  $U_c$  is the critical velocity for incipient motion of the bed material. For the discharge value of  $Q = 0.0678 \text{ m}^3/\text{s}$ , the critical water depth for the initiation of the sediment particles was observed at  $y = 12.1 \text{ cm}$ . For the experiments related with the application of collar at the abutments as a scour countermeasure, the  $U/U_c$  ratios were determined as 0.80 and 0.70, whereas the flow depths, calculated according to these ratios, were 15.2 cm and 17.4 cm, respectively. In addition to the flow intensity and the flow depth values, the Froude numbers corresponding to these two different flow depths were calculated as 0.24 and 0.48 for values of  $y = 15.2 \text{ cm}$  and  $y = 17.4 \text{ cm}$ , respectively. Moreover, for the experiments related with the temporal variation of scour without application of collars at the abutments, two different  $U/U_c$  ratios were used as a measure of the flow intensity. The  $U/U_c$  ratios were determined as 0.90 and 0.70 for these experimental runs for the same discharge of  $Q = 0.0678 \text{ m}^3/\text{s}$  and the corresponding flow depths were calculated as  $y = 13.5 \text{ cm}$  and  $y = 17.4 \text{ cm}$ , respectively. Accordingly, the Froude numbers were 0.29 for the flow depth of  $y = 13.5 \text{ cm}$ , and 0.48 for the flow depth of  $y = 17.4 \text{ cm}$ .

### **3.6 MEASUREMENTS AND INSTRUMENTATION**

The abutment model was first placed in the recessed section of the laboratory flume. For the experiments with the collar in place, it was also attached to the abutment at three different elevations on the abutments ( $Z_c$ ) as; at the bed level, 3.8 cm and 7.6 cm below the bed level for the flow depth of  $y = 15.2 \text{ cm}$ ; besides at the bed level, 4.35 cm and 8.7 cm below the bed level for the flow depth of  $y = 17.4 \text{ cm}$ .

The elevations of the collars tested in the experiments were determined in accordance with the ratios of  $Z_c/y=\pm 0.00$ ,  $Z_c/y=-0.25$  and  $Z_c/y=-0.50$ , where  $y$  denotes the depth of flow in the flume. The experimental arrangements of abutments and collars used in the tests are given in Table 3.1. Before each experiment, the sediment bed was levelled carefully in order to have a uniform bed surface.

Table 3.1 Experimental arrangements of abutments and collars

| Abutment- collar arrangement   | <b><math>Z_c/y=\pm 0.00, -0.25, -0.50</math></b><br>(with respect to the sediment bed) |            |           |      |            |
|--|--|------------|-----------|------|------------|
|  | Type   | La<br>(cm) | y<br>(cm) | Case | Bc<br>(cm) |
|  <p>Top View</p> <p>Flow</p> <p>La</p> <p>A</p> <p>Bc Ba Bc</p> <p>Abutment</p> <p>Flow</p> <p>Sediment bed</p> <p>Collar</p> <p>Section A-A</p> | 1  | 15         | 17.4      | a    | 5.0        |
|  |  |            |           | b    | 7.5        |
|  |  |            |           | c    | 10.0       |
|  | 2  | 15         | 15.2      | a    | 5.0        |
|  |  |            |           | b    | 7.5        |
|  |  |            |           | c    | 10.0       |
|  | 3  | 35         | 17.4      | a    | 5.0        |
|  |  |            |           | b    | 7.5        |
|  |  |            |           | c    | 10.0       |
|  | 4  | 35         | 15.2      | a    | 5.0        |
|  |  |            |           | b    | 7.5        |
|  |  |            |           | c    | 10.0       |

At the beginning of the experiment, the flume was filled with water very slowly without disturbing the levelled surface of the sediment bed. The water level in the flume was raised gradually by adjusting the tailgate, located at the downstream end of the flume, until the water depth was reached to the desired values to satisfy the required velocity ratios of  $U/U_c$  which were 0.90, 0.80 and 0.70 respectively. The same discharge of  $Q=0.0678 \text{ m}^3/\text{s}$  were used in all the experiments. After the required flow depths corresponding to the flow intensity values were achieved, the experiment was started.

For the experiments related with the application of collar at the abutments, 3-hour continuous run under clear-water scour conditions were performed for abutment lengths of  $L_a=15 \text{ cm}$  and  $L_a=35 \text{ cm}$ . The maximum scour depth and the scour formation around the abutment model were investigated at the end of each run. After the completion of each experiment, the flume was slowly drained without disturbing the scour formation. Thereafter, the maximum scour depth was gauged; also the sketches of the scour profiles were recorded for each test. The data related to these experimental results are given in Chapter 4. The maximum scour depth at the abutment was measured by a point gauge with an accuracy of  $\pm 0.1 \text{ mm}$ . The point gauge was mounted on a mobile cart on top of the flume, where it was moved manually along and across the flume section and used to measure the depths of scour and deposition around the abutment model. Moreover, a 3-dimensional bathymetry of the sand bed around the abutment model was investigated at the end of 3-hour continuous run under clear-water scour condition. The sediment recess of the flume was scanned to obtain the formation of scour hole and deposition around the abutment by an acoustic device with an accuracy of  $\pm 0.1 \text{ mm}$  (SeaTek 5 MHz Ultrasonic Ranging System). A photograph of the device is shown in Figure 3.10.



Figure 3.10 Seatek Ultrasonic Ranging System

In this study, the 3-dimensional bathymetry of the sediment bed was obtained only once for the abutment length of  $L_a=35$  cm without attaching a collar at a flow depth of  $y=17.4$  cm. At the end of the experiment, the bed levels at the upstream, downstream zones and around the abutment face were measured with transducer probes which were slightly submerged in the water. Figure 3.11 shows a photograph of the submerged transducer probes of the aquistic device. After scanning of the sediment bed, the depths of scour and deposition were obtained. Then, these depths were non-dimensionalized by dividing with the flow depth of  $y=17.4$  cm. The results of these experimental investigations related with the bathymetry of the sediment bed and the application of collars at abutments are given in Chapter 4.



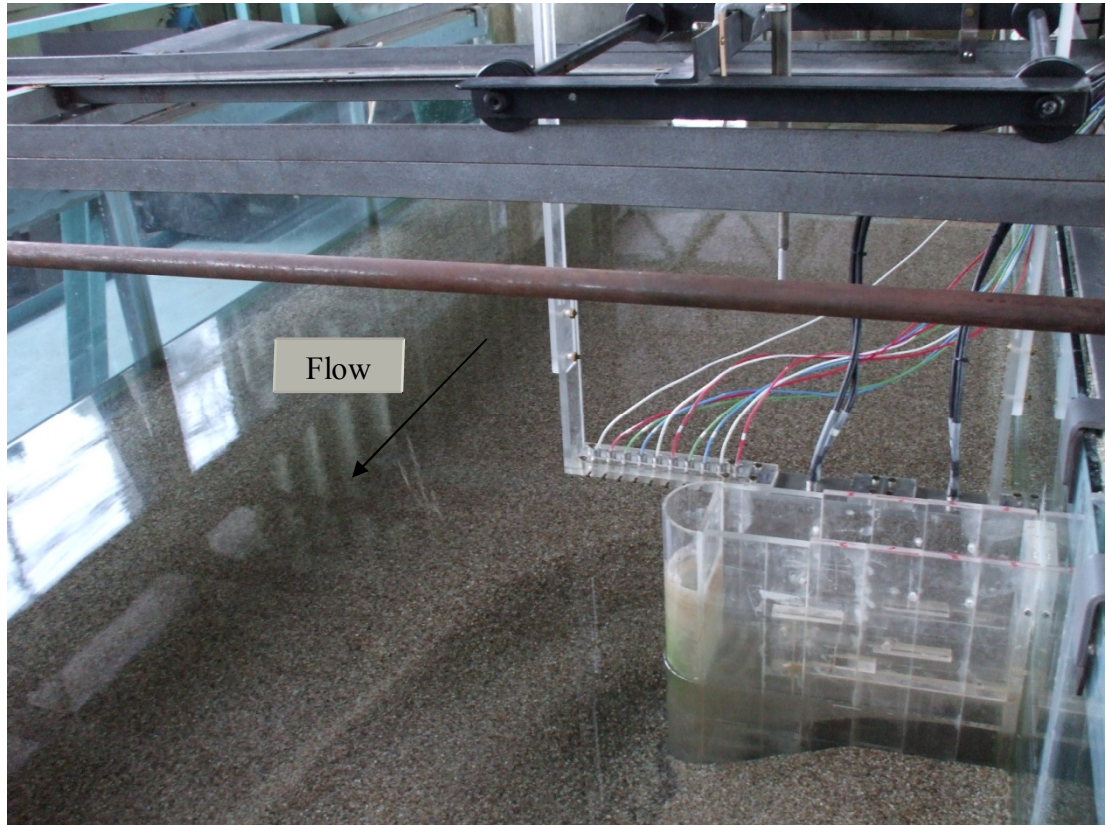


Figure 3.11 Acoustic device used in the experiments

Furthermore, the temporal variations of the scour hole forming around the abutment without a collar were obtained by performing 8-hour continuous runs under clear-water conditions. These experiments were conducted for the abutment lengths of  $L_a=15$  cm and  $L_a=35$  cm without a collar and for the flow depths of  $y=13.5$  cm and  $y=17.4$  cm. During these experiments the acoustic device mentioned above was used to record the temporal development of the scour hole around the abutments by locating the transducer probes at the prescribed locations of the scour and deposition zones around the abutment model. At the end of 8-hour continuous runs, the changes in the scour pattern with time were investigated for two different abutment lengths at two different water depths. The related data, details and results of these experiments are given in Chapter 5. At the end of each experiment, the flume was carefully drained and sediment bed was levelled and compacted with a steel plate that could slide over the rails mounted on the sidewalls of the flume.

## CHAPTER 4

### EFFECT OF FLOW DEPTH ON LOCAL SCOUR AT BRIDGE ABUTMENTS

#### 4.1 GENERAL

The main objective of this chapter is to investigate the effects of flow depth and collars, attached to the semi-circular end abutment models, on the development of local scour around bridge abutments under clear-water flow conditions. The results of the experimental investigations were compared with the data obtained by previous studies of Kayatürk's (2005), Doğan's (2008), and Daşkın's (2011) and the effect of flow depth on the performance of collars against abutment scour was analysed.

#### 4.2 DIMENSIONAL ANALYSIS

The dimensional analysis of the maximum scour depth  $(d_s)_{\max,c}$  at an abutment attached with a collar presented in this study is similar with the one given in Kayatürk's (2005) study. For clear-water scour conditions, the maximum scour depth at an abutment with a collar is a function of the following parameters:

$$(d_s)_{\max,c} = f \left\{ L_a, B_a, B_c, B, Z_c, T_c, U, y, S_0, g, \right. \\ \left. \rho_s, \rho, \mu, d_{50}, \sigma_g, t \right\} \quad (4.1)$$



where  $L_a$ =protrusion length of abutment,  $B_a$ =abutment width,  $B_c$ =collar width,  $B$ =channel width,  $Z_c$ =elevation of the collar with respect to the sand bed level,  $T_c$ =collar thickness,  $U$ =mean approach flow velocity,  $y$ =approach flow depth,  $S_0$ =slope of the channel,  $g$ =gravitational acceleration,  $\rho_s$ =density of the sediment,  $\rho$ =density of the fluid,  $\mu$ =dynamic viscosity of the fluid,  $d_{50}$ =median particle grain size,  $\sigma_g$ =geometric standard deviation of sediment size distribution, and  $t$ =time. Figure 4.1 shows a schematic illustration of the collar-abutment arrangement with the related parameters.

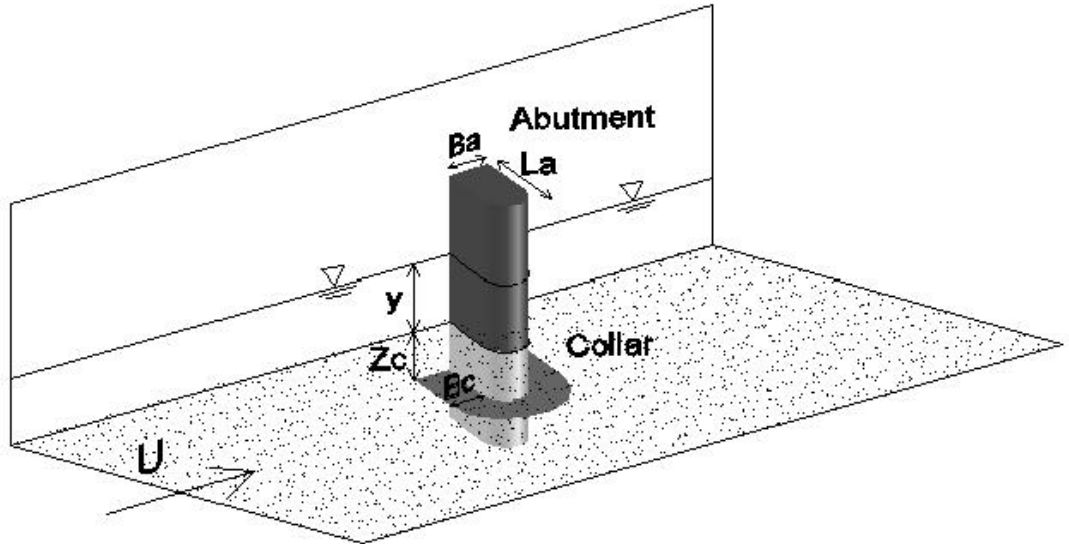


Figure 4.1 Schematic illustration of the collar-abutment arrangement

Using the Buckingham's  $\pi$  theorem, the maximum scour depth at an abutment with collar,  $(d_s)_{\max,c}$ , can be expressed in a non-dimensional form as:

$$\frac{(d_s)_{\max,c}}{y} = f \left\{ \frac{L_a}{y}, \frac{B_a}{y}, \frac{B_c}{y}, \frac{Z_c}{y}, \frac{T_c}{y}, \frac{\rho_s}{\rho}, \frac{U}{\sqrt{gy}}, \frac{B}{y}, \frac{\mu}{Uy\rho}, \frac{Ut}{y}, S_0, \sigma_g, \frac{d_{50}}{y} \right\} \quad (4.2)$$

Similar to the studies of Kayatürk's (2005), Doğan's (2008), and Daşkın's (2011), the experiments of this study were performed with one sediment size and constant channel bed slope, where channel width, collar thickness, abutment width, duration of the experiment, and discharge were kept constant. However, in this study apart from the previous ones, the experiments were conducted at two different approach flow depths corresponding to two different flow intensities,  $U/U_c$ . By replacing  $L_a/y$  by  $L_a/B$ ,  $B_c/y$  by  $L_a/B_c$  and  $U/\sqrt{gy}$  by  $U/U_c$  since the flow intensity includes the sediment properties, and also neglecting the viscous effects Equation (4.2) can be simplified as:

$$\frac{(d_s)_{\max,c}}{y} = f\left(\frac{L_a}{B_c}, \frac{Z_c}{y}, \frac{L_a}{B}, \frac{U}{U_c}\right) \quad (4.3)$$

where the scour depth is normalized with the flow depth.

The reduction in the scour depth around the bridge abutments with collars, with respect to the scour depth without collar application at abutments can be expressed as:

$$\frac{(d_s)_{\max} - (d_s)_{\max,c}}{(d_s)_{\max}} = f\left(\frac{L_a}{B_c}, \frac{Z_c}{y}, \frac{L_a}{B}, \frac{U}{U_c}\right) \quad (4.4)$$

where  $(d_s)_{\max}$  represents the maximum scour depth around the bridge abutments without collar application.

Within the scope of this study, the experiments were conducted for the Froude number,  $Fr = U/\sqrt{gy} = 0.24$ , and the Reynolds number,  $Re = (U\rho y)/\mu = 45296$  for the flow intensity of  $U/U_c = 0.80$ ; and for  $Fr = 0.48$ , and  $Re = 45240$  for the flow intensity of  $U/U_c = 0.70$ , where  $\mu \approx 1 \times 10^{-3} \text{ N}\cdot\text{sec}/\text{m}^2$ ,  $\rho \approx 1000 \text{ kg}/\text{m}^3$ .

## 4.3 DISCUSSION OF RESULTS

### 4.3.1 Application of Collars around the Bridge Abutment Models

In this study, 34 experiments were conducted under clear-water scour conditions for a period of 3 hours. The experiments were carried out with semi-circular end abutment models of  $L_a=15$  cm and  $L_a=35$  cm with and without a collar. In the experimental investigations including the collar application as a scour countermeasure, collars of  $B_c=5.0$  cm, 7.5 cm, and 10.0 cm were placed at three different elevations on the abutment models. The experiments for the abutment length of  $L_a=15$  cm with the collars of  $B_c=5.0$  cm, 7.5 cm, and 10.0 cm at  $Z_c/y=-0.50$  for two different approach flow depths of  $y=15.2$  cm and  $y=17.4$  cm have not been performed. The reason is that the maximum scour depths without a collar around the abutment were above the collar elevation of  $Z_c/y=-0.50$ . Therefore, there is no sense or need to locate the collars below these maximum scour depths. Furthermore, four experiments were conducted with the same abutment models without a collar at two different flow depths as stated above, to get the maximum scour depths around the abutments for the same time interval.

The results of all the experimental investigations performed with the abutment models with and without collars are given in Table 4.1. In this table, the data related to the abutment model, collar and flow properties as well as the maximum scour depths and the reduction in the maximum scour depths are presented. In Table 4.1,  $(d_s)_{\max}$  denotes the maximum scour depth around the abutment model without a collar, and  $(d_s)_{\max,c}$  represents the maximum scour depth around the abutment model with collars attached to the abutments at different elevations. The percent reductions in the maximum scour depth obtained with collars are presented in the last column of the table.

Table 4.1 Experimental data for  $Q=0.0678 \text{ m}^3/\text{s}$  and  $B_a=10 \text{ cm}$  at flow intensities of  $U/U_c=0.70$  ( $y=17.4 \text{ cm}$ ) and  $U/U_c=0.80$  ( $y=15.2 \text{ cm}$ )

| Run no     | La<br>(cm) | Bc<br>(cm) | La/Bc | La/B | Zc<br>(cm) | y<br>(cm) | Zc/y  | $\Theta$ | (ds)max<br>(cm) | (ds)max,c<br>(cm) | % Reduction in max.<br>scour depth |
|------------|------------|------------|-------|------|------------|-----------|-------|----------|-----------------|-------------------|------------------------------------|
| <b>R1</b>  | 15.0       | 5.0        | 3.0   | 0.10 | 0.00       | 17.4      | 0.00  | 2.56     | 5.8             | 4.32              | <b>25.5%</b>                       |
| <b>R2</b>  | 15.0       | 5.0        | 3.0   | 0.10 | -4.35      | 17.4      | -0.25 |          | 5.8             | 4.35              | 25.0%                              |
| <b>R3</b>  | 15.0       | 7.5        | 2.0   | 0.10 | 0.00       | 17.4      | 0.00  | 3.56     | 5.8             | 4.30              | <b>25.9%</b>                       |
| <b>R4</b>  | 15.0       | 7.5        | 2.0   | 0.10 | -4.35      | 17.4      | -0.25 |          | 5.8             | 4.35              | 25.0%                              |
| <b>R5</b>  | 15.0       | 10.0       | 1.5   | 0.10 | 0.00       | 17.4      | 0.00  | 4.69     | 5.8             | 4.00              | <b>31.0%</b>                       |
| <b>R6</b>  | 15.0       | 10.0       | 1.5   | 0.10 | -4.35      | 17.4      | -0.25 |          | 5.8             | 4.35              | 25.0%                              |
| <b>R7</b>  | 15.0       | 5.0        | 3.0   | 0.10 | 0.00       | 15.2      | 0.00  | 2.56     | 7.2             | 4.60              | 36.1%                              |
| <b>R8</b>  | 15.0       | 5.0        | 3.0   | 0.10 | -3.80      | 15.2      | -0.25 |          | 7.2             | 3.80              | <b>47.2%</b>                       |
| <b>R9</b>  | 15.0       | 7.5        | 2.0   | 0.10 | 0.00       | 15.2      | 0.00  | 3.56     | 7.2             | 5.20              | 27.8%                              |
| <b>R10</b> | 15.0       | 7.5        | 2.0   | 0.10 | -3.80      | 15.2      | -0.25 |          | 7.2             | 3.80              | <b>47.2%</b>                       |
| <b>R11</b> | 15.0       | 10.0       | 1.5   | 0.10 | 0.00       | 15.2      | 0.00  | 4.69     | 7.2             | 5.10              | 29.2%                              |
| <b>R12</b> | 15.0       | 10.0       | 1.5   | 0.10 | -3.80      | 15.2      | -0.25 |          | 7.2             | 3.80              | <b>47.2%</b>                       |
| <b>R13</b> | 35.0       | 5.0        | 7.0   | 0.23 | 0.00       | 17.4      | 0.00  | 2.23     | 11.3            | 7.20              | <b>36.3%</b>                       |
| <b>R14</b> | 35.0       | 5.0        | 7.0   | 0.23 | -4.35      | 17.4      | -0.25 |          | 11.3            | 7.60              | 32.7%                              |
| <b>R15</b> | 35.0       | 5.0        | 7.0   | 0.23 | -8.70      | 17.4      | -0.50 |          | 11.3            | 9.10              | 19.5%                              |
| <b>R16</b> | 35.0       | 7.5        | 4.7   | 0.23 | 0.00       | 17.4      | 0.00  | 2.93     | 11.3            | 7.20              | <b>36.3%</b>                       |
| <b>R17</b> | 35.0       | 7.5        | 4.7   | 0.23 | -4.35      | 17.4      | -0.25 |          | 11.3            | 7.40              | 34.5%                              |
| <b>R18</b> | 35.0       | 7.5        | 4.7   | 0.23 | -8.70      | 17.4      | -0.50 |          | 11.3            | 10.10             | 10.6%                              |
| <b>R19</b> | 35.0       | 10.0       | 3.5   | 0.23 | 0.00       | 17.4      | 0.00  | 3.69     | 11.3            | 5.70              | <b>49.6%</b>                       |
| <b>R20</b> | 35.0       | 10.0       | 3.5   | 0.23 | -4.35      | 17.4      | -0.25 |          | 11.3            | 8.70              | 23.0%                              |
| <b>R21</b> | 35.0       | 10.0       | 3.5   | 0.23 | -8.70      | 17.4      | -0.50 |          | 11.3            | 9.30              | 17.7%                              |
| <b>R22</b> | 35.0       | 5.0        | 7.0   | 0.23 | 0.00       | 15.2      | 0.00  | 2.23     | 16.0            | 13.00             | 18.8%                              |
| <b>R23</b> | 35.0       | 5.0        | 7.0   | 0.23 | -3.80      | 15.2      | -0.25 |          | 16.0            | 11.00             | 31.3%                              |
| <b>R24</b> | 35.0       | 5.0        | 7.0   | 0.23 | -7.60      | 15.2      | -0.50 |          | 16.0            | 10.50             | <b>34.4%</b>                       |
| <b>R25</b> | 35.0       | 7.5        | 4.7   | 0.23 | 0.00       | 15.2      | 0.00  | 2.93     | 16.0            | 11.20             | 30.0%                              |
| <b>R26</b> | 35.0       | 7.5        | 4.7   | 0.23 | -3.80      | 15.2      | -0.25 |          | 16.0            | 11.00             | 31.3%                              |
| <b>R27</b> | 35.0       | 7.5        | 4.7   | 0.23 | -7.60      | 15.2      | -0.50 |          | 16.0            | 10.00             | <b>37.5%</b>                       |
| <b>R28</b> | 35.0       | 10.0       | 3.5   | 0.23 | 0.00       | 15.2      | 0.00  | 3.69     | 16.0            | 10.10             | 36.9%                              |
| <b>R29</b> | 35.0       | 10.0       | 3.5   | 0.23 | -3.80      | 15.2      | -0.25 |          | 16.0            | 10.10             | 36.9%                              |
| <b>R30</b> | 35.0       | 10.0       | 3.5   | 0.23 | -7.60      | 15.2      | -0.50 |          | 16.0            | 9.60              | <b>40.0%</b>                       |

The results of the experimental investigations of local scour at bridge abutment models with and without collars are presented in the following sections:

#### **4.3.1.1 The Abutment of $L_a = 15$ cm at the Flow Depth of $y = 17.4$ cm (Experiments R1~R6)**

The maximum scour reductions for three different collar widths are observed when the collars are placed at  $Z_c/y = \pm 0.00$ . The experimental results show that for  $L_a = 15$  cm and  $y = 17.4$  cm, the scour formation does not penetrate below the collars when they are attached to the abutment models at an elevation of  $Z_c/y = -0.25$ . Since the maximum scour depths occur at the elevation of the collars, it is observed that the scour reduction performances of the collars do not change with the width of the collars, when they are placed at  $Z_c/y = -0.25$ . Although the collar width does not affect the maximum scour reductions at  $Z_c/y = -0.25$ , when collars are placed at  $Z_c/y = \pm 0.00$ , the best performance is observed for the collar of  $B_c = 10$  cm.

When the scour formations around the abutment models for three different collar widths at  $Z_c/y = \pm 0.00$  are compared, the maximum scour depth is observed at the toe of the abutment model with collar of  $B_c = 5$  cm; while for the abutments with collars of  $B_c = 7.5$  cm and  $B_c = 10$  cm, the maximum scour depths are located at the downstream end of the abutment models. This result shows that the similar tendency is observed with respect to the location of the maximum scour depths for the collars of  $B_c = 7.5$  cm and  $B_c = 10$  cm at  $Z_c/y = \pm 0.00$ .

The bed material is swept away at the downstream of the abutment model in all of the experiments. The deposition patterns are resulted in a longer distance from the abutment for the cases with collars at  $Z_c/y = \pm 0.00$ ; whereas deposition formations are observed in a closer region around the abutment model for the cases with collars at  $Z_c/y = -0.25$ . However, only for the abutment model with collar of  $B_c = 7.5$  cm at  $Z_c/y = -0.25$ , it is observed that there exists another scour formation apart from the one which is formed around the abutment model. This secondary scour formation is relatively small with respect to the primary scour formation including the maximum scour depth.

This secondary scour hole is formed just downstream of the deposition formation located at the downstream of the abutment model. In this region the scour depth is measured as 1.3 cm and it is surrounded by a deposition pattern having relatively small height compared with the major deposition pattern close to the abutment model (see Figure 4.10a for similar type of scour formation).

Among the experiments the maximum collar efficiency is observed at the elevation of  $Z_c/y=\pm 0.00$  for the collar of  $B_c=10$  cm. Moreover, this result is the most efficient collar configuration similar to the one concluded in Daşkın's (2011) study. However, the scour reduction performances of collars tested in this study are lower than the observations in Daşkın's (2011) study for the abutment of  $L_a=15$  cm.

#### **4.3.1.2 The abutment of $L_a=15$ cm at the Flow Depth of $y=15.2$ cm (Experiments R7~R12)**

The best collar performances are obtained at  $Z_c/y=-0.25$  for the three different collar widths tested with the abutment models of  $L_a=15$  cm at the flow depth of  $y=15.2$  cm. This result shows that for the same abutment of  $L_a=15$  cm, the maximum scour reductions are obtained at different collar elevations of  $Z_c/y$  for the two different  $U/U_c$  ratios. As the flow depth decreases, the maximum scour reduction efficiencies of collars occur when they are placed below the sand bed level. However, according to the results obtained in Daşkın's (2011) study, the maximum scour reduction was observed for the abutment of  $L_a=15$  cm when collar is placed at an elevation of  $Z_c/y=\pm 0.00$ . In the experimental investigations of Daşkın's (2011) study, the abutment models were tested with collars at a higher  $U/U_c$  ratio where the flow depth was  $y=13.5$  cm. Therefore, it can be concluded that as the flow depth decreases below a certain threshold value, the maximum scour reduction efficiencies of collars occur at  $Z_c/y=\pm 0.00$ .

In this part, the maximum scour reductions are observed at the same elevation of collars for the three different collar widths. Thus, it can be noticed that when collars are attached at an elevation of  $Z_c/y=-0.25$ , scour does not penetrate below the collars regardless of their widths,  $B_c$ . Although the maximum scour reductions are the same for the cases of collars at  $Z_c/y=-0.25$ ; when they are placed at an elevation of  $Z_c/y=\pm 0.00$ , the best scour reduction is observed for the collar of  $B_c=5$  cm.

According to the experimental results, it is also observed that the formation of scour and deposition patterns around the abutment model are similar in the case of collars of  $B_c=7.5$  cm and  $B_c=10$  cm such that there is a secondary scour hole formation at the downstream of the deposition pattern formed around the abutment. This scour formation is similar to the one observed for the same abutment length with collar of  $B_c=7.5$  cm placed at  $Z_c/y=-0.25$  at the flow depth of  $y=17.4$  cm. However, this scour formation does not occur when the collar of  $B_c=5$  cm applied to the abutment at the flow depth of  $y=15.2$  cm. When the collars of  $B_c=7.5$  cm and  $B_c=10$  cm are placed at  $Z_c/y=\pm 0.00$  and  $Z_c/y=-0.25$ , the depths of the secondary scour holes are measured for these four cases approximately as 1~2 cm which are close to the depth of scour hole observed in the previously stated case for  $L_a=15$  cm (see Figure 3.8).

#### **4.3.1.3 The abutment of $L_a = 35$ cm at the Flow Depth of $y = 17.4$ cm (Experiments R13~R21)**

The maximum scour reductions are obtained at  $Z_c/y=\pm 0.00$ , for the collars of  $B_c= 5, 7.5, 10$  cm tested with the abutment model of  $L_a=35$  cm at  $y=17.4$  cm. This result shows that for the same flow depth of  $y=17.4$  cm, the maximum scour reductions occur at the same collar elevation of  $Z_c/y$  for two different abutments of  $L_a=15$  cm and  $L_a=35$  cm. For the three different collar widths, the scour reduction efficiencies of collars decrease when they are placed deeper below the sand bed level. As the elevations of collars  $Z_c/y$  decrease, the scour reduction performances of collars show a decreasing trend.

According to the experimental results, it is observed that the maximum scour reduction efficiencies of collars of  $B_c = 5$  cm and  $B_c = 7.5$  cm are equal to each other at  $Z_c/y = \pm 0.00$ . Among the experiments, the best collar performance is obtained at the elevation of  $Z_c/y = \pm 0.00$  for the collar of  $B_c = 10$  cm. Daşkın (2011) obtained similar results such that the same collar width gives the maximum scour reduction for the abutment of  $L_a = 35$  cm. However, according to the results of the experimental study, Daşkın (2011) observed the maximum collar efficiency at the elevation of  $Z_c/y = -0.25$  for the collar of  $B_c = 10$  cm. Moreover, it should be noticed that Daşkın (2011) obtained the maximum collar efficiencies for the collars of  $B_c = 5$  cm and  $B_c = 7.5$  cm at  $Z_c/y = -0.50$  which are different from the results observed in this study for the same collar widths. In addition, it should be also noted that the scour reduction performances of collars tested in this study are higher than the observations obtained in Daşkın's (2011) study for the abutment of  $L_a = 35$  cm.

When the scour formations around the abutment models for three different collar widths are compared, the maximum scour depth is generally observed at the downstream part of the abutment toe except the two cases. These are observed for the collar of  $B_c = 5$  cm at  $Z_c/y = \pm 0.00$  and  $Z_c/y = -0.25$ . In these two cases, the maximum scour depths are observed at the upstream part of the abutment toe which differs from the other cases.

During scour formation, the sand bed material is swept away towards the downstream of the abutment. The deposition patterns have almost similar trends for all the cases. However, it should be noticed that in all the experiments conducted with three different collar widths placed at three different elevations, a secondary scour hole formation is observed at the downstream of the abutment model. This scour formation is similar with the ones resulted in the experiments carried out for the abutment model of  $L_a = 15$  cm. The depths of these scour holes for the case of  $L_a = 35$  cm are also relatively small with respect to the main scour formations obtained around the abutment model as observed in the previously reported cases with the abutment model of  $L_a = 15$  cm.



For the case of  $L_a=35$  cm, the scour depths are measured approximately as 3~4.5 cm which are greater than the previous cases. These scour holes are observed about 1 m downstream of the abutment model. It should be also noticed that a deposition formation occurs around this scour pattern having a smaller height with respect to the deposition formed close to the abutment model (see Figure 3.5 and Figure 3.6).

#### **4.3.1.4 The abutment of $L_a = 35$ cm at the Flow Depth of $y = 15.2$ cm (Experiments R22~R30)**

The maximum scour reductions for all three collar widths are observed when the collars are placed to the abutment model at  $Z_c/y=-0.50$ . It can be noticed that for the same abutment of  $L_a=35$  cm, the maximum scour reduction performances of collars change with respect to their elevations of  $Z_c/y$  for two different flow depths. The scour reduction performances of collars are higher at  $Z_c/y=\pm 0.00$  when they are tested at a flow depth of  $y=17.4$  cm. When the results of these experimental investigations are compared with the results of Daşkın's (2011) study, it can be concluded that for the abutment of  $L_a=35$  cm, as the flow depth decreases, the decrease in the elevation of collars below the bed level mostly leads to higher scour reduction efficiencies.

It can be noted that as the elevations of collars  $Z_c/y$  decrease, the scour reduction performances of collars show an increasing trend. According to the experimental results, it can be concluded that the best collar performance for the abutment of  $L_a=35$  cm at the flow depth of  $y=15.2$  cm is obtained with the collar of  $B_c=10$  cm placed at  $Z_c/y=-0.50$ .

It can also be noticed that the scour reduction performances of collars tend to increase with the increase in the collar widths. Daşkın (2011) obtained a similar result for the maximum scour reduction performances of collars with respect to the collar width.

According to the results of Daşkın's (2011) study, the maximum collar efficiency was obtained for the abutment of  $L_a=35$  cm with the collar of  $B_c= 10$  cm. Moreover, it was also observed that the maximum scour reductions increase with the increase in the collar widths which is similar with the results of this study.

When the scour and deposition formations are considered for the case of  $L_a=35$  cm at the flow depth of  $y=15.2$  cm, a formation of secondary scour hole does not exist in all the cases of the tests conducted with three different collar widths. However, for the same abutment length at the flow depth of  $y=17.4$  cm, this formation was present in all the sets of the experiments.

In Daşkın's (2011) study, when the scour formations around the abutment of  $L_a=35$  cm are considered, there exists only one scour hole which is close to the abutment model in all the sets of collars tested. Therefore, it can be concluded that as the flow depth decreases which corresponds to the increase in the flow velocity, the secondary scour formation does not occur at the downstream of the abutment models. Table 4.2 shows the cases of the experiments in which the secondary scour formation exists.

Table 4.2 List of the experiments where the secondary scour hole is observed

| <b>La<br/>(cm)</b> | <b>Bc<br/>(cm)</b> | <b>Zc<br/>(cm)</b> | <b>y<br/>(cm)</b> | <b>Zc/y</b> |
|--------------------|--------------------|--------------------|-------------------|-------------|
| 15                 | 7.5                | -4.35              | 17.4              | -0.25       |
| 15                 | 7.5                | 0.00               | 15.2              | 0.00        |
| 15                 | 7.5                | -3.80              | 15.2              | -0.25       |
| 15                 | 10                 | 0.00               | 15.2              | 0.00        |
| 15                 | 10                 | -3.80              | 15.2              | -0.25       |
| 35                 | 5                  | 0.00               | 17.4              | 0.00        |
| 35                 | 5                  | -4.35              | 17.4              | -0.25       |
| 35                 | 5                  | -8.70              | 17.4              | -0.50       |
| 35                 | 7.5                | 0.00               | 17.4              | 0.00        |
| 35                 | 7.5                | -4.35              | 17.4              | -0.25       |
| 35                 | 7.5                | -8.70              | 17.4              | -0.50       |
| 35                 | 10                 | 0.00               | 17.4              | 0.00        |
| 35                 | 10                 | -4.35              | 17.4              | -0.25       |
| 35                 | 10                 | -8.70              | 17.4              | -0.50       |

#### 4.3.2 Comparison of Scour for Various Collar Applications

The experimental results related to the effects of abutment length, collar width, collar elevation and flow depth on the reduction of maximum scour depth at abutments are given in Figure 4.2. In Figure 4.3, the results of Daşkın's (2011) study on the reduction of maximum scour depth at abutments are presented. According to the results of this study, it can be observed that the maximum value of the percent reduction of scour depth among all the experiments is obtained for  $L_a/B_c=3.5$  when the collar of  $B_c=10$  cm is tested at  $Z_c/y=\pm 0.00$  at the flow depth of  $y=17.4$  cm.

In Figure 4.2, it can be seen that for  $L_a/B_c \leq 3$ , the maximum reductions in scour depths are obtained at different  $Z_c/y$  values for the two flow depths. The maximum scour reduction performances of collars were obtained at the bed level for the flow depth of  $y=17.4$  cm, whereas the maximum scour reductions occur at  $Z_c/y=-0.25$  when the collars are tested at  $y=15.2$  cm.

According to Figure 4.3, it can be observed that for the same abutment length of  $L_a=15$  cm, the maximum scour reductions are obtained at  $Z_c/y=\pm 0.00$  except one data point for  $L_a/B_c \leq 3.0$ . Therefore, it can be concluded that as the flow depth decreases which corresponds to the increase in flow velocity, the locations of collars providing the maximum scour reductions fluctuate between the bed level and  $Z_c/y=-0.25$ .

Daşkın (2011) observed that for  $L_a/B_c$  values between 1.5 and 3.0, the scour reduction performances of collars increase with the increase in collar width. Likewise, for the same range of  $L_a/B_c$ , a similar trend can be observed in this study for the flow depth of  $y=17.4$  cm. At this flow depth, the scour reduction performance of collars increases with the increase in the collar width similar to Daşkın's (2011) observations. However, for the same range of  $L_a/B_c$ , such a trend cannot be observed in this study for the flow depth of  $y=15.2$  cm. The maximum scour reductions of collars are the same when they are tested at  $y=15.2$  cm. This is because the scour penetrates down to the collar level and cannot exceed this depth.

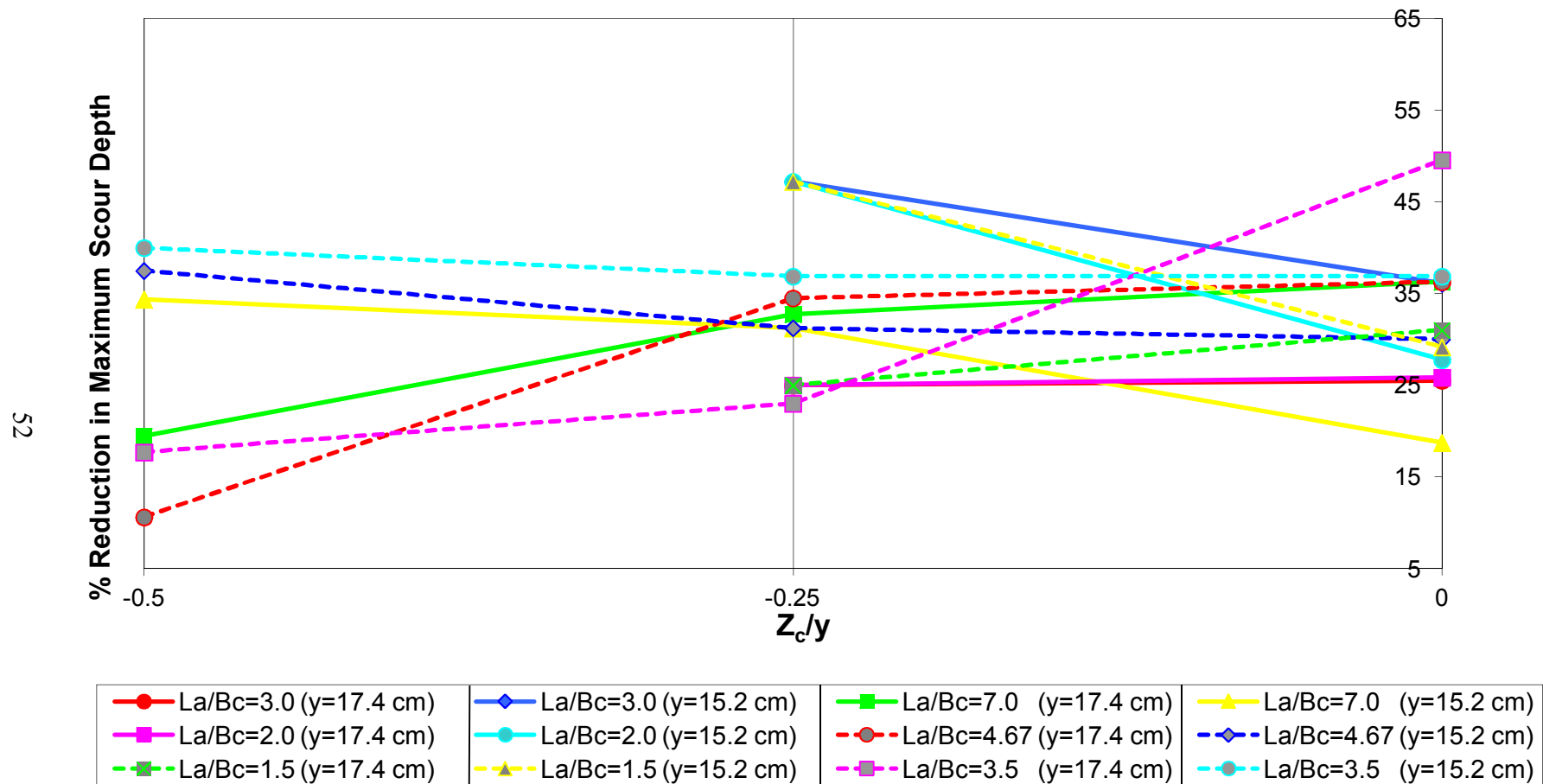


Figure 4.2 Effect of collar size and elevation on the maximum scour depth around the abutments of  $L_a=15$  cm and  $L_a=35$  cm ( $Q=0.0678$  m<sup>3</sup>/s,  $y=15.2$  cm and  $y=17.4$  cm,  $d_{50}=1.5$  mm)

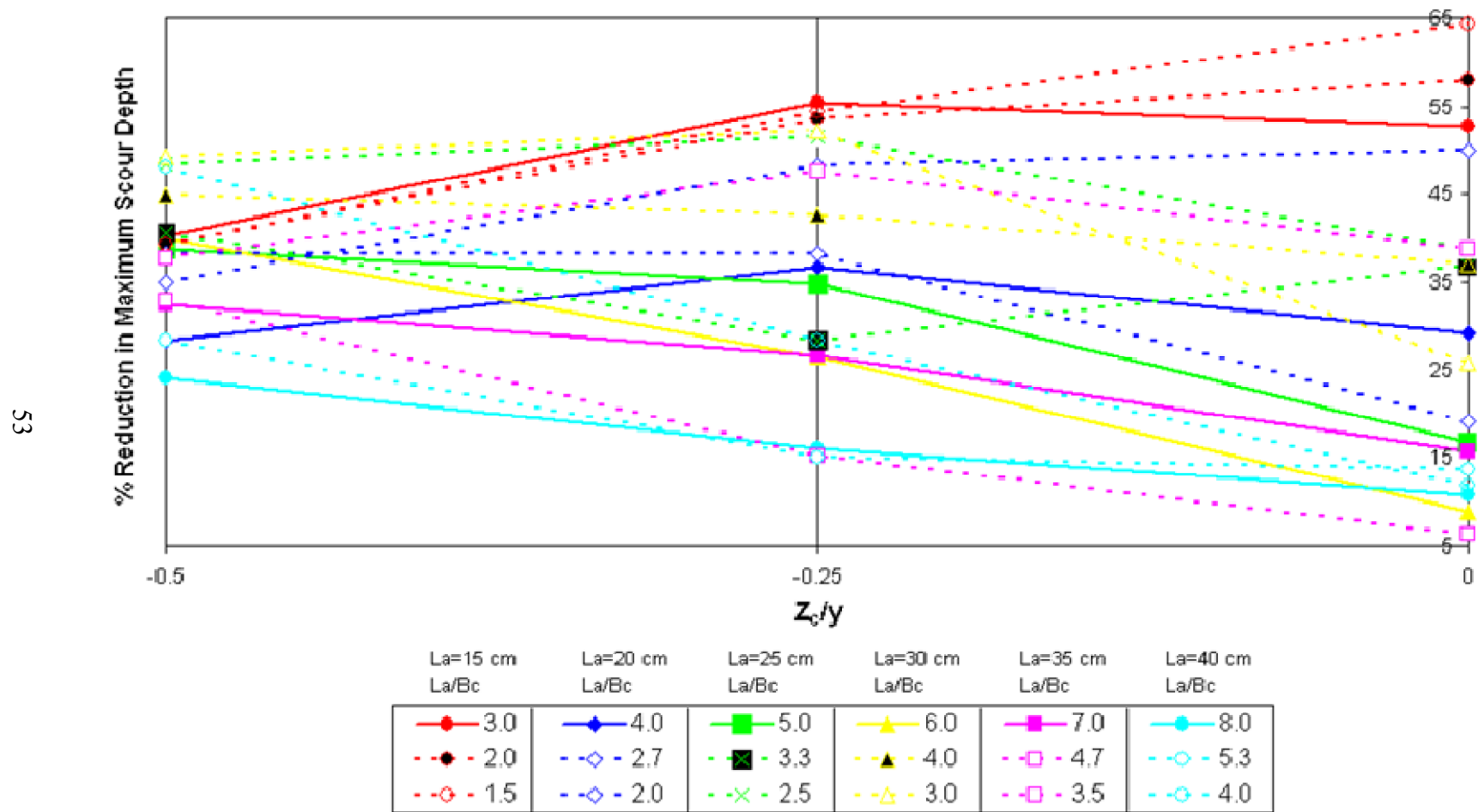


Figure 4.3 Effect of collar size and elevation on the maximum scour depth around the abutments of various lengths ( $Q=0.0678 \text{ m}^3/\text{s}$ ,  $y=13.5 \text{ cm}$ ,  $d_{50}=1.5 \text{ mm}$ ) (Daşkın, 2011)

According to the results of this study, for the flow depth of  $y=15.2$  cm, as the abutment length increases, the performances of collars decrease similar to Daşkın's (2011) result. Unlike this result, the maximum scour reductions increase with the increase in the abutment length for the flow depth of  $y=17.4$  cm. In Figure 4.2, it can also be observed that for the range of  $3.5 \leq L_a/B_c \leq 7.0$  for abutment of  $L_a=35$  cm, the scour reduction performances of collars increase as the collar width increases both for the two flow depths. This result is similar with the observations of Daşkın (2011). In Figure 4.2, it can be seen that for  $L_a/B_c$  values between 3.5 and 7.0, the scour reduction performances of collars increase when the collars are located at the bed level at the flow depth of  $y=17.4$  cm. On the contrary, when the collars are tested at  $y=15.2$  cm, the efficiencies of collars increase with the decrease in  $Z_c/y$  values. For this range of  $L_a/B_c$  values corresponding to abutment of  $L_a=35$  cm, Daşkın (2011) obtained the maximum scour reduction when the collar of  $B_c=10$  cm placed at  $Z_c/y=-0.25$ . The results of this study are similar with Daşkın's (2011) observations in terms of the collar widths which provide the maximum scour reduction for  $L_a=35$  cm for the two different flow depths. However, the efficiencies of collars increase when they are placed at the bed level for the flow depth of  $y=17.4$  cm, and at  $Z_c/y=-0.25$  for the flow depth of  $y=15.2$  cm.

The results of the experiments including  $[Z_c/y]_{\text{opt}}$  and  $[(d_s)_{\text{max},c}/y]_{\text{opt}}$  values are presented in Table 4.3. In this table,  $[Z_c/y]_{\text{opt}}$  and  $[(d_s)_{\text{max},c}/y]_{\text{opt}}$  values represent the optimum design parameters of the collar applications corresponding to the largest percent reductions in the maximum scour depths for the two different abutment models tested at two different flow depths. The data related to the cross-sectional areas of the abutment models and collars are also presented in Table 4.3. The  $\theta$  value denotes the ratio of ‘the total area of the abutment with collar’ to ‘the area of the abutment’ on the horizontal plane, and can be expressed as:

$$\theta = \frac{A_{\text{total}}}{A_{\text{abutment}}} \quad (4.5)$$

The  $\theta$  values are used to show the effect of the areal sizes of the abutment models with collars on the reduction of scour around the abutments. The increase in the  $\theta$  value corresponds to the increase in the collar width for the same abutment model tested with collars. In Table 4.4, the results of the experimental investigations of Daşkın’s (2011) study are also given for comparison.

Table 4.3 Optimum design parameters of the abutment-collar arrangements

|                        |                                    |   |                   | <b>RESULTS OF PRESENT STUDY</b>        |  |                                   |
|------------------------|------------------------------------|---|-------------------|--|--|-----------------------------------|
| <b>L<sub>a</sub>/B</b> | <b>L<sub>a</sub>/B<sub>c</sub></b> | <b>θ<br/>(A<sub>total</sub>/A<sub>abutment</sub>)</b> | <b>y<br/>(cm)</b> | <b>[Z<sub>c</sub>/y]<sub>opt</sub></b> | <b>[(d<sub>s</sub>)<sub>max,c</sub>/y]<sub>opt</sub></b> | <b>[%Reduction]<sub>opt</sub></b> |
| 0.10                   | 3.00                               | 2.56  | 17.4              | 0.00                                   | 0.25   | 25.52                             |
|                        | 2.00                               | 3.56  | 17.4              | 0.00                                   | 0.25   | 25.86                             |
|                        | 1.50                               | 4.69  | 17.4              | 0.00                                   | 0.23   | 31.03                             |
| 0.10                   | 3.00                               | 2.56  | 15.2              | -0.25                                  | 0.25   | 47.22                             |
|                        | 2.00                               | 3.56  | 15.2              | -0.25                                  | 0.25   | 47.22                             |
|                        | 1.50                               | 4.69  | 15.2              | -0.25                                  | 0.25   | 47.22                             |
| 0.23                   | 7.00                               | 2.23  | 17.4              | 0.00                                   | 0.41   | 36.28                             |
|                        | 4.67                               | 2.93  | 17.4              | 0.00                                   | 0.41   | 36.28                             |
|                        | 3.50                               | 3.69  | 17.4              | 0.00                                   | 0.33   | 49.56                             |
| 0.23                   | 7.00                               | 2.23  | 15.2              | -0.50                                  | 0.69   | 34.38                             |
|                        | 4.67                               | 2.93  | 15.2              | -0.50                                  | 0.66   | 37.50                             |
|                        | 3.50                               | 3.69  | 15.2              | -0.50                                  | 0.63   | 40.00                             |

Table 4.4 Optimum design parameters of the abutment-collar arrangements in Daşkın's study (2011)

|                        |                                    |   |                   | <b>DAŞKIN'S RESULTS (2011)</b>         |  |                                   |
|------------------------|------------------------------------|---|-------------------|--|--|-----------------------------------|
| <b>L<sub>a</sub>/B</b> | <b>L<sub>a</sub>/B<sub>c</sub></b> | <b>θ<br/>(A<sub>total</sub>/A<sub>abutment</sub>)</b> | <b>y<br/>(cm)</b> | <b>[Z<sub>c</sub>/y]<sub>opt</sub></b> | <b>[(d<sub>s</sub>)<sub>max,c</sub>/y]<sub>opt</sub></b> | <b>[%Reduction]<sub>opt</sub></b> |
| 0.10                   | 3.00                               | 3.15  | 13.5              | -0.25                                  | 0.37   | 55.36                             |
|                        | 2.00                               | 4.31  | 13.5              | 0.00                                   | 0.35   | 58.04                             |
|                        | 1.50                               | 5.63  | 13.5              | 0.00                                   | 0.30   | 64.29                             |
| 0.13                   | 4.00                               | 2.81  | 13.5              | -0.25                                  | 0.56   | 36.67                             |
|                        | 2.67                               | 3.77  | 13.5              | -0.50                                  | 0.55   | 38.33                             |
|                        | 2.00                               | 4.85  | 13.5              | 0.00                                   | 0.44   | 50.00                             |
| 0.17                   | 5.00                               | 2.63  | 13.5              | -0.50                                  | 0.70   | 38.71                             |
|                        | 3.33                               | 3.48  | 13.5              | -0.50                                  | 0.68   | 40.65                             |
|                        | 2.50                               | 4.43  | 13.5              | -0.25                                  | 0.56   | 51.61                             |
| 0.20                   | 6.00                               | 2.51  | 13.5              | -0.50                                  | 0.79   | 39.89                             |
|                        | 4.00                               | 3.30  | 13.5              | -0.50                                  | 0.73   | 44.94                             |
|                        | 3.00                               | 4.17  | 13.5              | -0.25                                  | 0.63   | 52.25                             |
| 0.23                   | 7.00                               | 2.43  | 13.5              | -0.50                                  | 0.96   | 32.46                             |
|                        | 4.67                               | 3.18  | 13.5              | -0.50                                  | 0.95   | 32.98                             |
|                        | 3.50                               | 3.98  | 13.5              | -0.25                                  | 0.74   | 47.64                             |
| 0.27                   | 8.00                               | 2.37  | 13.5              | -0.50                                  | 1.19   | 24.06                             |
|                        | 5.33                               | 3.08  | 13.5              | -0.50                                  | 1.13   | 28.30                             |
|                        | 4.00                               | 3.85  | 13.5              | -0.50                                  | 0.81   | 48.11                             |



In Figure 4.4, the variations of  $[(d_s)_{\max,c} / y]_{\text{opt}}$  versus  $\theta$  values are shown as a function of  $L_a/B$ . The variations of these parameters obtained in Daşkın's (2011) study are presented in Figure 4.5 for comparison. In the plots,  $(Z_c/y)_{\text{opt}}$  values corresponding to each data points are also given. In Figure 4.4, it can be seen that for  $L_a/B=0.23$ ,  $[(d_s)_{\max,c} / y]_{\text{opt}}$  values decrease with the increase in  $\theta$  values. This trend is similar with the results of Daşkın's (2011) study. In that study, it was observed that for all  $L_a/B$  values,  $[(d_s)_{\max,c} / y]_{\text{opt}}$  values decreased with the increase in  $\theta$  values. Similarly, according to the results of this study, for  $L_a/B=0.10$  at the flow depth of  $y=17.4$  cm, it is observed that  $[(d_s)_{\max,c} / y]_{\text{opt}}$  values decrease with the increase in  $\theta$  values. However, the similar trend cannot be observed for  $L_a/B=0.10$  at the flow depth of  $y=15.2$  cm. For  $L_a/B=0.10$  at  $y=15.2$  cm, it is observed that  $[(d_s)_{\max,c} / y]_{\text{opt}}$  values do not change with the change in the  $\theta$  values. The reason is that for this case, the maximum scour reductions are observed at the elevation of collars both for the three collar widths. Therefore, as it can be seen in Figure 4.4,  $[(d_s)_{\max,c} / y]_{\text{opt}}$  values remain constant regardless of the increase in the collar widths at  $y=15.2$  cm. The optimum location of the collar,  $(Z_c/y)_{\text{opt}}$  corresponding to  $[(d_s)_{\max,c} / y]_{\text{opt}}$  values can also be obtained from these figures for the given  $L_a/B$  and  $\theta$  values.

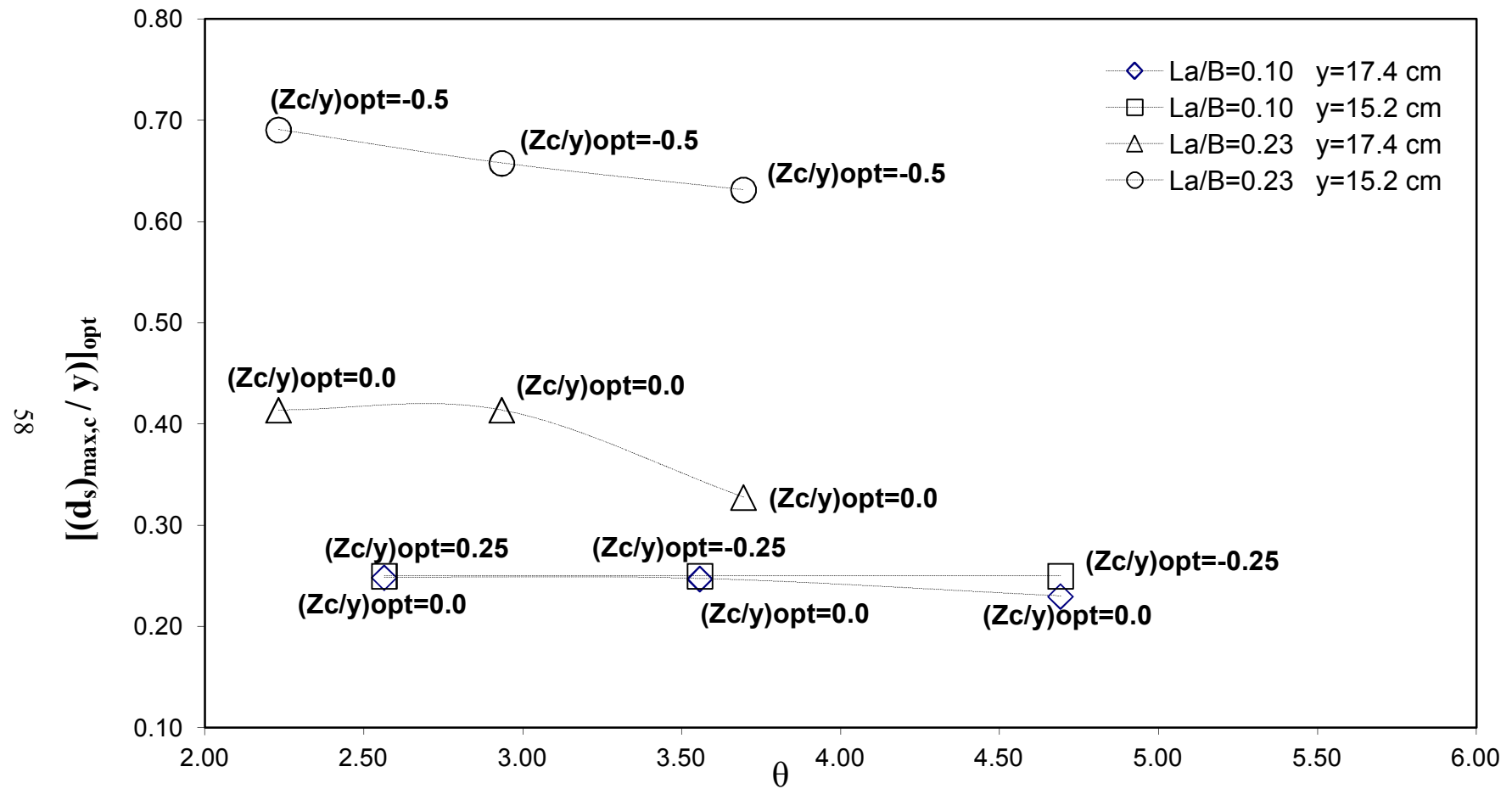


Figure 4.4 Variation of  $[(d_s)_{max,c} / y]_{opt}$  with  $\theta$  ( $Q=0.0678 \text{ m}^3/\text{s}$ ,  $y=17.4 \text{ cm}$ ,  $F_r=0.48$ ,  $U/U_c=0.70$ ,  $d_{50} = 1.50 \text{ mm}$ ,  $t=3 \text{ hours}$ )

( $Q=0.0678 \text{ m}^3/\text{s}$ ,  $y=15.2 \text{ cm}$ ,  $F_r=0.24$ ,  $U/U_c=0.80$ ,  $d_{50} = 1.50 \text{ mm}$ ,  $t=3 \text{ hours}$ )

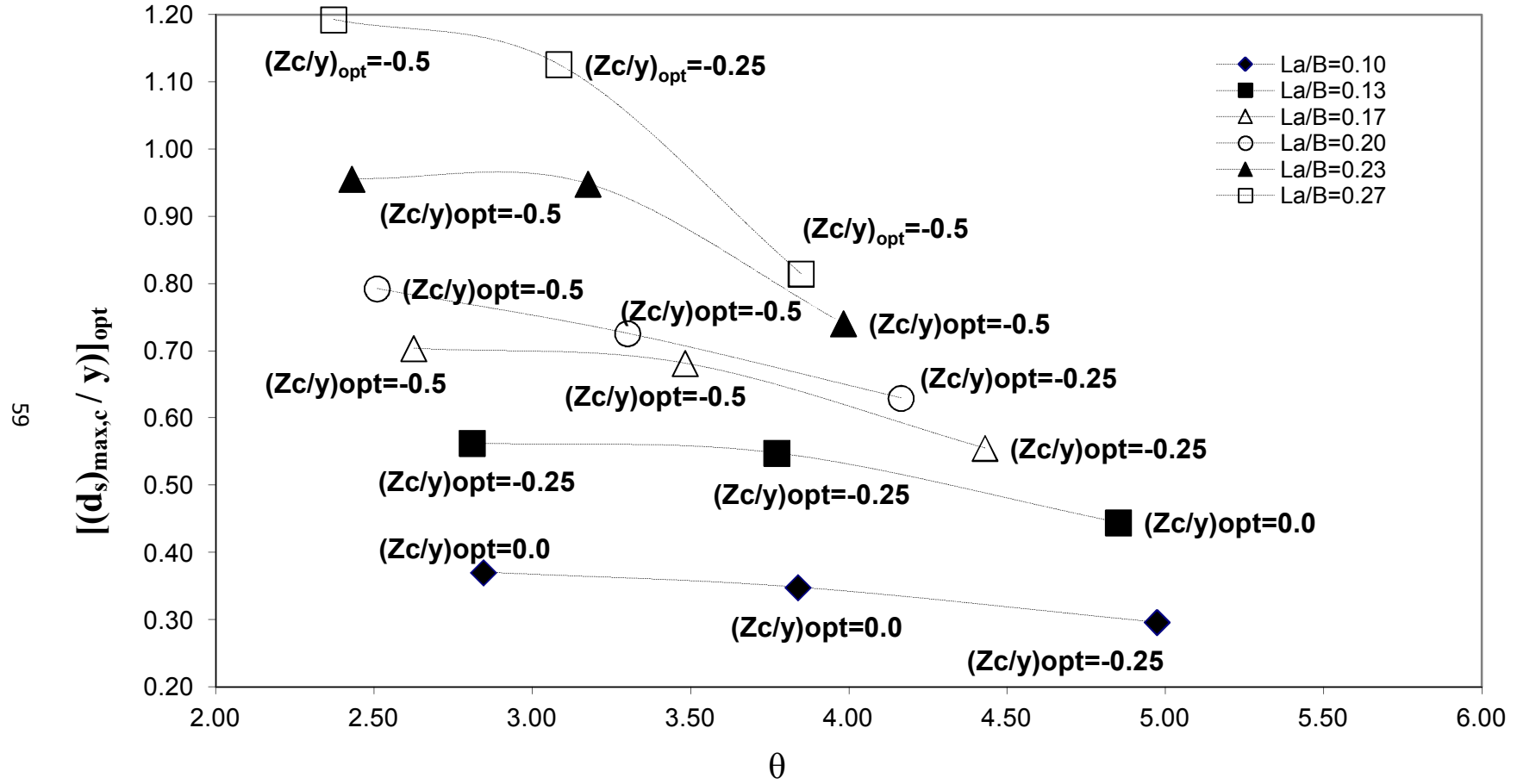


Figure 4.5 Variation of  $[(d_s)_{\max,c} / y]_{\text{opt}}$  with  $\theta$  ( $Q=0.0678 \text{ m}^3/\text{s}$ ,  $y=13.5 \text{ cm}$ ,  $F_r=0.29$ ,  $U/U_c=0.90$ ,  $d_{50} = 1.50 \text{ mm}$ ,  $t=3 \text{ hours}$ )

(Daşkın, 2011)

An alternative presentation of the data plotted in Figure 4.4 is given in Figure 4.6. In this figure, the variations of  $[(d_s)_{\max,c} / y]_{\text{opt}}$  versus  $\sqrt{\theta(L_a/B_c)}$  values are presented. The results of the experimental investigations obtained by previous studies of Kayatürk's (2005), Doğan's (2008), and Daşkın's (2011) are also included with the best fit lines of the data points. Based on Figure 4.6,  $[(d_s)_{\max,c} / y]_{\text{opt}}$  value of an abutment can be estimated for known  $\theta$  and  $L_a/B_c$  values within the ranges of the parameters used in the four different studies. It should be kept in mind that the abutment models used in the studies of Kayatürk's (2005) and Doğan's (2008) were rectangular in plan, whereas semi-circular end abutment models were used both in Daşkın's (2011) study and in this study. In Figure 4.6, it can be noticed that the best fit lines of the data points of the present study and Daşkın's (2011) study fall below the other two best fit lines of the previous studies due to the short experimental period of  $t=3$  hours. In the other two studies, the experiments were conducted for a period of 6 hours which may lead the data points to fall above the data points of the present study and the Daşkın's (2011) study. Although the shape of the abutment model, duration of the experiments and the mean diameter of the sand bed material are the same in Daşkın's (2011) study with the present study,  $[(d_s)_{\max,c} / y]_{\text{opt}}$  values of this study are lower than the results of Daşkın's (2011) study between the same  $\sqrt{\theta(L_a/B_c)}$  ranges on the horizontal axis. According to Figure 4.6, it can be observed that for the range of  $\sqrt{\theta(L_a/B_c)}$  between 2.5 – 3.0 and 3.5 – 4.0, the  $[(d_s)_{\max,c} / y]_{\text{opt}}$  values of the two studies are close to each other but the data points of the present study remain always lower than the data points of the other study. This is related to the larger flow depth and smaller  $U/U_c$  ratio used in the present study.

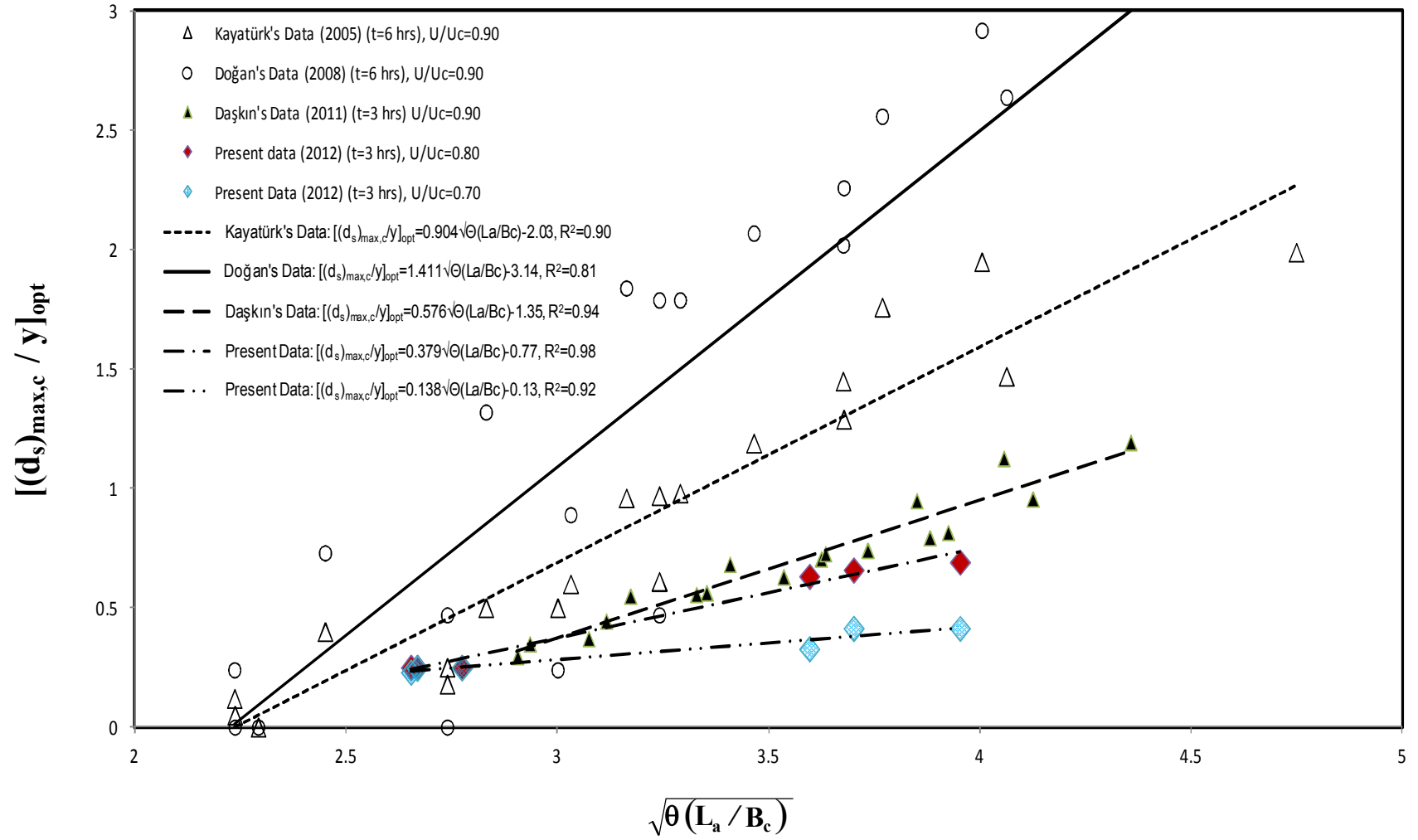


Figure 4.6 Variation of  $[(d_s)_{max,c} / y]_{opt}$  with  $\sqrt{\theta(L_a/B_c)}$

The variations of  $[Z_c/y]_{\text{opt}}$  versus  $L_a/B_c$  values of the present study, as well as the data obtained by Kayatürk (2005), Doğan (2008) and Daşkın (2011) are presented in Figures 4.7 and 4.8. According to these figures, the optimum location of collars,  $[Z_c/y]_{\text{opt}}$  can be determined for a known value of  $L_a/B_c$  within the range of the parameters used in the studies. Based on the results of the present study, for the experiments conducted at the large flow depths ( $y=17.4$  cm), the optimum collar elevation is obtained at the bed level for all  $L_a/B_c$  ratios (see Figure 4.7). However, as the flow depth decreases ( $y=15.2$  cm,  $y=13.5$  cm), the optimum collar elevations decrease and  $[Z_c/y]_{\text{opt}}$  values are observed below the bed level for larger  $L_a/B_c$  ratios. In Figures 4.7 and 4.8,  $[Z_c/y]_{\text{opt}}$  values are classified into zones as a function of  $L_a/B_c$  and can be summarized as below:

The present study:

- Flow depth of  $y=17.4$  cm ( $U/U_c=0.70$ )

$$[Z_c/y]_{\text{opt}} = 0 \quad \text{for } 1.5 \leq L_a/B_c \leq 7.0 \quad (4.6)$$

- Flow depth of  $y=15.2$  cm ( $U/U_c=0.80$ )

$$[Z_c/y]_{\text{opt}} = -0.25 \quad \text{for } 1.5 \leq L_a/B_c \leq 3.0 \quad (4.7)$$

$$[Z_c/y]_{\text{opt}} = -0.50 \quad \text{for } 3.0 < L_a/B_c \leq 7.0$$

The above relations are valid within the range of  $L_a/B_c$  between 1.5 and 7.

Daşkın's study (2011):

- Flow depth of  $y=13.5$  cm ( $U/U_c=0.90$ )

$$[Z_c/y]_{\text{opt}} = 0 \quad \text{for } L_a/B_c \leq 2.0$$

$$-0.50 \leq [Z_c/y]_{\text{opt}} \leq -0.25 \quad \text{for } 2.0 \leq L_a/B_c \leq 5.0 \quad (4.8)$$

$$[Z_c/y]_{\text{opt}} = -0.50 \quad \text{for } 5.0 < L_a/B_c \leq 8.0$$

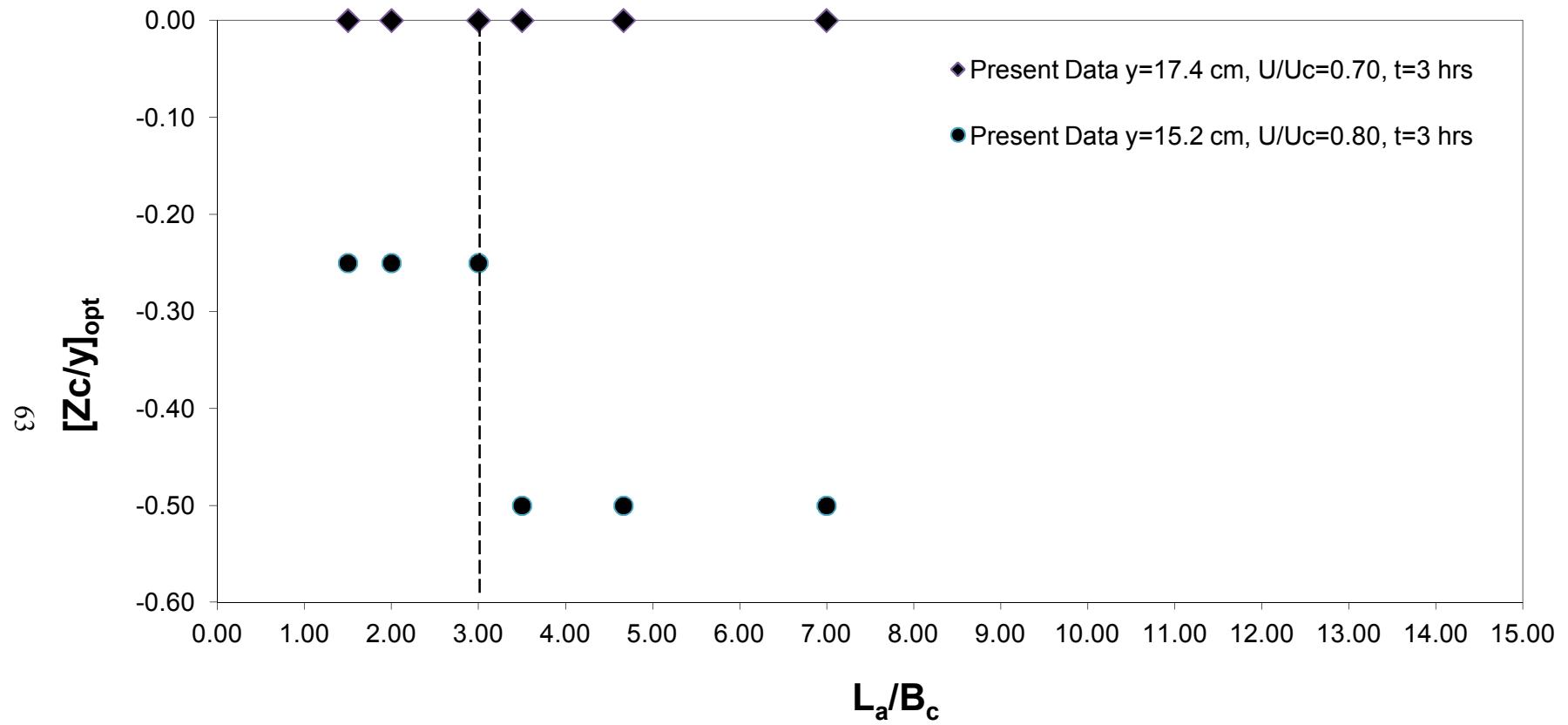


Figure 4.7 Variation of  $[Z_c/y]_{\text{opt}}$  with  $L_a/B_c$

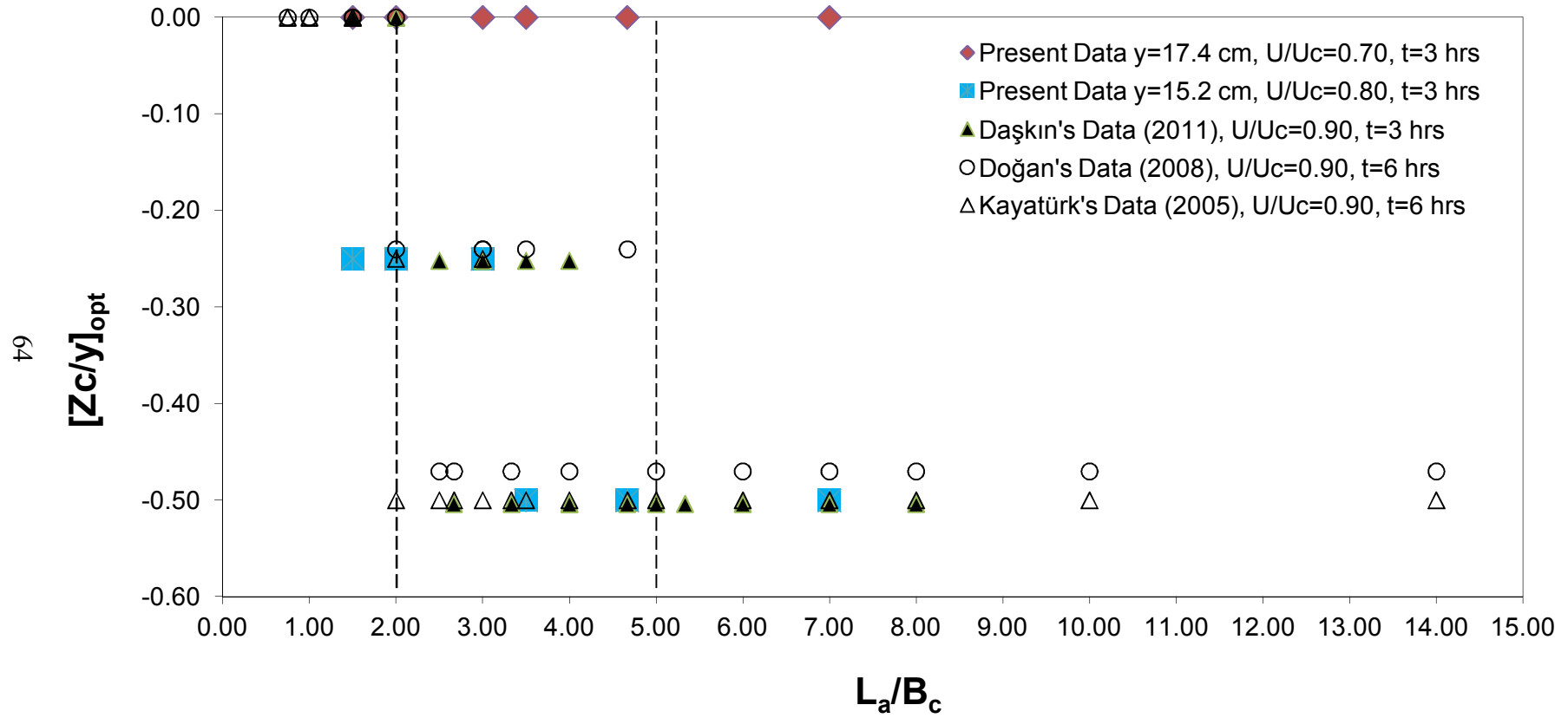


Figure 4.8 Variation of  $[Z_c/y]_{\text{opt}}$  with  $L_a/B_c$



The above relations of Daşkın's study are valid within the range of  $L_a/B_c$  between 1.5 and 8.

Doğan's study (2008):

$$\begin{aligned}
 [Z_c/y]_{\text{opt}} &= 0 & \text{for } L_a/B_c \leq 2.0 \\
 -0.47 \leq [Z_c/y]_{\text{opt}} &\leq -0.24 & \text{for } 2.0 < L_a/B_c < 5.0 \\
 [Z_c/y]_{\text{opt}} &= -0.47 & \text{for } 5.0 \leq L_a/B_c \leq 14.0
 \end{aligned} \tag{4.9}$$

Kayatürk's study (2005):

$$\begin{aligned}
 [Z_c/y]_{\text{opt}} &= 0 & \text{for } L_a/B_c = 2.0 \\
 -0.50 \leq [Z_c/y]_{\text{opt}} &\leq -0.25 & \text{for } 2.0 \leq L_a/B_c \leq 3.0 \\
 [Z_c/y]_{\text{opt}} &= -0.50 & \text{for } 3.0 < L_a/B_c \leq 14.0
 \end{aligned} \tag{4.10}$$

The above relations of Doğan's and Kayatürk's studies are valid within the range of  $L_a/B_c$  between 0.75 and 14.

The variations of optimum % reduction in scour depth ( $[\%Reduction]_{opt}$ ) with respect to  $L_a/B_c$  values of the present study and the previous ones are shown in Figure 4.9. The general trend here is that as  $L_a/B_c$  increases, the % reduction in scour depth decreases. All the data except the ones obtained at larger flow depth of  $y=17.4$  cm shows this similar trend. At this flow depth, data is not well correlated. When the best fit lines for the present data obtained at  $y=15.2$  cm is compared with Kayatürk's (2005) and Doğan's (2011) data, there observed a considerable difference. This is basically related to the fact that  $L_a/B_c$  range in the present study is very limited, and test durations,  $U/U_c$  values and the abutment shapes in the present study and the above mentioned ones are different.

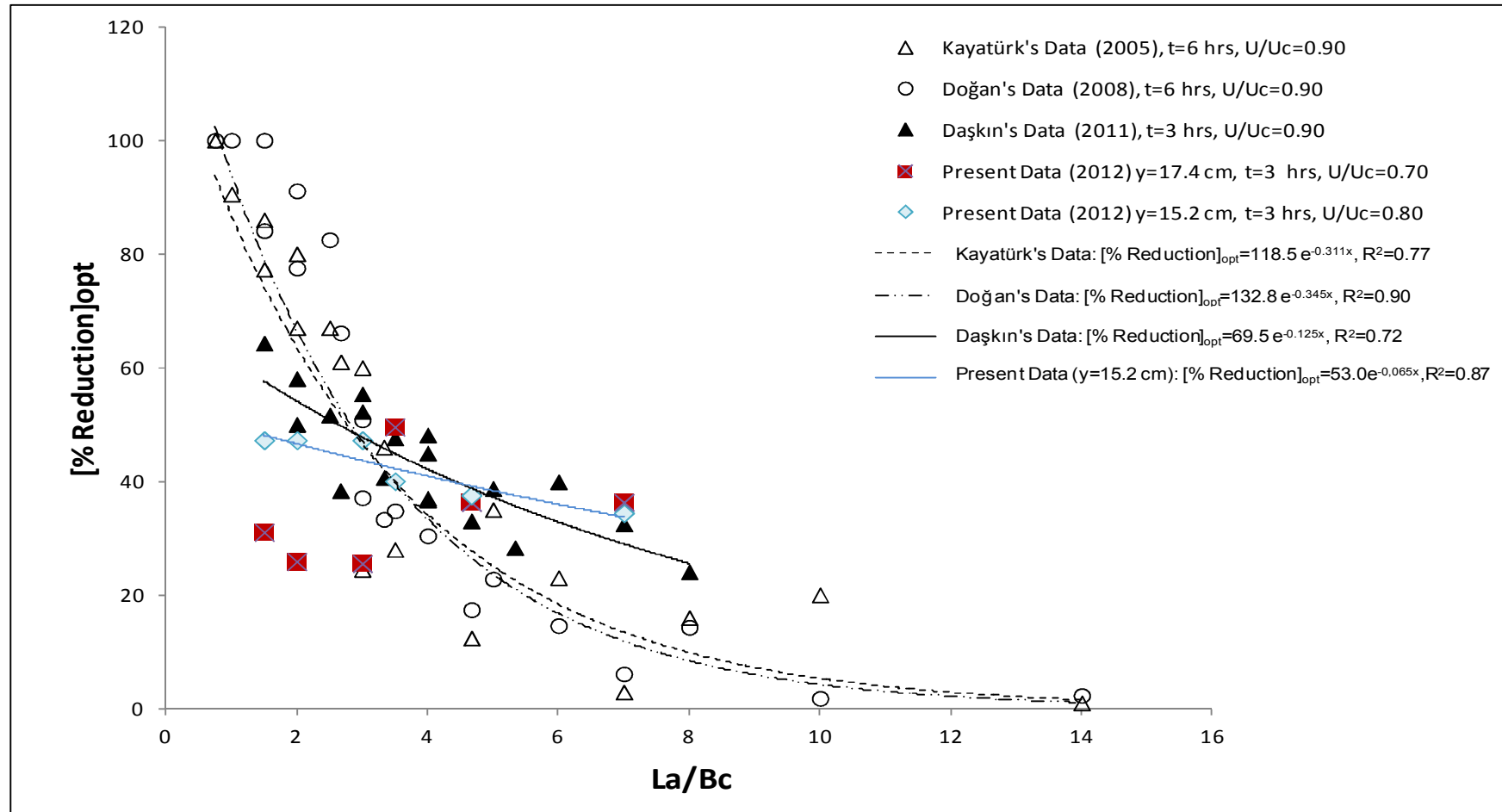


Figure 4.9 Variation of  $[\% \text{Reduction}]_{\text{opt}}$  with  $La/Bc$

### 4.3.3 Comparison of Scour Holes for Different Flow Depths

The results of the 3-dimensional bathymetry investigations of the sand bed around the abutment model related to the effect of flow depth on the formation of scour are presented in this section. Figure 4.10 shows the 3-dimensional views of the scour formations obtained at two different flow depths for the same abutment model of  $L_a=35$  cm. In Figure 4.10a, the view of the scour and deposition patterns around the abutment model obtained in the present study at a flow depth of  $y=17.4$  cm is given. On the other hand, Figure 4.10b shows the view of the scour and deposition patterns of the same abutment model tested in Daşkın's (2011) study at a flow depth of  $y=13.5$  cm. According to the results of these two studies, it can be observed that the depth of the scour hole decreases as the flow depth increases. Furthermore, the scour hole forms in a larger region around the abutment model in Daşkın's (2011) study than the one obtained in this study.

In Figure 4.10, the depths of scour and deposition formations are non-dimensionalized by dividing with the corresponding flow depths of  $y=17.4$  cm and  $y=13.5$  cm. In the present study, the dimensionless maximum scour depth,  $z/y$  is obtained as  $-0.64$ ; whereas for the case of  $y=13.5$  cm, the dimensionless maximum scour depth is measured as  $z/y=-1.41$ . Moreover, the dimensionless maximum deposition levels observed in the present study and in the previous one are as  $z/y=0.31$  and  $z/y=0.64$ , respectively. Therefore, it can be concluded that both the depth of scour and the deposition level around the abutment model increase with the decrease in the flow depth.

According to the results of the experiments, it is also noticed that the deposition formation at the downstream of the abutment models differ from each other with respect to the existence of a secondary scour hole. In the present study, it is observed that at the downstream end of the deposition pattern, a smaller scour hole forms apart

from the one which is close to the abutment model. The dimensionless depth of this scour hole is measured approximately as  $z/y = -0.29$  which is almost two times smaller than the maximum scour depth observed close to the abutment. Although such a scour formation does not exist in Daşkın's (2011) study, the distances measured between the ends of the deposition formations with the abutment models are almost the same both in these two cases.

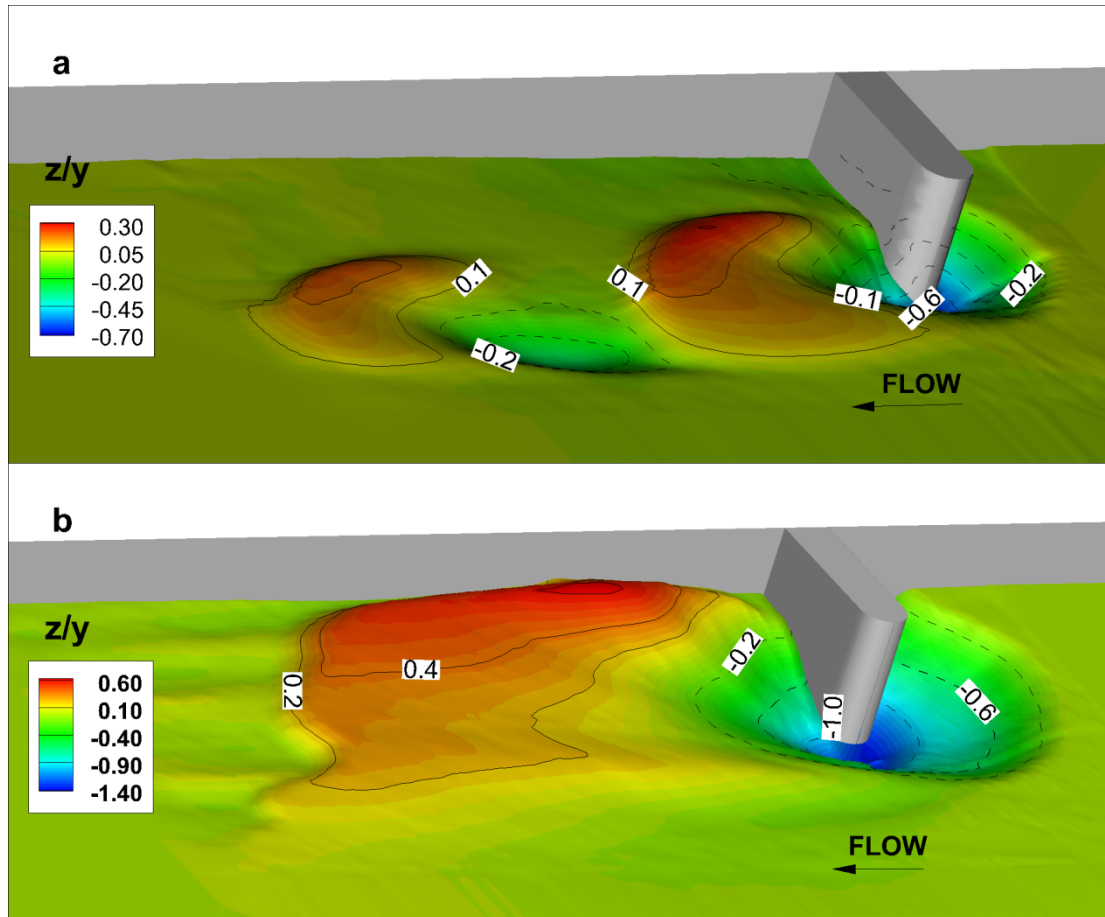


Figure 4.10 3-D views of the scour and deposition patterns around the abutment model of  $L_a = 35$  cm: a) at flow depth of  $y = 17.4$  cm; b) at flow depth of  $y = 13.5$  cm

In order to make a more quantitative comparison on the formation of local scour, two-dimensional (2D) plots of the predetermined sections around the abutment models are given in the following sections.

In Figure 4.11, a schematic illustration is presented to indicate the location of these sections around the abutment model.

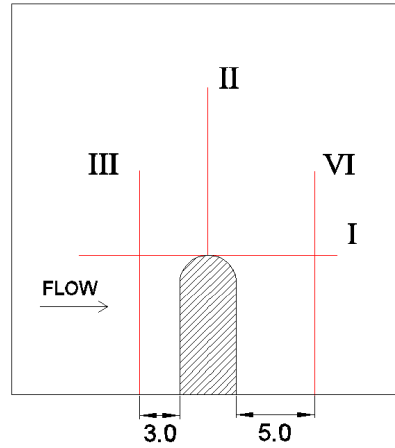


Figure 4.11 Schematic illustration of the sections taken around the abutment model of  $L_a=35$  cm (dimensions are given in cm)

The 2D plots of the longitudinal profiles of the sand bed just at the toe of the abutment models through section I are presented in Figure 4.12. According to this figure, the dimensionless maximum scour depths are measured approximately as  $z/y=-0.64$  and  $z/y=-1.32$  at the flow depths of  $y=17.4$  cm and  $y=13.5$  cm, respectively. Although the depth of scour hole increases with the decrease in the flow depth, the locations of the maximum scour depths are observed approximately at the same streamwise location of  $x/y \approx -0.3$ .

The scour formation around the abutment tested at  $y=13.5$  cm resulted in a wider scour hole which is observed approximately between  $-3 < x/y < 4$ . At the flow depth of  $y=17.4$  cm, however, the scour formation is resulted between  $-1 < x/y < 2$  which is almost two times smaller than the previous case. Therefore, it may be concluded that the maximum scour depth and the width of the scour hole increases with the decrease in the flow depth.

When the deposition profiles of the two cases are compared with each other, it can be noticed that the dimensionless maximum deposition levels are observed as  $z/y=0.30$  and  $z/y=0.40$  at flow depths of  $y=17.4$  cm and  $y=13.5$  cm, respectively. Moreover, the deposition pattern is formed in a smaller region in the larger flow depth. Based on Figure 4.12, the deposition profiles are measured approximately between  $2 < x/y < 7$  in the larger flow depth, and measured about between  $4 < x/y < 10$  in the smaller flow depth. As a result, it can be concluded that the maximum deposition level and the longitudinal distance of the deposition increase as the flow depth decreases.

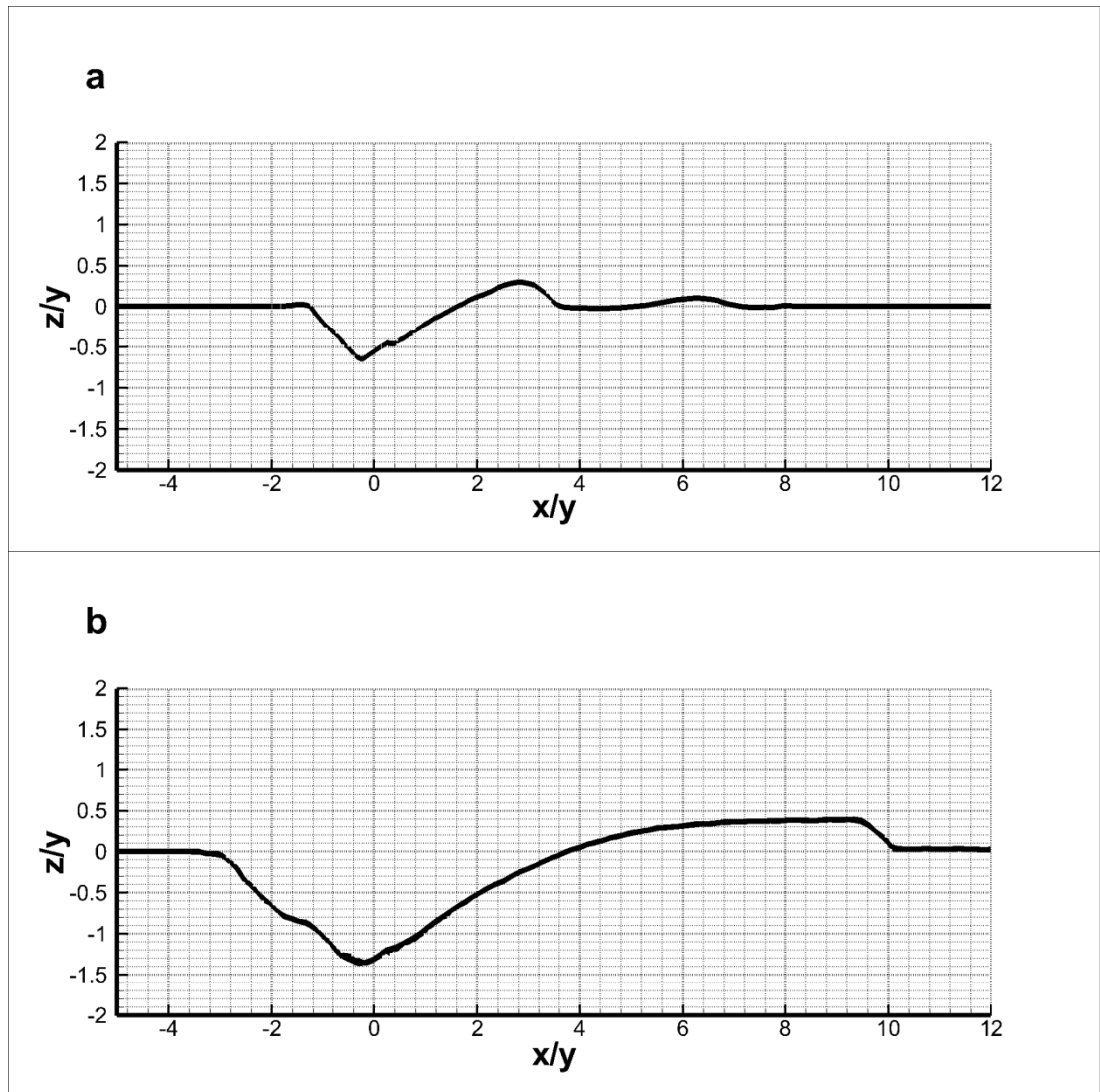


Figure 4.12 Section I: a) at flow depth of  $y=17.4$  cm; b) at flow depth of  $y=13.5$  cm

The 2D plots of the lateral profiles of the sand bed taken at the toe of the abutment models which are perpendicular to the flow direction are shown in Figure 4.13. In the plots,  $\xi/y$  stands for the dimensionless values of the bathymetry levels in the transversal direction. At this section for the larger flow depth, the maximum scour depth is observed just in front of the toe of the abutment model and measured approximately as  $z/y=-0.59$ . Similarly, in the case of the experiment conducted at  $y=13.5$  cm, the maximum scour depth is formed close to the abutment model and observed approximately as  $z/y=-1.32$ .

According to Figure 4.13, it can also be noticed that the lateral extent of the scour hole measured in the case of  $y=17.4$  cm is smaller than the previous case. Based on the plots, scour is observed up to the value of about  $\xi/y=3.2$  in the present study, and in the case of Daşkın's (2011) study, it is formed up to the value of approximately  $\xi/y=5.6$ . Thus, it can be concluded that the scour depth and the lateral distance of the scour hole from the toe of the abutment increase with the decrease in the flow depth.



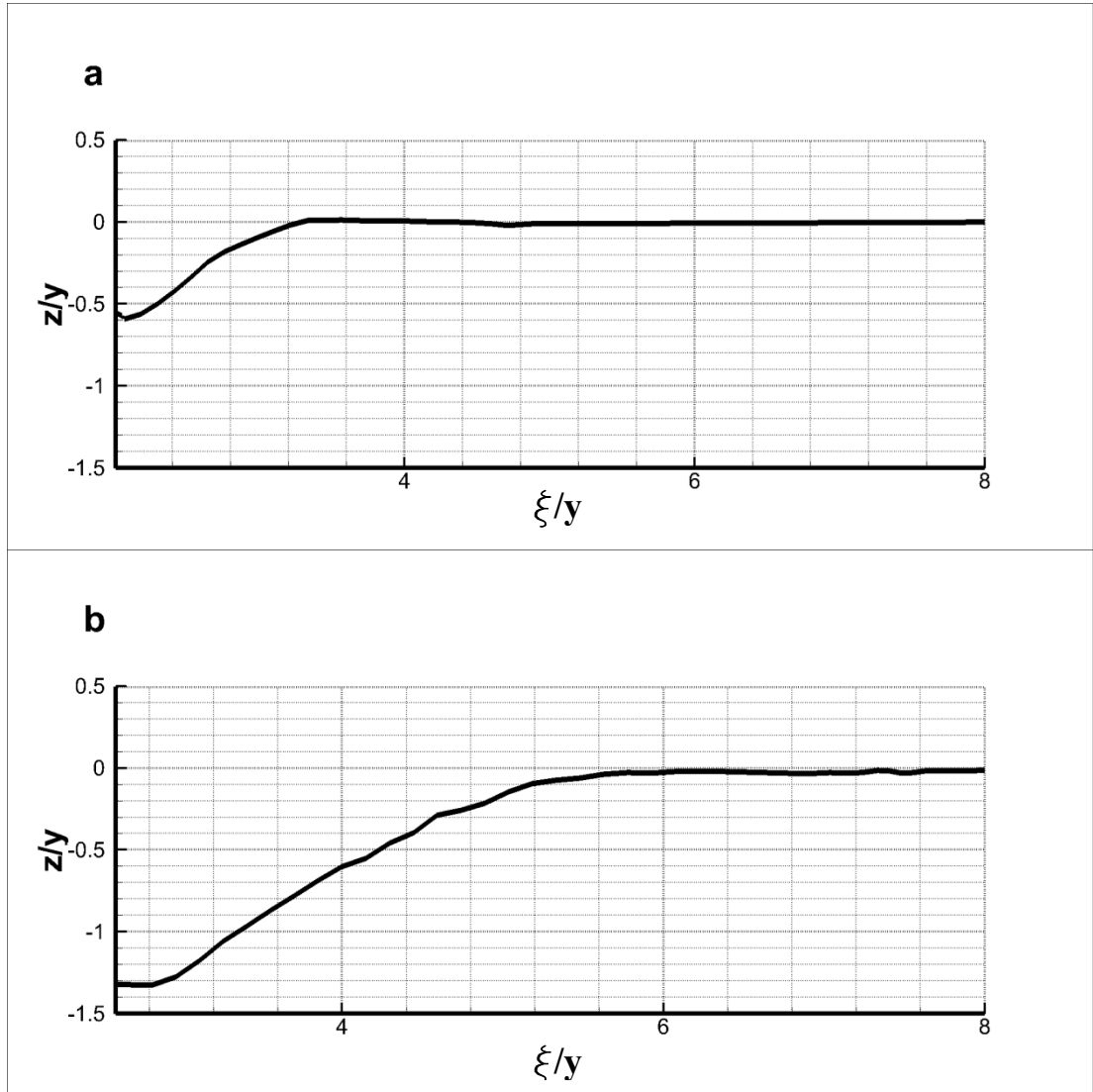


Figure 4.13 Section II: a) at flow depth of  $y=17.4$  cm; b) at flow depth of  $y=13.5$  cm

The lateral profiles of the sand bed at the upstream of the abutment model are presented in Figure 4.14. According to this figure, it can be seen that the dimensionless lateral distances of the maximum scour depth from the flume wall are almost the same for the two cases. However, as observed in the previous plots, the dimensionless maximum scour depth is higher in Daşkın's (2011) study than the one observed in the present study at this section. The maximum scour depths measured for the flow depths of  $y=13.5$  cm and  $y=17.4$  cm are approximately as  $z/y= -1.38$  and  $z/y= -0.55$ , respectively. The maximum scour observed in the smaller flow depth is

approximately 2.5 times of the value observed in the larger flow depth. This is the largest differentiation observed among all the sections compared.

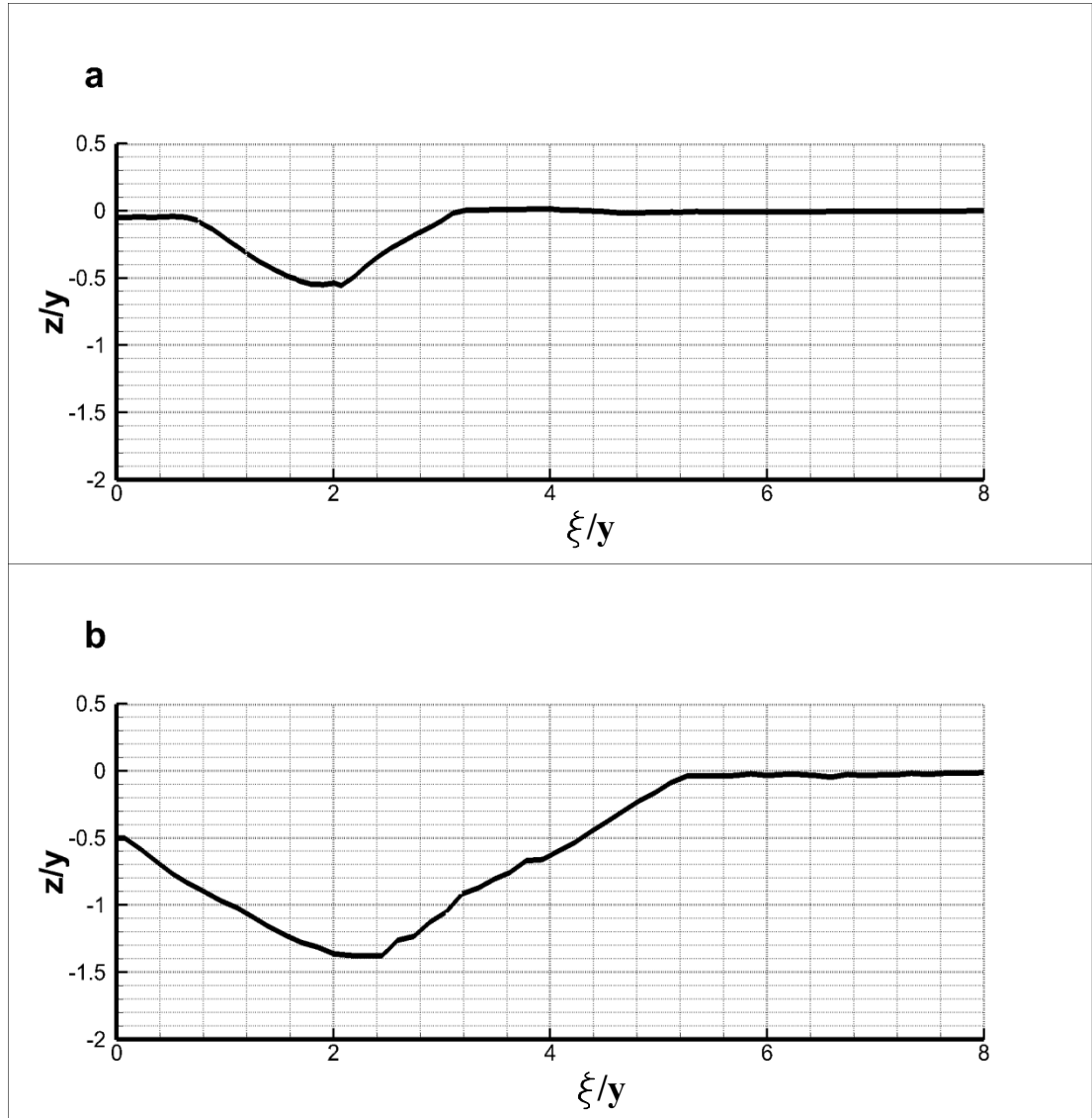


Figure 4.14 Section III: a) at flow depth of  $y=17.4$  cm; b) at flow depth of  $y=13.5$  cm

The 2D plots of the lateral profiles of the sand bed at the downstream of the abutment model are provided in Figure 4.15. According to this figure, it can be observed that the scour formation obtained in the present study has milder slopes than the scour formation resulted in the previous study. In the case of higher flow depth, the dimensionless scour depth is measured approximately as  $z/y=-0.11$  between the values of  $0 < \xi/y < 1.2$  in the lateral direction. In contrast to this result,

Daşkın (2011) obtained a scour formation with sharp slopes at both sides of the hole which is extending between the values of  $0.6 < \xi/y < 6.10$ .

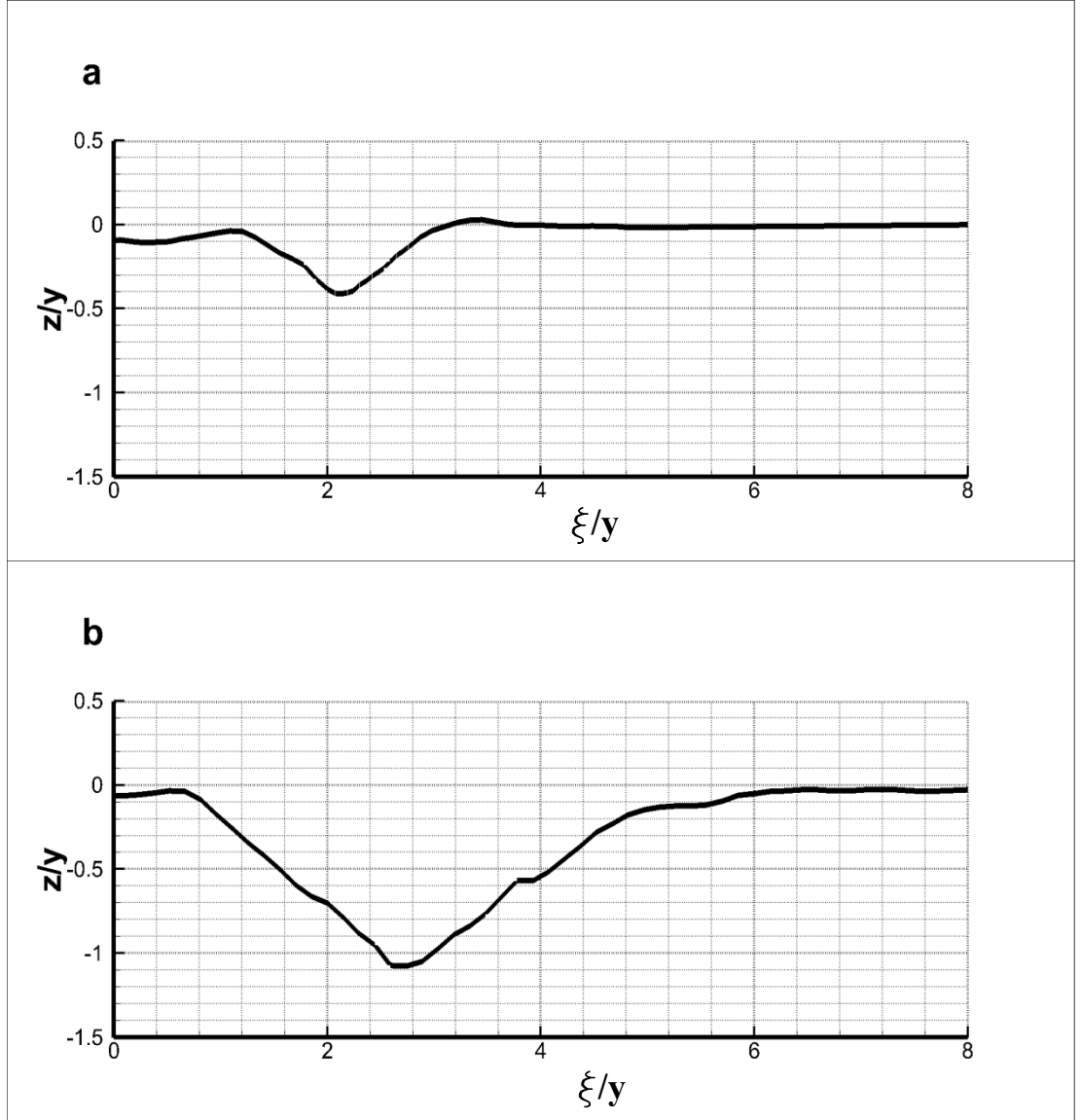


Figure 4.15 Section IV: a) at flow depth of  $y=17.4$  cm; b) at flow depth of  $y=13.5$  cm

## **CHAPTER 5**

### **TIME DEVELOPMENT OF LOCAL SCOUR AT BRIDGE ABUTMENTS**

#### **5.1 GENERAL**

The primary objective of this chapter is to investigate the effects of flow depth and abutment length on the temporal development of local scour at bridge abutments. The development of scour around the abutments without a collar was studied for a time period of 8 hours under clear-water scour conditions, and observed scour depths were compared to analyse the effects of flow depth and abutment length on the time development of local scour.

#### **5.2 DISCUSSION OF RESULTS**

In this study, 20 experiments were carried out to investigate the temporal variations of the scour hole forming around the abutment model for a period of 8 hours under clear-water scour conditions. The experiments were conducted with semi-circular end abutment models of  $L_a=15$  cm and  $L_a=35$  cm without a collar for the flow depths of  $y=13.5$  cm and  $y=17.4$  cm. The data acquisition by the use of the aquistic device and the experimental procedure of this study are given in Chapter 3.

The temporal development of the scour hole was recorded at five different sections around the abutment model for each experimental set. The locations of the prescribed sections are presented in the following parts of the study, and the results of the experimental investigations will be analysed with respect to the development of the scour and deposition formations obtained at these sections.

In the figures, the depths of the scour and deposition formations are non-dimensionalized by dividing with the corresponding flow depths of  $y=17.4$  cm and  $y=13.5$  cm for each section taken around the abutment models. Moreover, in the plots,  $\xi/y$  stands for the dimensionless values of the bathymetry levels in the transverse direction of the flume channel. Likewise,  $r/y$  values correspond to the dimensionless values of the bathymetry levels around the peripheral surface of the abutment model.

### **5.2.1 Time Development of Scour Hole at Short Abutment ( $L_a=15$ cm)**

The time development of scour hole at the abutment model of  $L_a=15$  cm will be first investigated in the following sections for two different flow depths of  $y=13.5$  cm and  $y=17.4$  cm. The location of the sections around the abutment model and the experimental results for the two different flow depths are presented in each case.

#### **5.2.1.1 Time Development of Scour at the Flow Depth of $y=13.5$ cm**

The results of the experimental investigations of the temporal development of local scour around the abutment of  $L_a=15$  cm at the flow depth of  $y=13.5$  cm are given in this section. In Figure 5.1, a schematic illustration of the locations of the sections around the abutment model is presented. In this figure, sections 1, 2 and 3 are located perpendicular to the flow direction; i.e. section 1 is at the upstream of the abutment, section 2 is at the toe of the abutment and section 3 is at the downstream of the abutment. Moreover, section 4 is located at the toe of the abutment parallel to the flow direction and the last section is located at the peripheral surface of the abutment. In the following figures of 5.2 through 5.6, the notations of P1 to P26 are given to indicate the number of the transducer probes which are used to record the bathymetry levels at the prescribed sections.

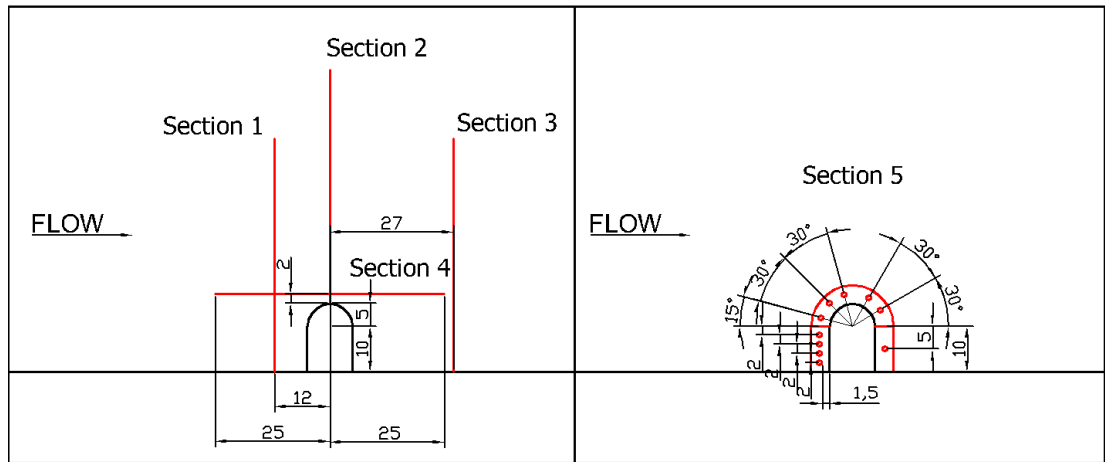


Figure 5.1 Schematic illustration of the sections taken around the abutment model of  $L_a=15$  cm for the flow depth of  $y=13.5$  cm (linear dimensions are given in cm)

The 2D lateral profile of the temporal development of local scour around the abutment model at section 1 is presented in Figure 5.2. According to this figure, it can be observed that the depth and the width of the scour hole increases with time. Throughout the experiment period, despite the increase in the depth of scour, the side slopes of the scour hole are observed to be almost parallel to each other. This result shows that as the scour hole deepens at this section, i.e. at the upstream of the abutment, the scour hole almost conserves its shape. Moreover, the scour profiles tend to close each other in progress of time.

In Figure 5.2, it can also be noticed that there is a rapid development of scour during the time period of three hours. After this time period, the scour hole continues to develop at a slower rate in such a way that the scour profiles follow almost the same trend with the previous ones. At the end of the eight hours experimental period, the maximum local scour depth occurs close to the flume wall at about  $\xi/y=0.5$ , and is measured approximately as  $z/y=0.74$ .

The lateral profile of the temporal development of local scour at the toe of the abutment model perpendicular to the flow direction is shown in Figure 5.3. In this figure, it is seen that scour hole deepens rapidly in three hours period of time as in the case of scour formation at section 1. However, at the end of the eight hours test duration, the dimensionless maximum scour depth,  $z/y$  is observed higher at the toe of the abutment model than the one measured at the upstream of the abutment model at section 1. The maximum local scour depth is measured approximately as  $z/y=-0.82$  just at the toe of the abutment model at the end of the experiment period.

Based on the figures at these two sections, the time development of the scour hole tends to be similar at both sections with respect to the rate of development of scour. Moreover, the side slopes of the scour hole remain almost unchanged during the experimental period.

The time development of local scour at the downstream of the abutment model is presented in Figure 5.4. According to this figure, it is seen that during the first hour of test duration, the lateral profile of the sand bed show small scour and deposition formations. At the second hour, it is observed that a significant amount of deposition forms at the downstream of the abutment model between approximately  $0 < \xi/y < 2.5$ . This is related to the movement of the deposition hill in the streamwise direction. At this time instant it already reached to the test section. After this time period, the maximum level of the deposition pattern moves towards the flume wall and the amount of deposition slowly decreases between the range of  $0.5 < \xi/y < 2.5$ . At the end of the experiment, the maximum level of the deposition hill is measured about  $z/y=0.38$ .

The time variation of the local scour around the abutment model at section 4 is given in Figure 5.5. The development of the scour hole at this section which is located just at the toe of the abutment model has a uniform trend through the experiment period. According to Figure 5.5, it is seen that the depth and the length of the scour hole increase gradually as time progresses. In Figure 5.5, it can also be noticed that a

deposition formation exists at the downstream zone of the abutment model. As time passes, this deposition zone moves in the streamwise direction and after six hours, it leaves the domain on which the measurements are recorded.

In Figure 5.6, the time development of local scour around the peripheral surface of the abutment model is presented. According to this figure, it is seen that there is a rapid development of scour at the upstream side of the abutment model up to five hours of experiment period. After five hours of test duration, the rate of scour development decreases all around the abutment model, and at the end of eight hours, the maximum local scour depth occurs at the upstream part of the abutment at around  $r/y=0.4$ , where its magnitude is about  $z/y \approx -1.0$ .



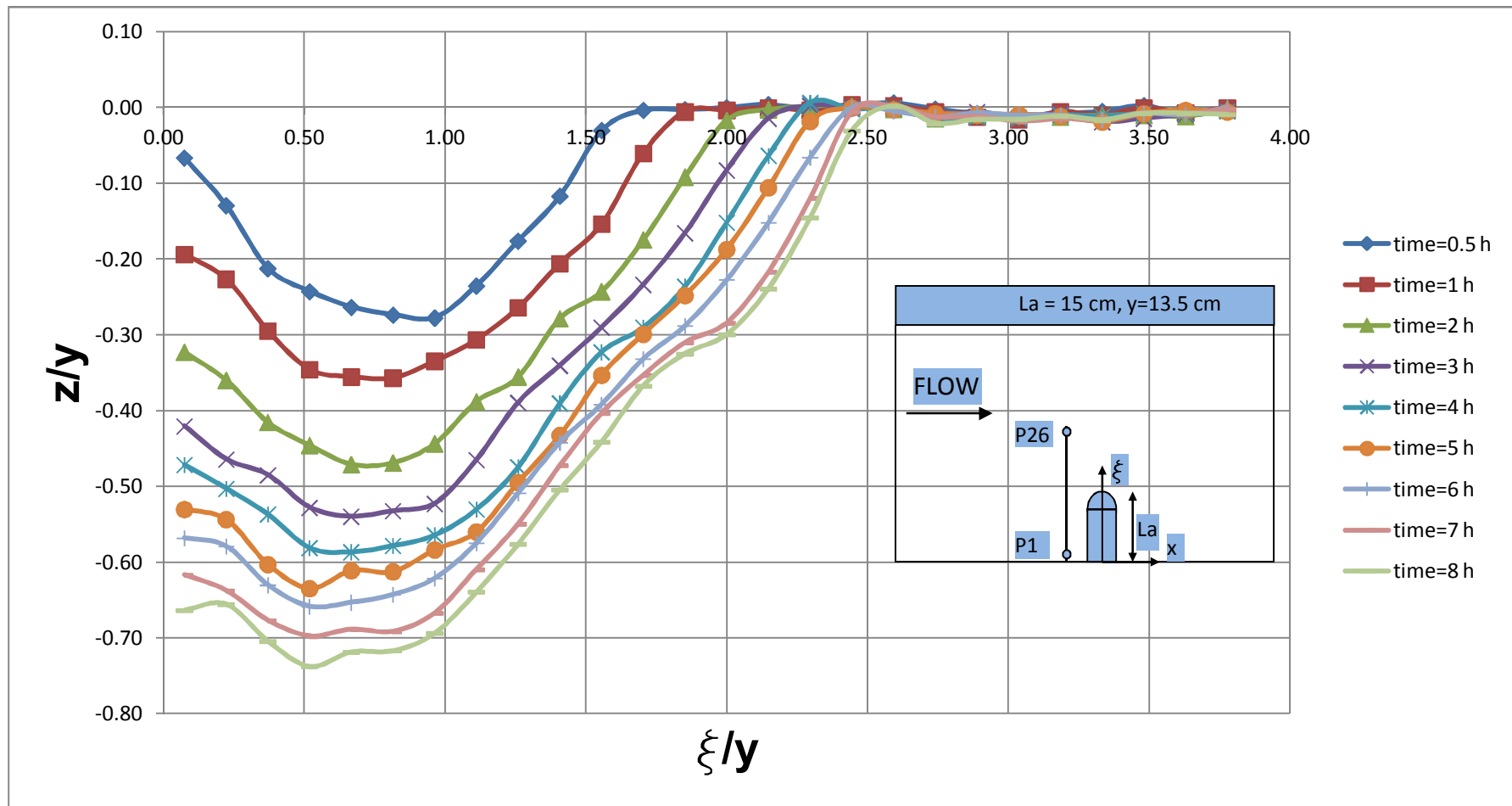


Figure 5.2 Time development of local scour around the abutment model of  $L_a=15 \text{ cm}$  at section 1

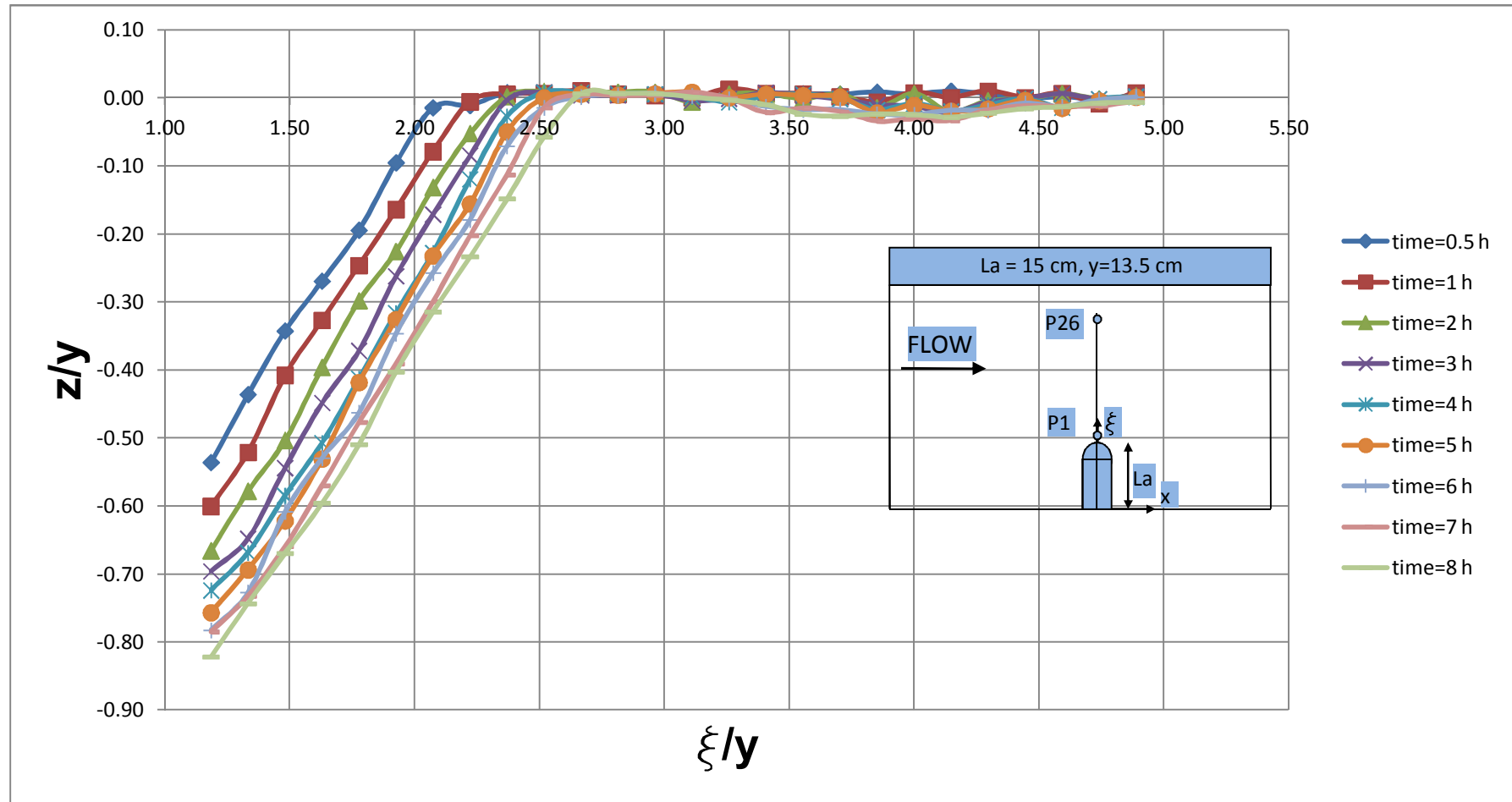


Figure 5.3 Time development of local scour around the abutment model of  $L_a=15 \text{ cm}$  at section 2

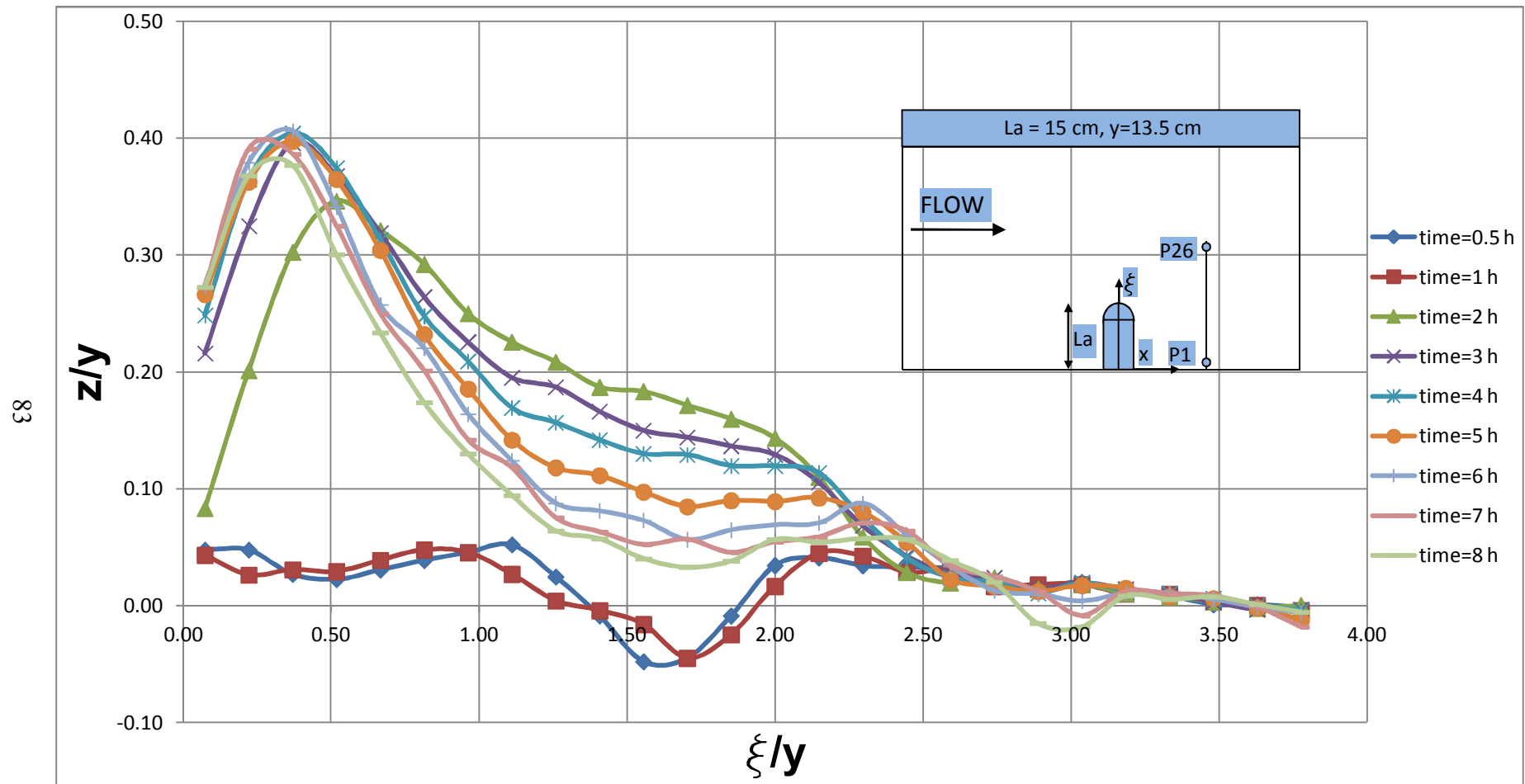


Figure 5.4 Time development of local scour around the abutment model of  $L_a=15$  cm at section 3

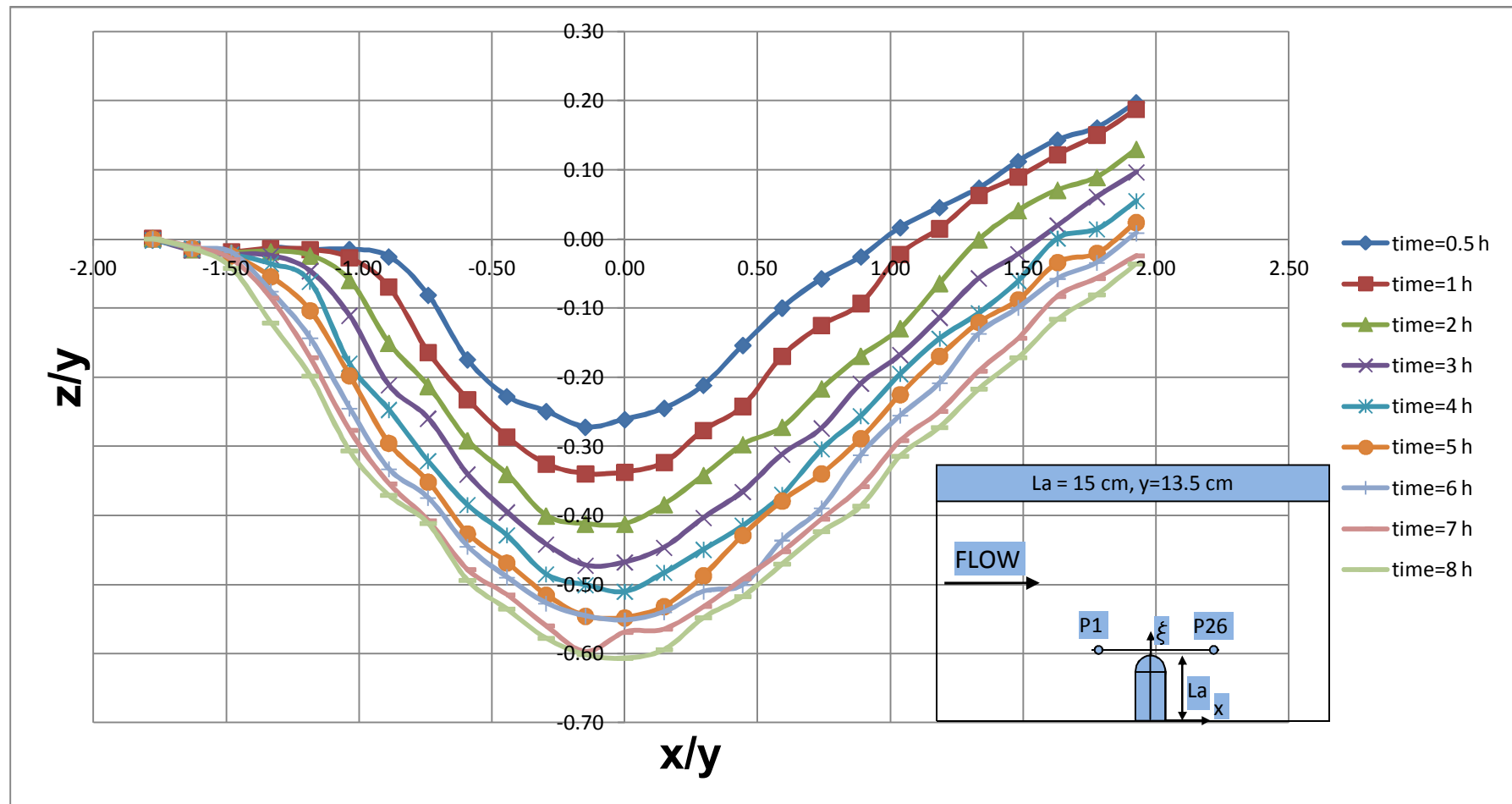


Figure 5.5 Time development of local scour around the abutment model of  $L_a=15$  cm at section 4

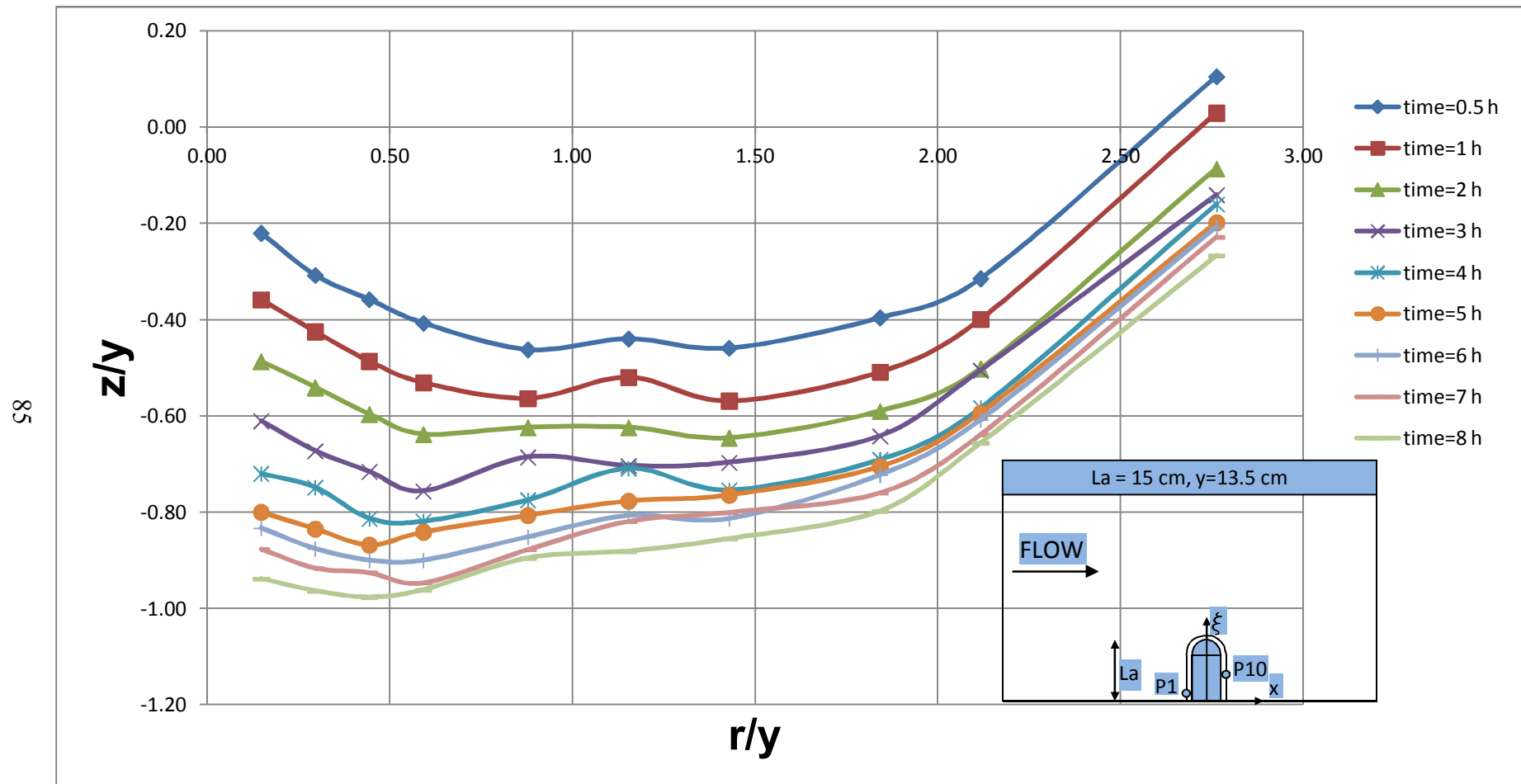


Figure 5.6 Time development of local scour around the abutment model of  $L_a=15$  cm at section 5

### 5.2.1.2 Time Development of Scour at the Flow Depth of $y=17.4$ cm

The results of the experiments of the time development of local scour around the abutment at the flow depth of  $y=17.4$  cm are presented in Figures 5.8 to 5.12. A schematic illustration of the location of the sections around the abutment is given in Figure 5.7. In this figure, the locations of the transversal sections are slightly different from the previous layout of the sections for the experiments at the flow depth of  $y=13.5$  cm. Sections 1, 2 and 3 are located perpendicular to the flow direction similar to Figure 5.1; however, the sections at the upstream and downstream of the abutment model are located at a closer distance to the model compared to the previous case. The scour hole is smaller at the flow depth of  $y=17.4$  cm and hence the sections are particularly located close to the abutment.

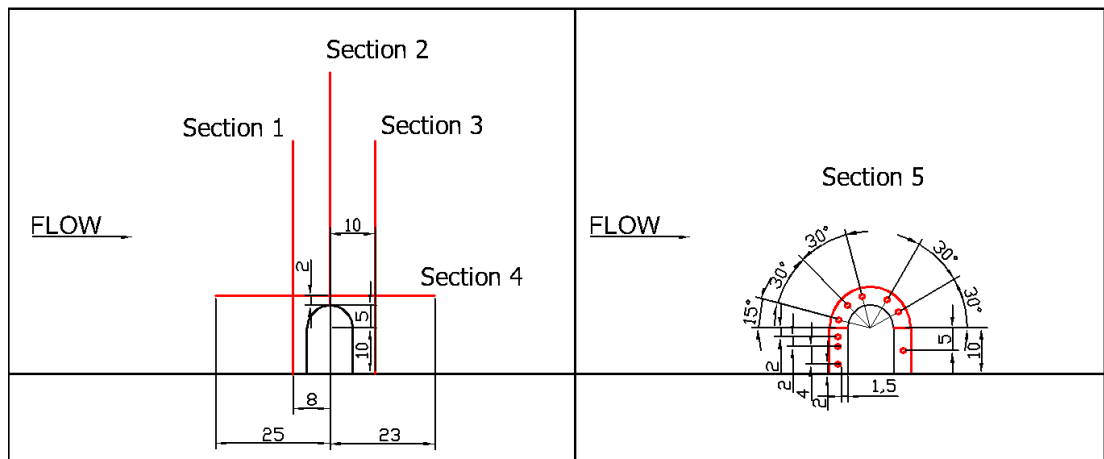


Figure 5.7 Schematic illustration of the sections taken around the abutment model of  $L_a=15$  cm for the flow depth of  $y=17.4$  cm (linear dimensions are given in cm)

The lateral profile of the time development of local scour around the abutment model at section 1 is presented in Figure 5.8. According to this figure, it is seen that there is a rapid development of scour hole at the upstream of the abutment model up to three hours of experiment period.

After this time period, the scour hole continues to develop at a slower rate until the end of the experiment. Throughout the experimental period, the rate of development of scour in the lateral direction is much smaller than the increase in the depth of scour in this case. The side slopes of the scour hole are almost parallel to each other through the test period, and the bathymetry lines corresponding to the sides of the scour hole are observed so close to each other after three hours of experimental duration.

When the scour formations around the abutment models for two different flow depths are compared, it is observed that at the upstream of the abutment, the development of scour hole is rapid during the first three hours of the experiment in both cases. Thereafter, the rate of development of scour decreases in each case according to the results of the experiments. Besides the side slopes of the scour holes are observed parallel to each other throughout the test period in both of these cases. Moreover, nondimensional maximum scour depth at this section is approximately 7 times smaller compared to the one observed at the smaller flow depth (Figure 5.2). These results lead to the formation of a wider scour hole at  $y=13.5$  cm than the other scour formation.

Thus, it can be concluded that at the upstream of the abutment, the time development of scour hole basically shows similarities for the two different flow depths with respect to the trend of the development of the scour holes in general. However, at higher flow depth, the maximum scour depth is smaller.

The temporal development of local scour at the toe of the abutment model perpendicular to the flow direction is given in Figure 5.9. According to this figure, it can be noticed that there is a rapid development of scour at locations close to the toe of the abutment model. In Figure 5.9, it is also observed that the side slopes of the scour hole are parallel to each other throughout the test period. Moreover, there is not a particular change in the bathymetry levels in the lateral direction for the region where  $\xi/y > 1.25$  throughout the experiment.

In Figure 5.10, the time development of local scour at the downstream of the abutment model is presented. In the lateral direction, there is a particular change in the bathymetry levels between approximately  $0.55 < \xi/y < 1.55$  throughout the experiment period. Except this zone, there is not any significant change in the bathymetry profiles up to the end of the experiment. At the beginning of the test period, a deposition pattern forms within this zone, and as time progresses, this deposited zone is gradually scoured. At the end of the experiment, there observed two ridges of deposition pattern formed at two sides of the scoured zone at this region.

In Figure 5.11, the time development of local scour around the abutment model at section 4 is presented. In this figure, both scour and deposition pattern are observed at  $t=0.5$  h. As time passes, the deposition pattern located between  $0.5 < x/y < 1.2$  is eroded, whereas the scour hole becomes deeper and wider.

The temporal development of local scour around the peripheral surface of the abutment model is shown in Figure 5.12. According to this figure, it is observed that the maximum local scour depth occurs at approximately  $r/y=0.85$  corresponding to the upstream side of the toe of the abutment model, where the maximum scour depth is recorded as  $z/y=-0.12$ .

When the scour formations around the abutment models for two different flow depths are compared, it is obtained that the maximum local scour depth shifts to the upstream part of the abutment toe with the increase in the flow depth.



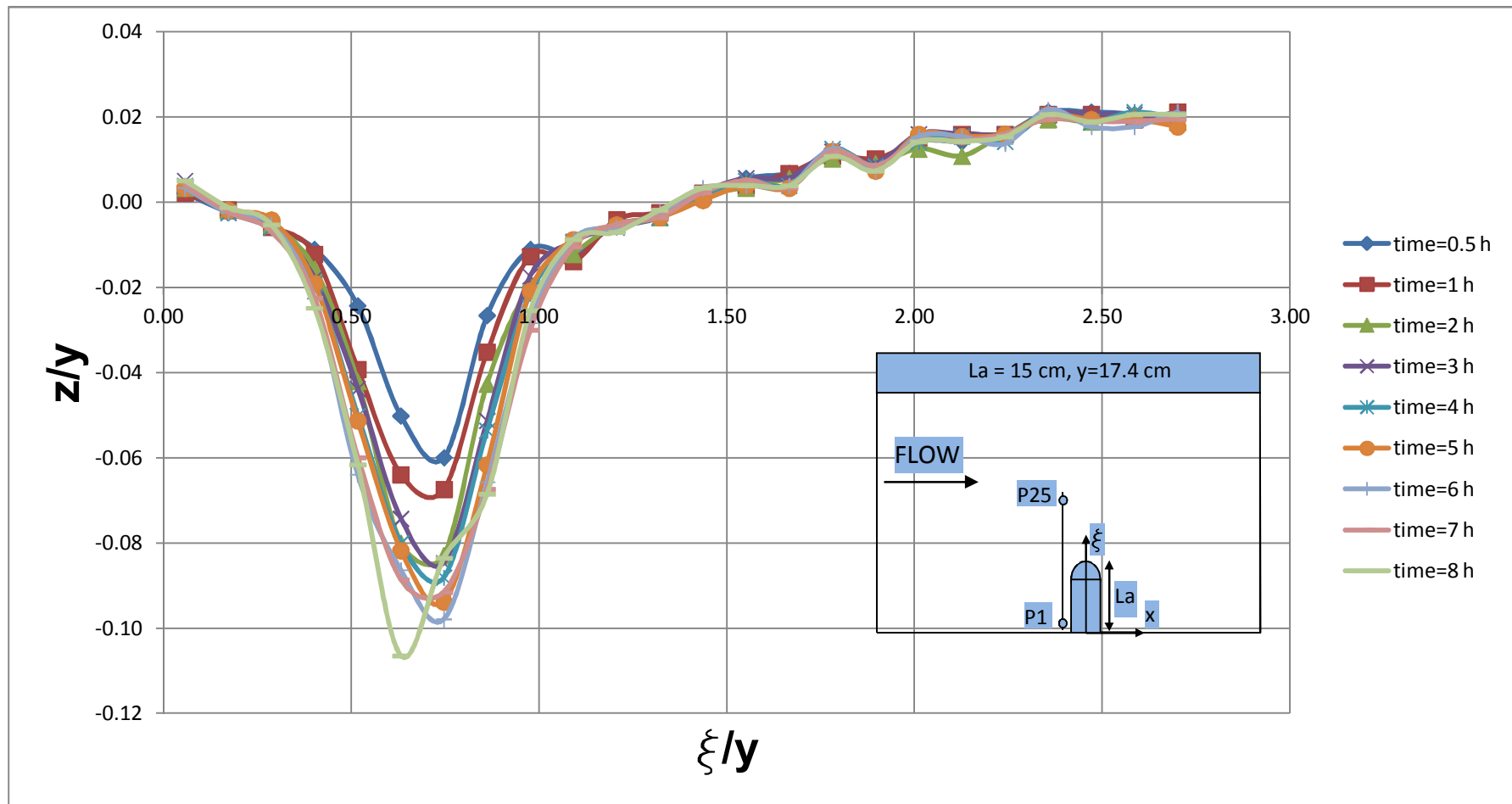


Figure 5.8 Time development of local scour around the abutment model of  $L_a=15 \text{ cm}$  at section 1

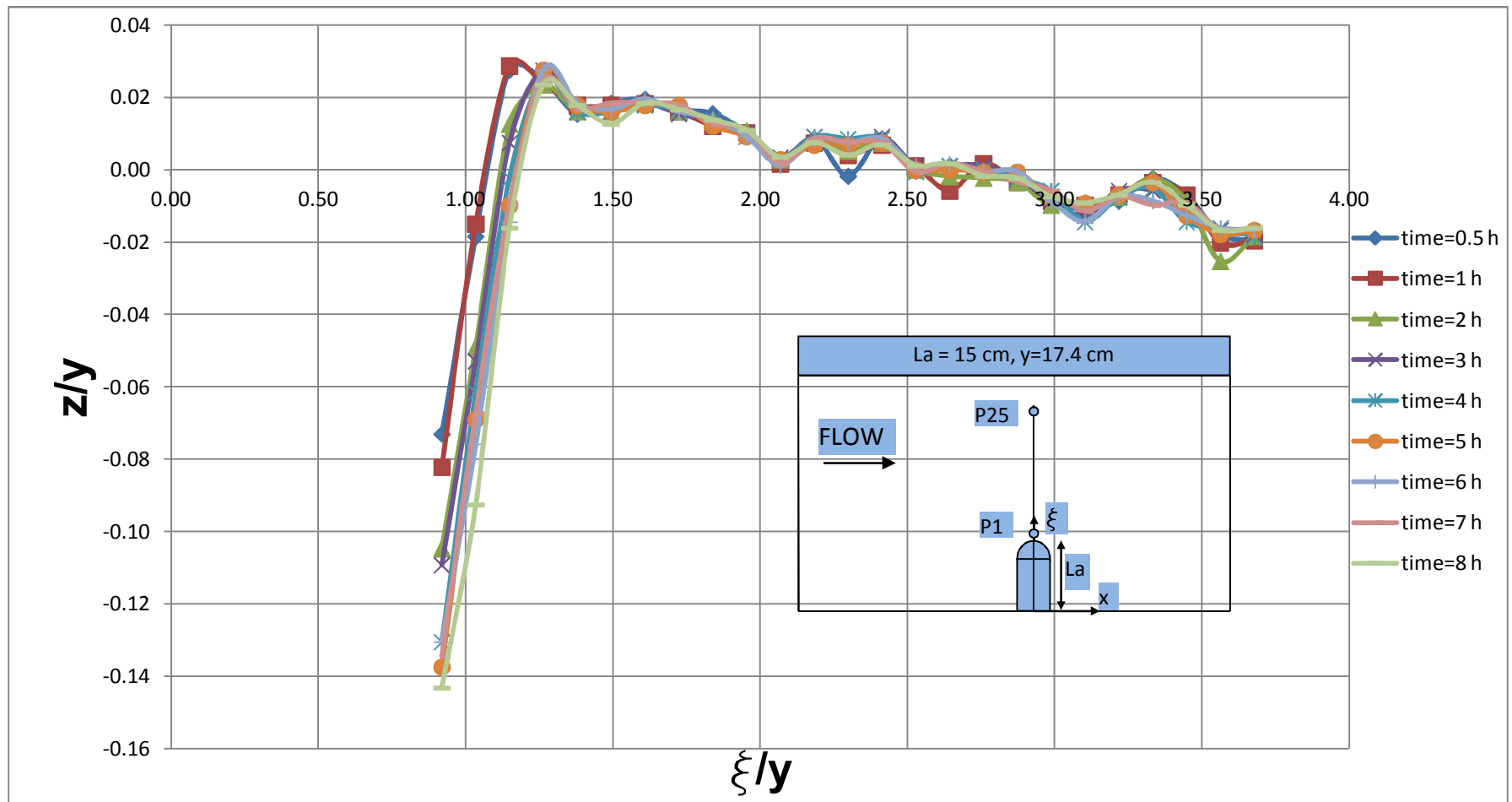


Figure 5.9 Time development of local scour around the abutment model of  $L_a=15$  cm at section 2

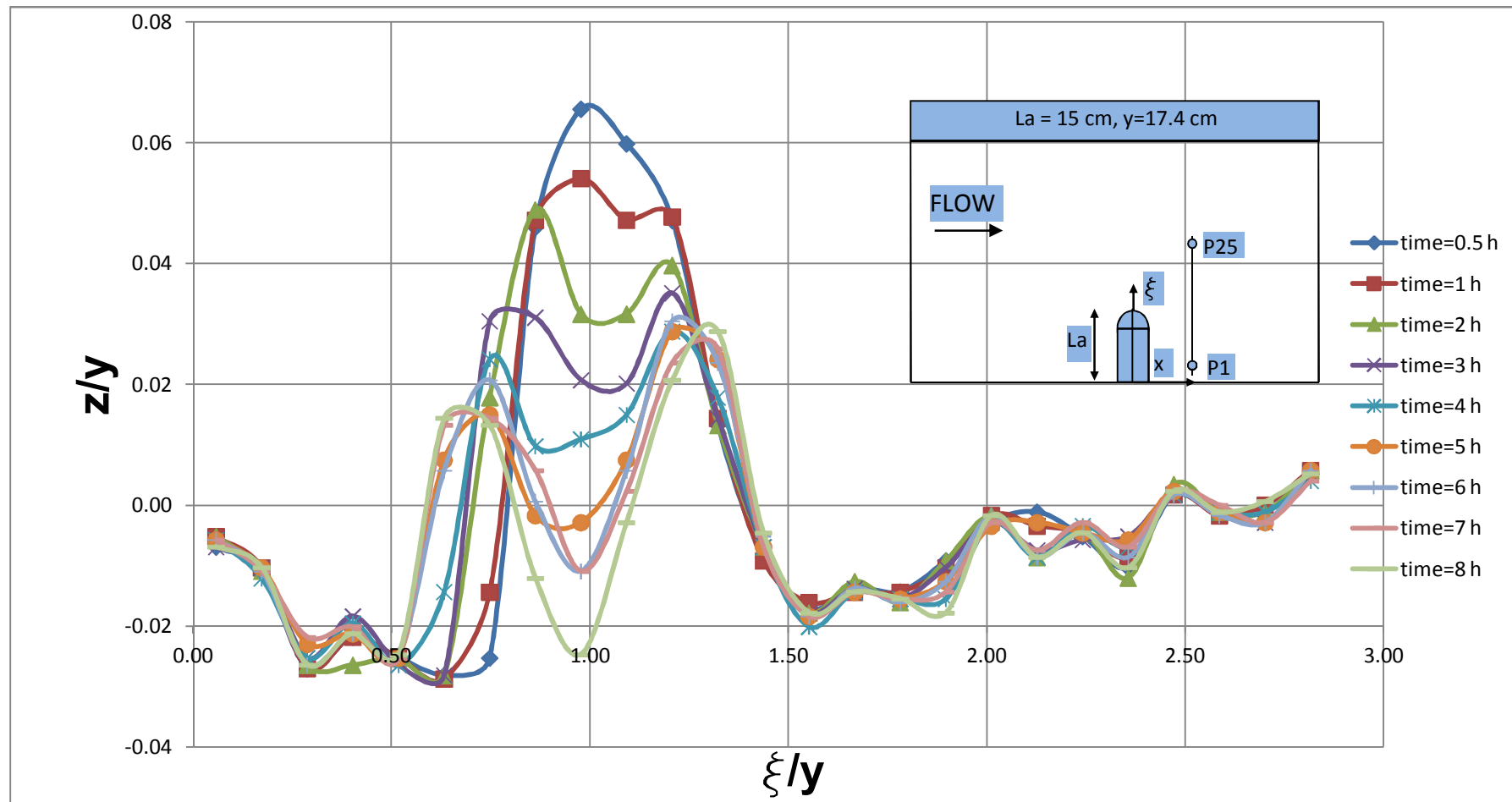


Figure 5.10 Time development of local scour around the abutment model of  $L_a=15 \text{ cm}$  at section 3

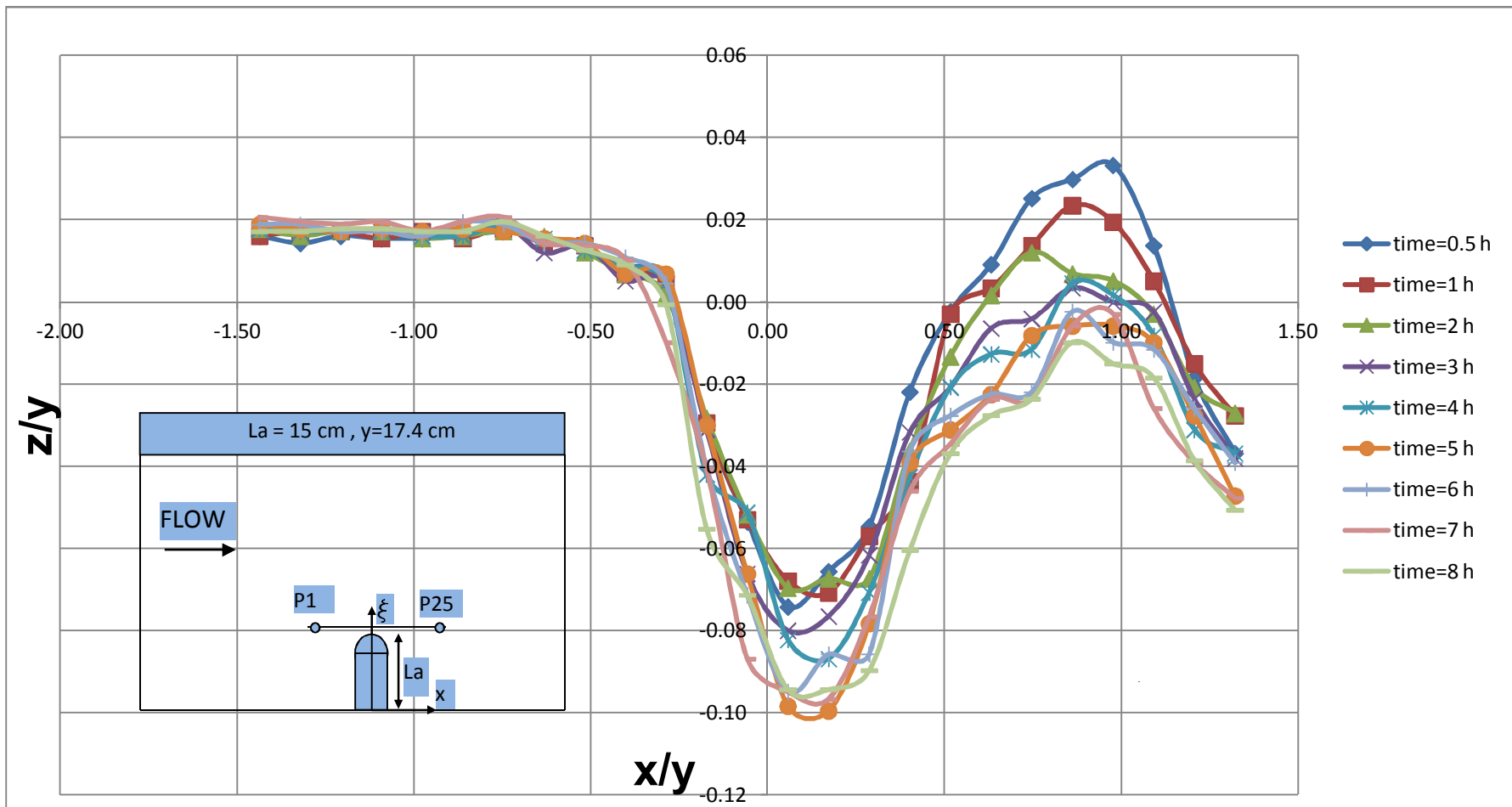


Figure 5.11 Time development of local scour around the abutment model of  $L_a=15 \text{ cm}$  at section 4

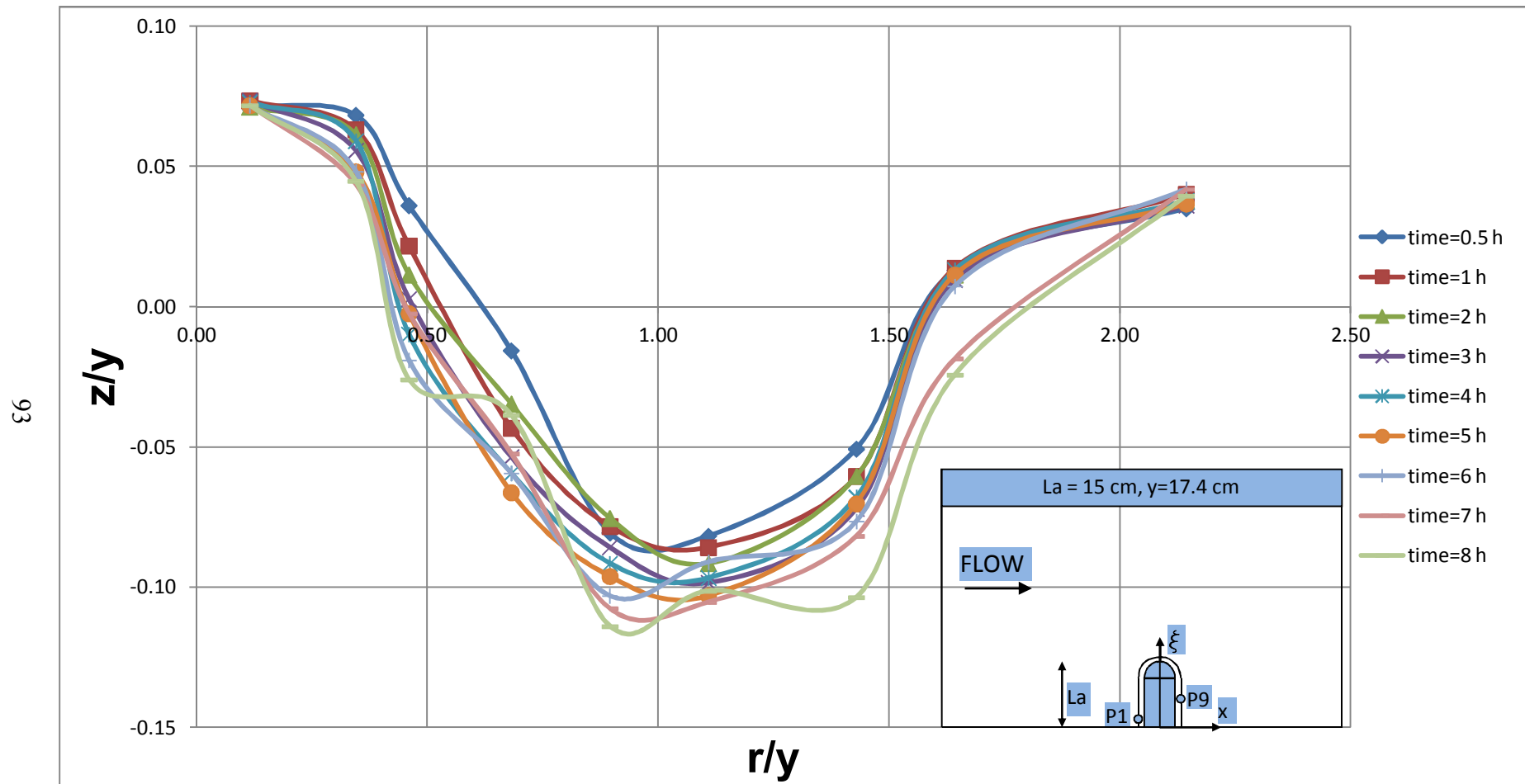


Figure 5.12 Time development of local scour around the abutment model of  $L_a=15$  cm at section 5

### 5.2.2 Time Development of Scour Hole at Long Abutment ( $L_a=35$ cm)

The time development of scour hole around the abutment model of  $L_a=35$  cm will be investigated in the following sections for two different flow depths of  $y=13.5$  cm and  $y=17.4$  cm. The location of the sections around the abutment model and the experimental results for the two different flow depths are presented in each case.

#### 5.2.2.1 Time Development of Scour at the Flow Depth of $y=13.5$ cm

The results of the experimental investigations of the time development of local scour around the abutment of  $L_a=35$  cm at the flow depth of  $y=13.5$  cm are given in Figures 5.14 to 5.18. A schematic illustration of the locations of the sections around the abutment model is presented in Figure 5.13. In this case, sections 1, 2 and 3 are located perpendicular to the flow direction similar to Figure 5.1; however, the sections at the downstream and upstream of the abutment are located at a longer distance from the abutment model. The reason is that the scour hole is formed in a larger area in the case of experiments with the abutment of  $L_a=35$  cm.

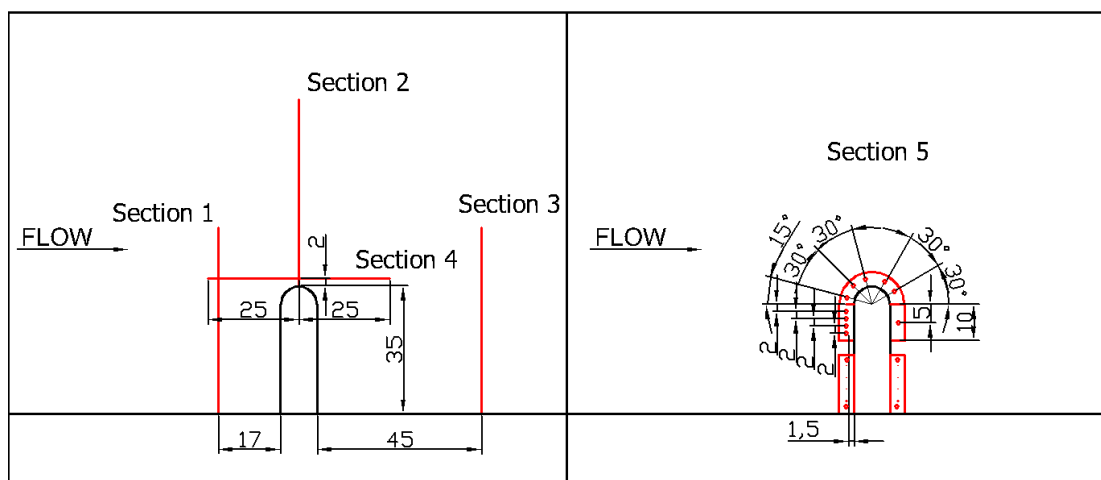


Figure 5.13 Schematic illustration of the sections taken around the abutment model of  $L_a=35$  cm at the flow depth of  $y=13.5$  cm (linear dimensions are given in cm)

In Figure 5.14, the time development of local scour around the abutment model at section 1 is presented. During the first three hours of experiment period, the rate of development of scour is rapid at this section as in the case of the experiment at the same flow depth with the abutment of  $L_a=15$  cm. Thereafter, the scour hole continues to develop at a slower rate up to the end of the experiment. According to Figure 5.14, it can also be noticed that the side slopes of the scour hole decreases with time, and this decline in slope is associated with the development of a wider scour hole at this section, compared to the short abutment case.

Based on the results of the experiments carried out at the same flow depth with two different abutment models of  $L_a=15$  cm and  $L_a=35$  cm, the rate of development of scour is observed to be higher for the long abutment case. Besides, the results of the experiments on temporal development of local scour indicate that at the upstream of the abutment, scour hole is formed within a wider distance in the lateral direction at  $L_a=35$  cm. Moreover, when the time development of the side slopes of these two cases are compared, it is noticed that as a part of the development of local scour, the side slopes of the scour hole are observed milder in the case of  $L_a=35$  cm. Thus, it should be noted that at the same flow depth, as the abutment length increases, the rate of development of scour hole increases, and a comparably wider and deeper scour forms with the progress of time.

The lateral profile of the temporal development of local scour at the toe of the abutment model perpendicular to the flow direction is given in Figure 5.15. In this figure, it is seen that scour hole deepens rapidly just at the toe of the abutment model in three hours period. After this time period, the development of scour continues gradually until the end of the experiment. In Figure 5.15, it is also noticed that the side slopes of the scour hole are almost parallel to each other throughout the test period. As time progresses, scour hole is also developed in the lateral direction along with the increase in the depth of scour in the downward direction. Moreover, there is not a particular change in the bathymetry levels in the lateral direction beyond approximately  $\xi/y=6$  up to the end of the experiment period.

When the results of the time development of local scour at the same flow depth for two different abutment lengths are compared, there is a remarkable difference between the two cases with respect to the development of the side slopes of the scour formations. In the long abutment case, the scour hole does not have a continuous slope; rather there are two slopes that are connected with a much milder slope.

In Figure 5.16, the time development of local scour at the downstream of the abutment model is presented. According to this figure, it is seen that there is a rapid development of deposition pattern at the downstream of the abutment, and this formation is shifting towards the flume channel wall until the end of third hour. During this movement, the slope of the deposition hill on the main channel side continuously increases, and after three hours it remains constant. On the other hand, the slope of the deposition hill on the channel wall side remains constant throughout the whole experiment. The height of the deposition hill is also constant throughout the rest of the experiment after this time. On the contrary, there is continuous erosion towards the main channel. According to the results of the experiments conducted with abutments of  $L_a=15$  cm and  $L_a=35$  cm at the same flow depth, the dimensionless maximum deposition level at the downstream of the abutment model is approximately 90 % larger compared to the one observed in the small abutment case (Figure 5.4).

The time development of local scour around the abutment model at section 4 is presented in Figure 5.17. Similar to the short abutment case (Figure 5.5), throughout the whole experimental period, the scour hole slopes at the downstream and upstream sides remain parallel. Moreover, at these two abutment lengths, the growth of the scour hole is rapid for the first three hours. The only difference is that the scour hole is larger for the long abutment case.

In Figure 5.18, the temporal development of local scour around the peripheral surface of the abutment model is shown. Based on this figure, it is observed that the maximum scour depth is  $1.8z/y$  which is approximately 80 % larger compared to the



one observed in the short abutment case (Figure 5.6). Different from the short abutment case, the maximum scour depth is observed at approximately  $r/y=1.75$  which is located at the upstream side of the toe of the abutment model.

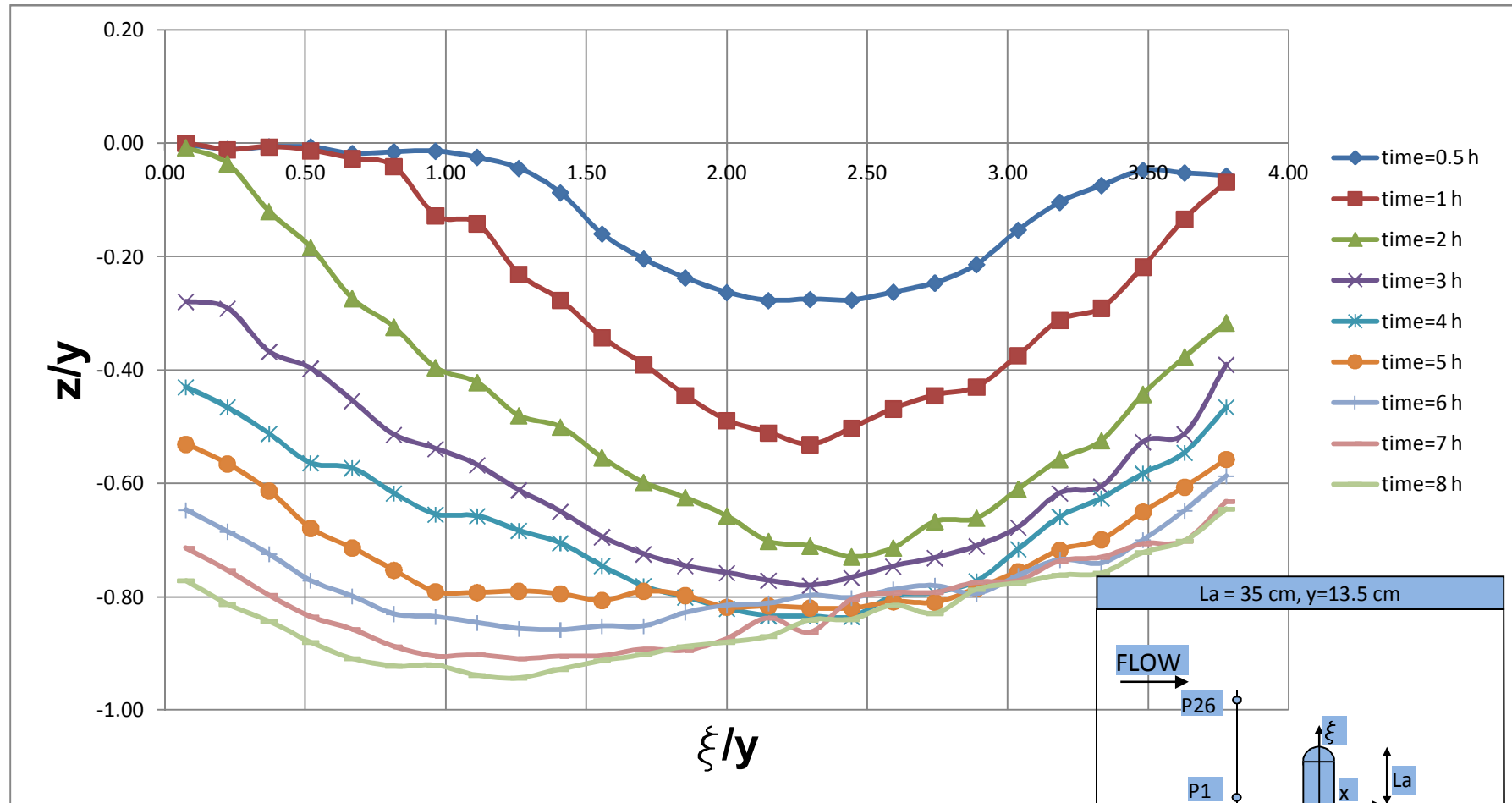


Figure 5.14 Time development of local scour around the abutment model of  $L_a=35$  cm at section 1

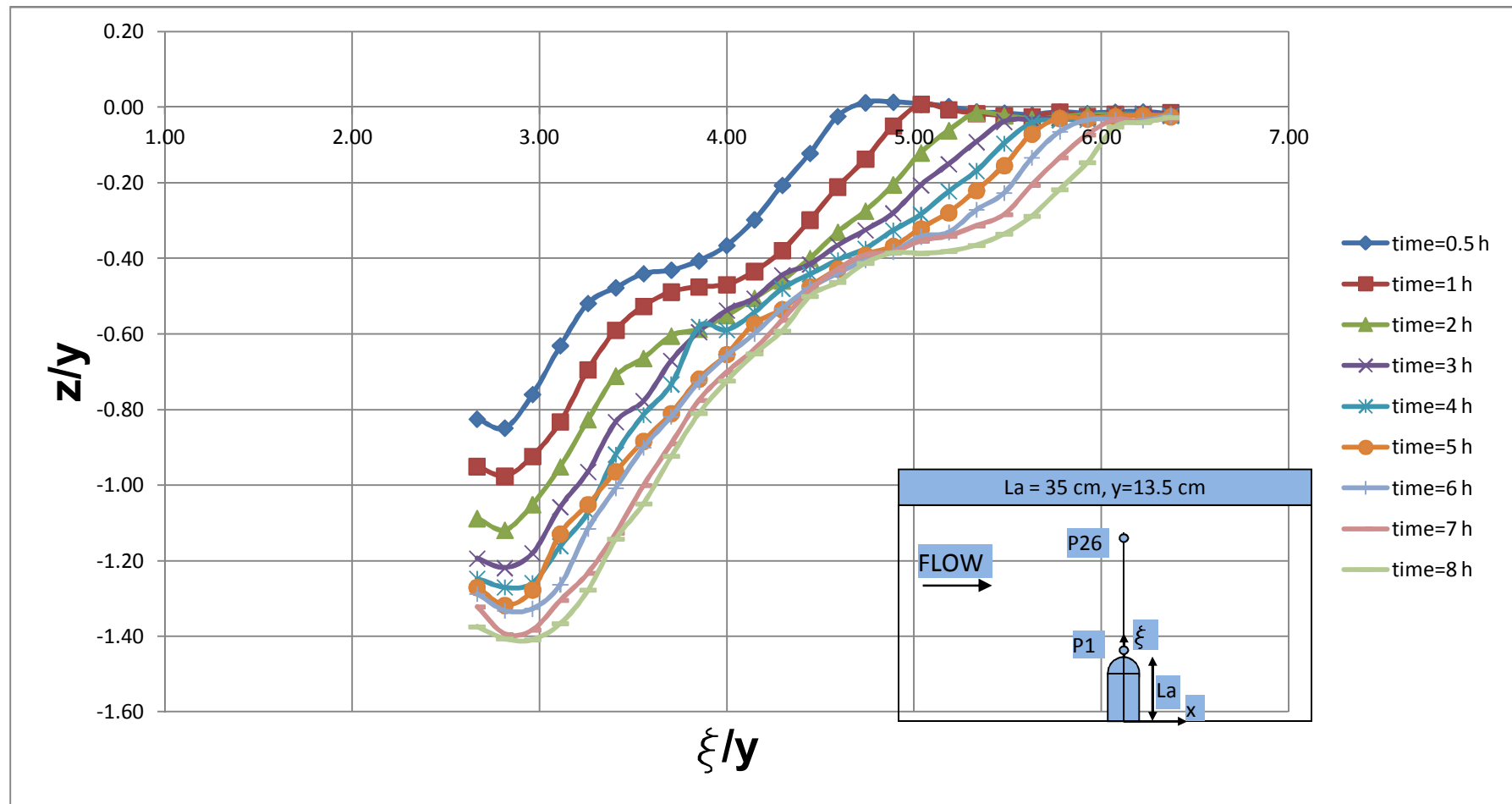


Figure 5.15 Time development of local scour around the abutment model of  $L_a=35 \text{ cm}$  at section 2

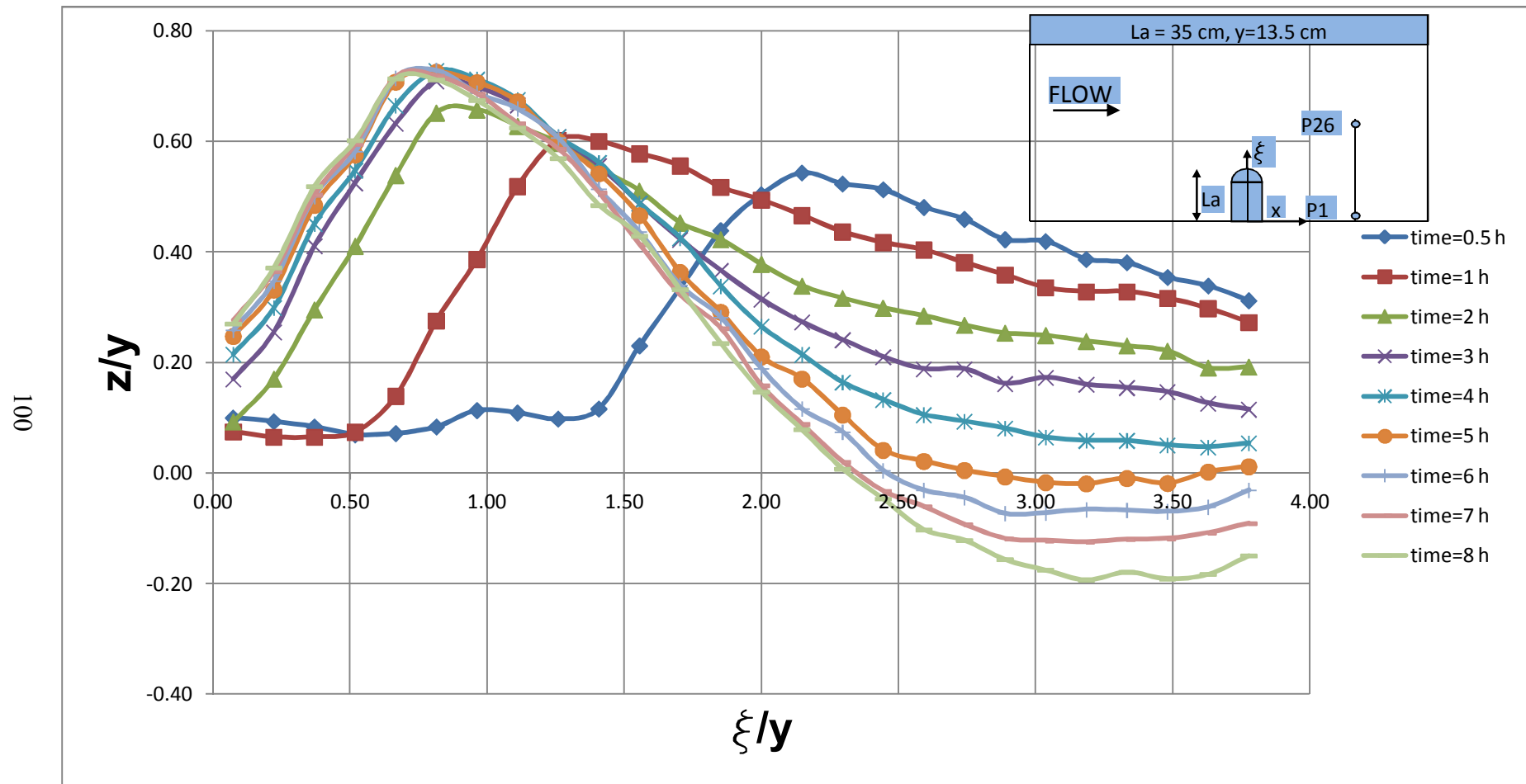


Figure 5.16 Time development of local scour around the abutment model of  $L_a=35 \text{ cm}$  at section 3

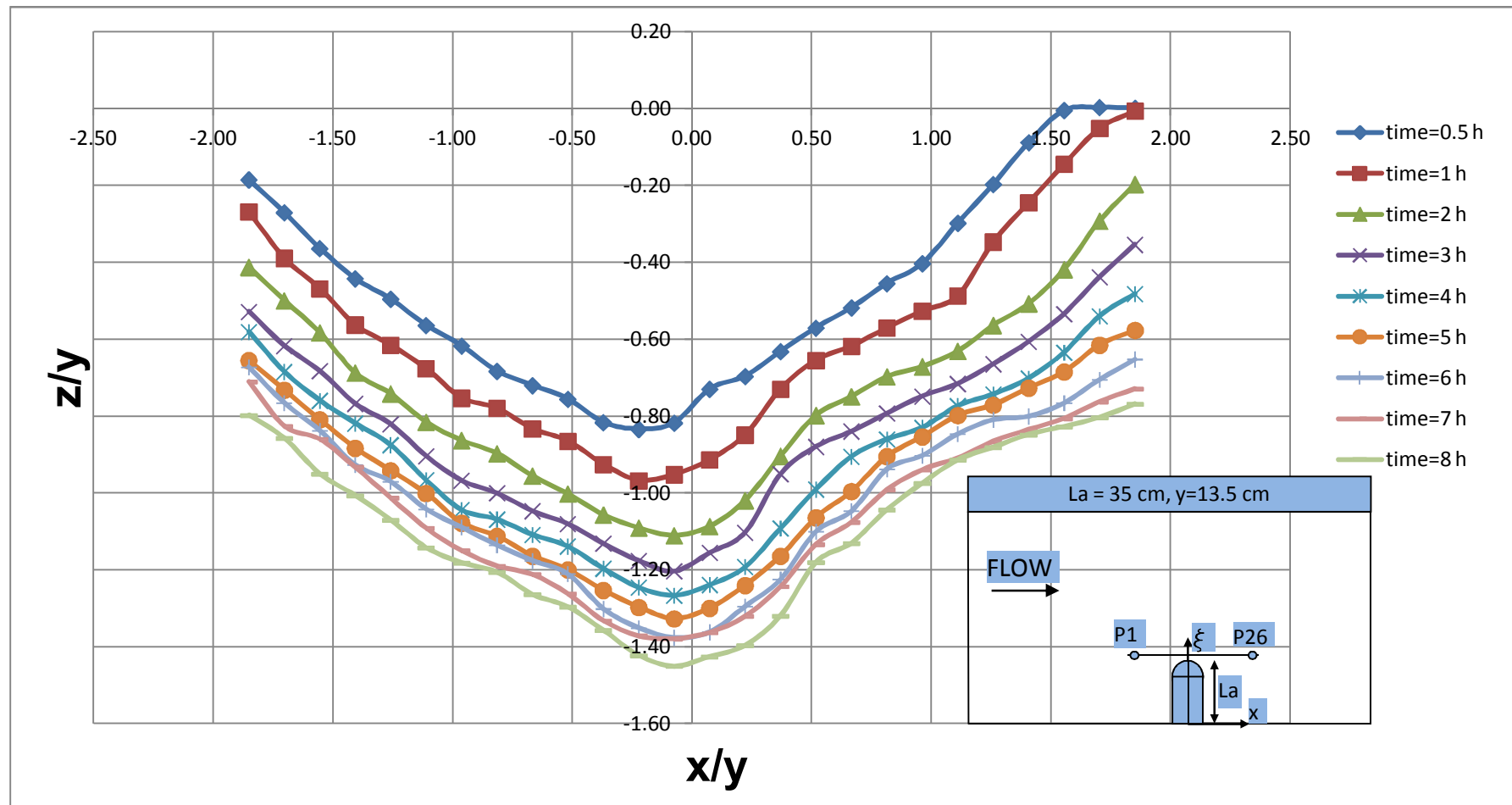


Figure 5.17 Time development of local scour around the abutment model of  $L_a=35$  cm at section 4

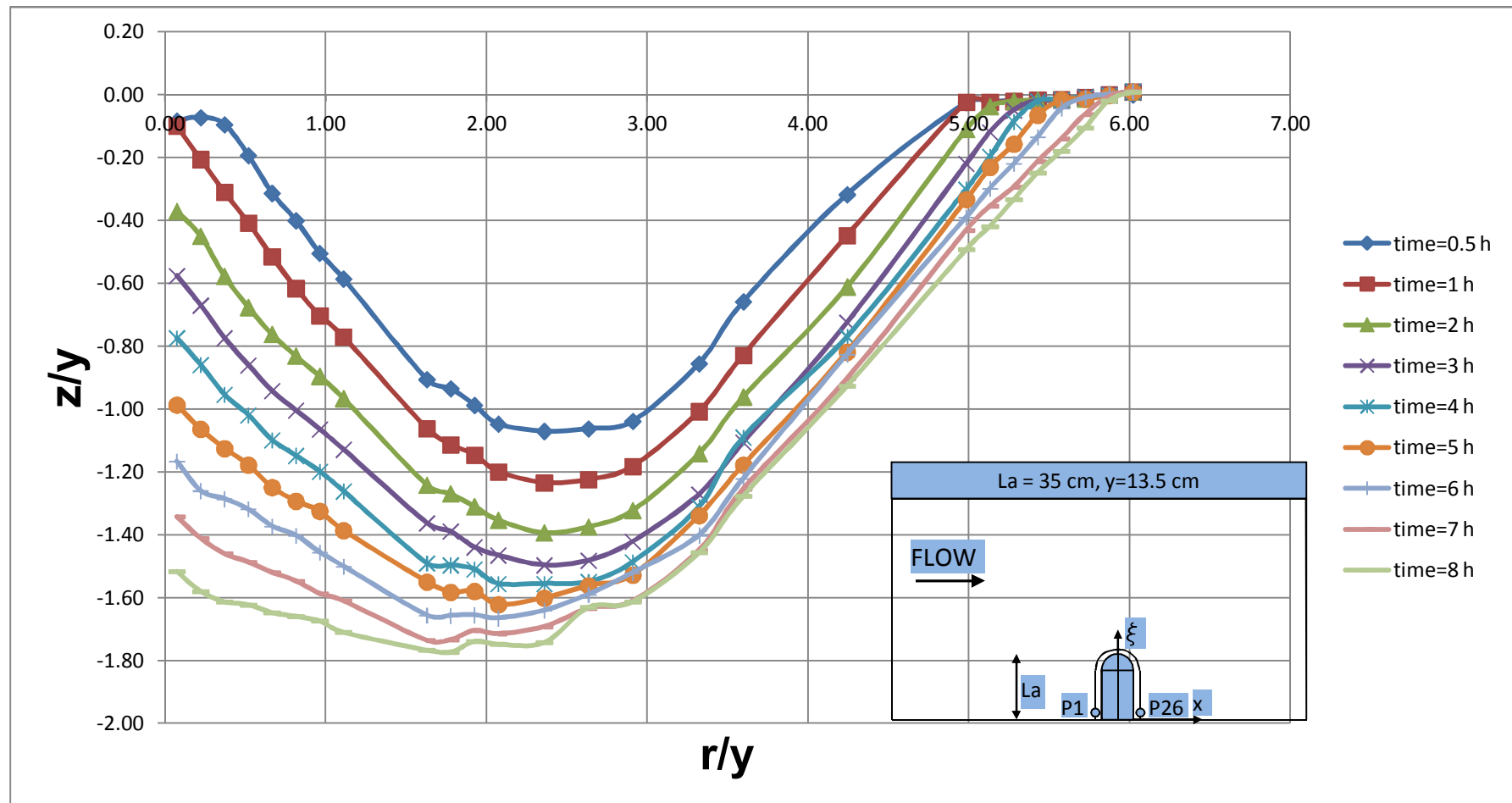


Figure 5.18 Time development of local scour around the abutment model of  $L_a=35 \text{ cm}$  at section 5

### 5.2.2.2 Time Development of Scour at the Flow Depth of $y=17.4$ cm

The results of the experimental investigations of the time development of local scour around the abutment of  $L_a=35$  cm at the flow depth of  $y=17.4$  cm are given in Figures 5.20 to 5.24. A schematic illustration of the locations of the sections around the abutment model is presented in Figure 5.19. In this figure, sections 1, 2 and 3 are located perpendicular to the flow direction similar to Figure 5.13. However, there exists a slight difference in the locations of the transversal sections compared with the previous layout for the case with abutment of  $L_a=15$  cm at the same flow depth. In this case, the sections at the downstream and upstream of the abutment are placed at a longer distance from the abutment model.

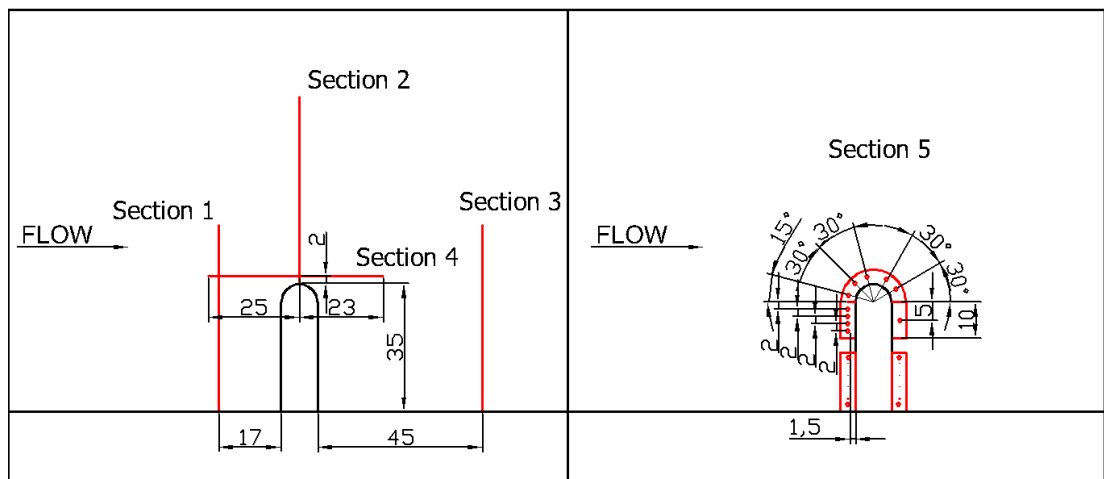


Figure 5.19 Schematic illustration of the sections taken around the abutment model of  $L_a=35$  cm at the flow depth of  $y=17.4$  cm (linear dimensions are given in cm)

In Figure 5.20, the lateral profile of the time development of local scour around the abutment model through section 1 is presented. Unlike the previous experimental results, the time development of local scour at the upstream of the abutment shows a particularly different trend among other cases.

In this figure, it is remarkable that during the first three hours of experiment period, there is no significant scour development and after this period of time, scour starts to develop rapidly up to the end of the experiment period. This is because the scour hole cannot reach the test section until the end of third hour. Moreover, the side slopes of the scour formation are observed milder during the first three hours of experiment. Thereafter, side slopes become steeper with time, and at the end of the experiment duration there observed a particular change in the sides and the depth of the scour.

In Figure 5.21, the lateral profile of the temporal development of local scour at the toe of the abutment model perpendicular to the flow direction is presented. Based on this figure, it is seen that scour hole deepens rapidly in three hours period of time as in the case of time development of local scour for the same abutment length tested at the flow depth of  $y=13.5$  cm (Figure 5.15). Thereafter, the scour hole continues to develop at a slower rate up to the end of the experiment.

Similar to the experiment performed using the same abutment at a lower flow depth, scour hole is composed of two stages where there is a milder slope in between those two. Furthermore, maximum scour depth observed at this section is only 60 % of the value observed for the same abutment at the flow depth of  $y=13.5$  cm.

In Figure 5.22, the time development of local scour at the downstream of the abutment model is presented. Similar to the findings with the same abutment model at the lower flow depth, the deposition hill is moving towards the channel wall. Unlike the case of the smaller flow depth, this movement is continueing until the end of the experiment. The slope of the hill on the main channel side remains constant after three hours period of time, similar to the experiment at the lower flow depth.

In Figure 5.23, the temporal development of local scour around the abutment model through section 4 is given. In this figure, it is seen that scour hole deepens rapidly just at the toe of the abutment model in three hours period of time as in the case of



the time development of local scour for the same abutment length tested at  $y=13.5$  cm (Figure 5.17). Thereafter, the scour hole continues to develop gradually till the end of the experiment. According to Figure 5.23, it is also noticed that the side slopes of the scour hole are almost parallel to each other throughout the test period.

The time development of local scour around the peripheral surface of the abutment model is presented in Figure 5.24. According to the results of the experiments conducted with the abutment of  $L_a=35$  cm at two different flow depths, the maximum scour depth is observed at the same point at  $r/y=1.75$ . However, the nondimensional maximum scour depth is 0.73 which is approximately 40 % of the scour depth observed in the case of the lower flow depth (Figure 5.18).

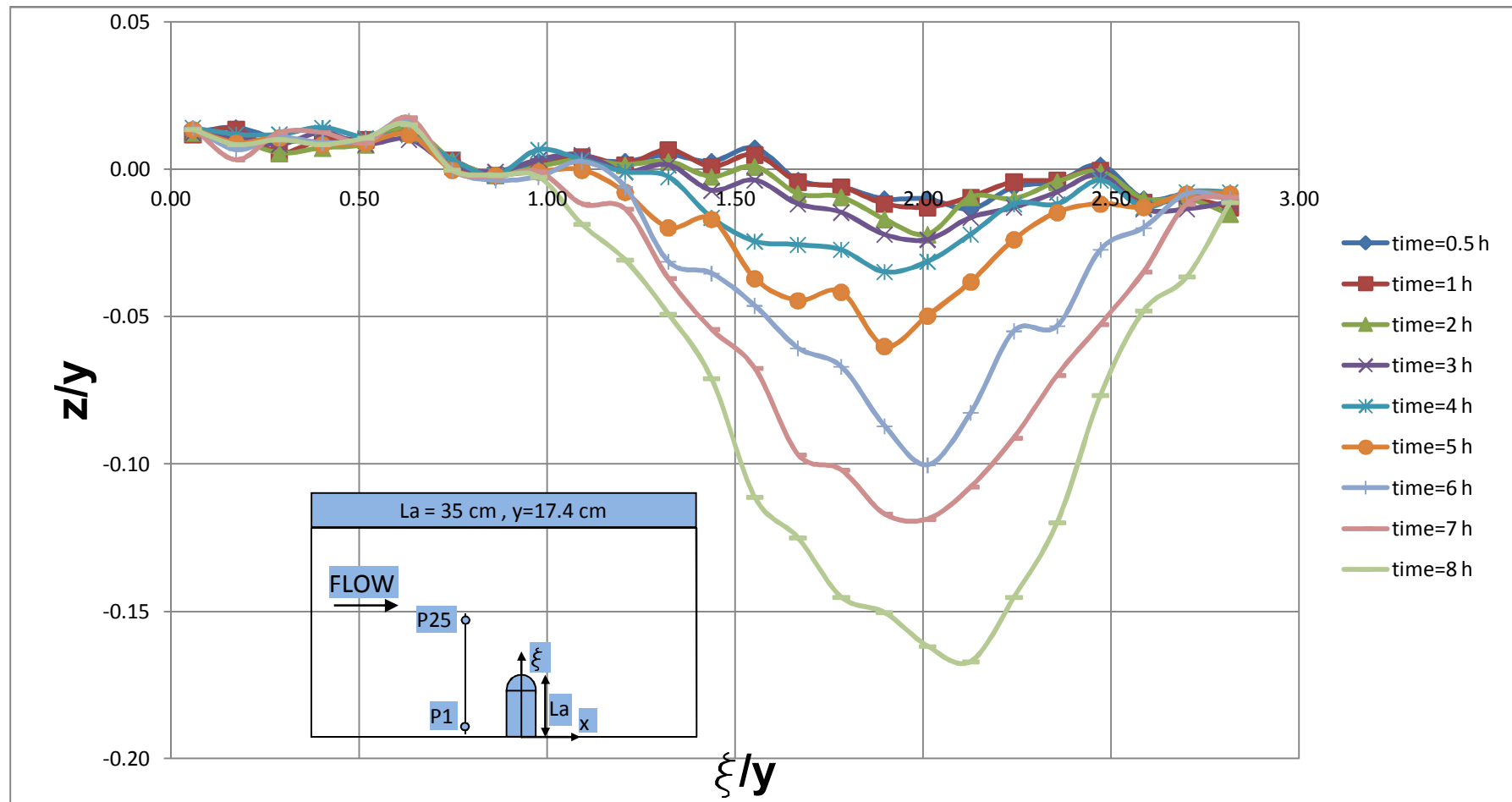


Figure 5.20 Time development of local scour around the abutment model of  $L_a=35 \text{ cm}$  at section 1

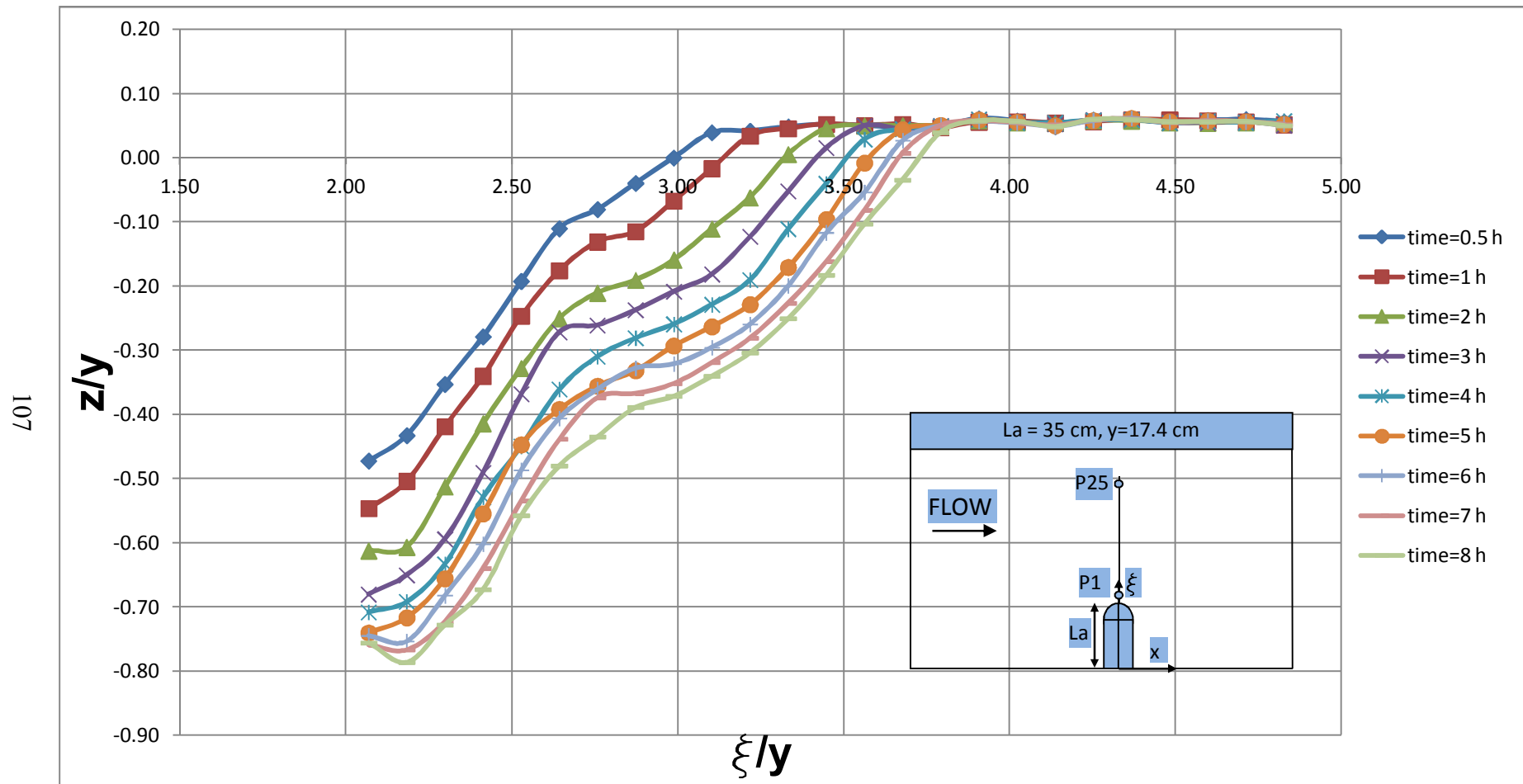


Figure 5.21 Time development of local scour around the abutment model of  $L_a=35$  cm at section 2

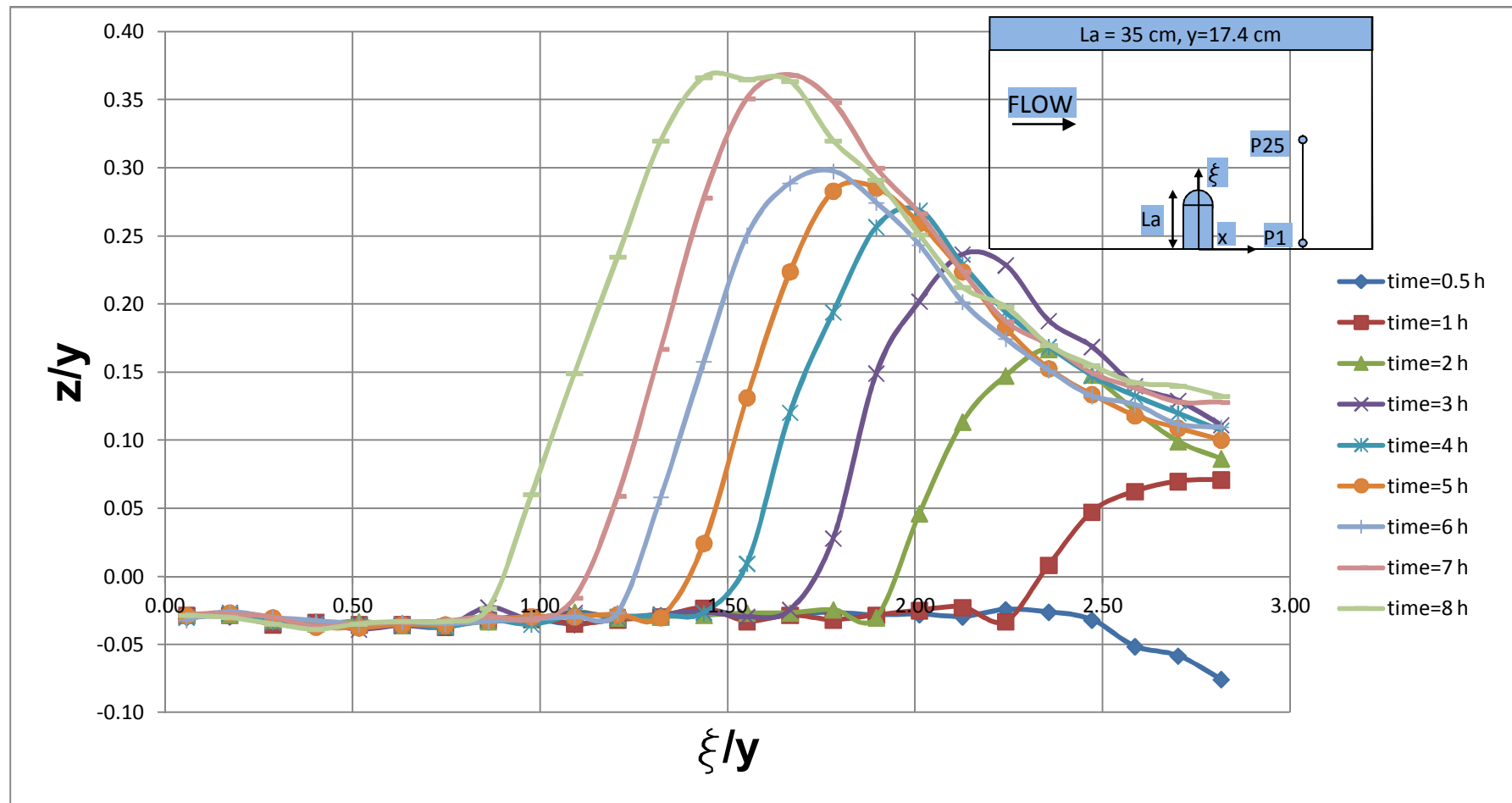


Figure 5.22 Time development of local scour around the abutment model of  $L_a=35 \text{ cm}$  at section 3

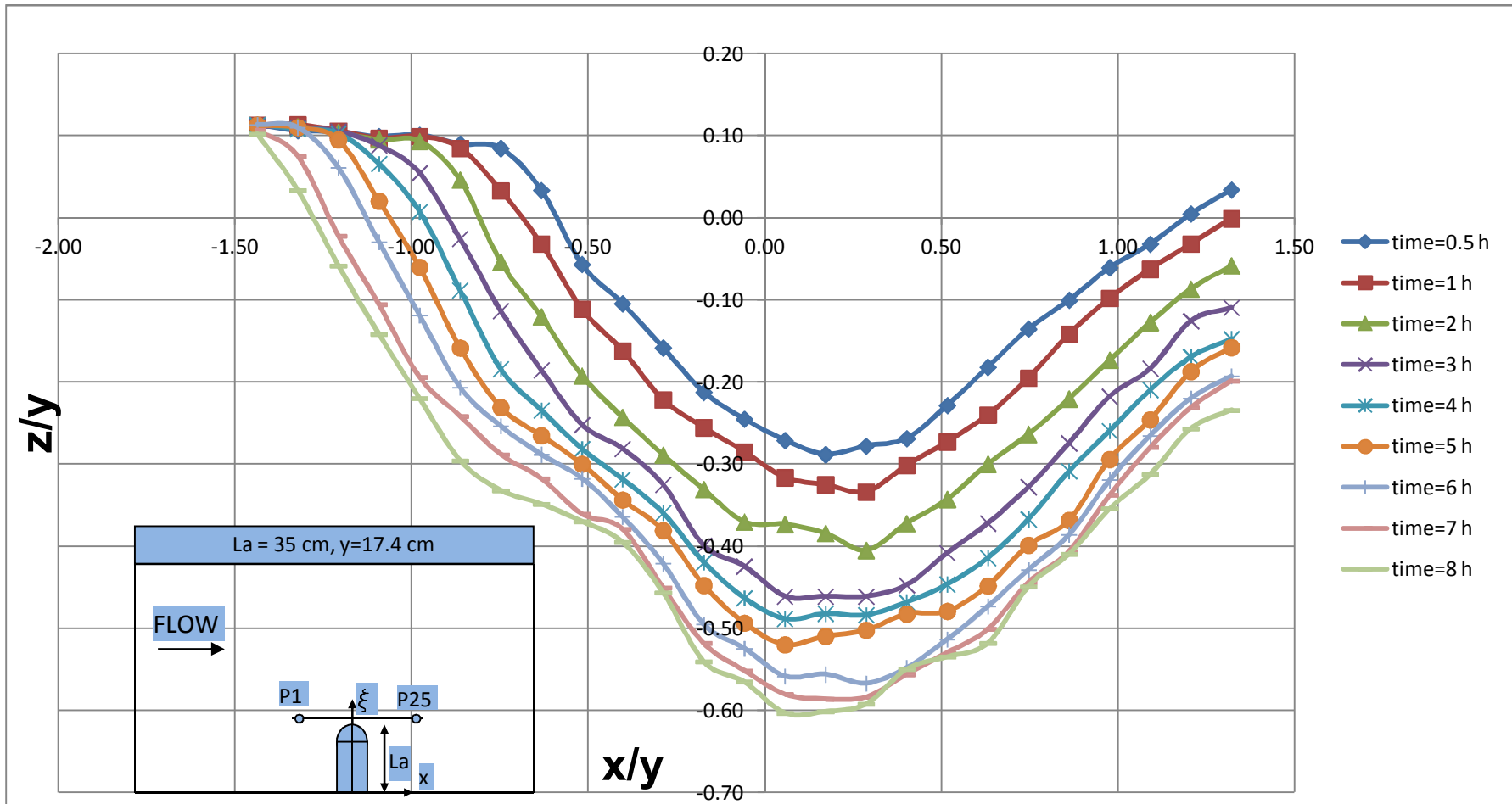


Figure 5.23 Time development of local scour around the abutment model of  $L_a=35 \text{ cm}$  at section 4

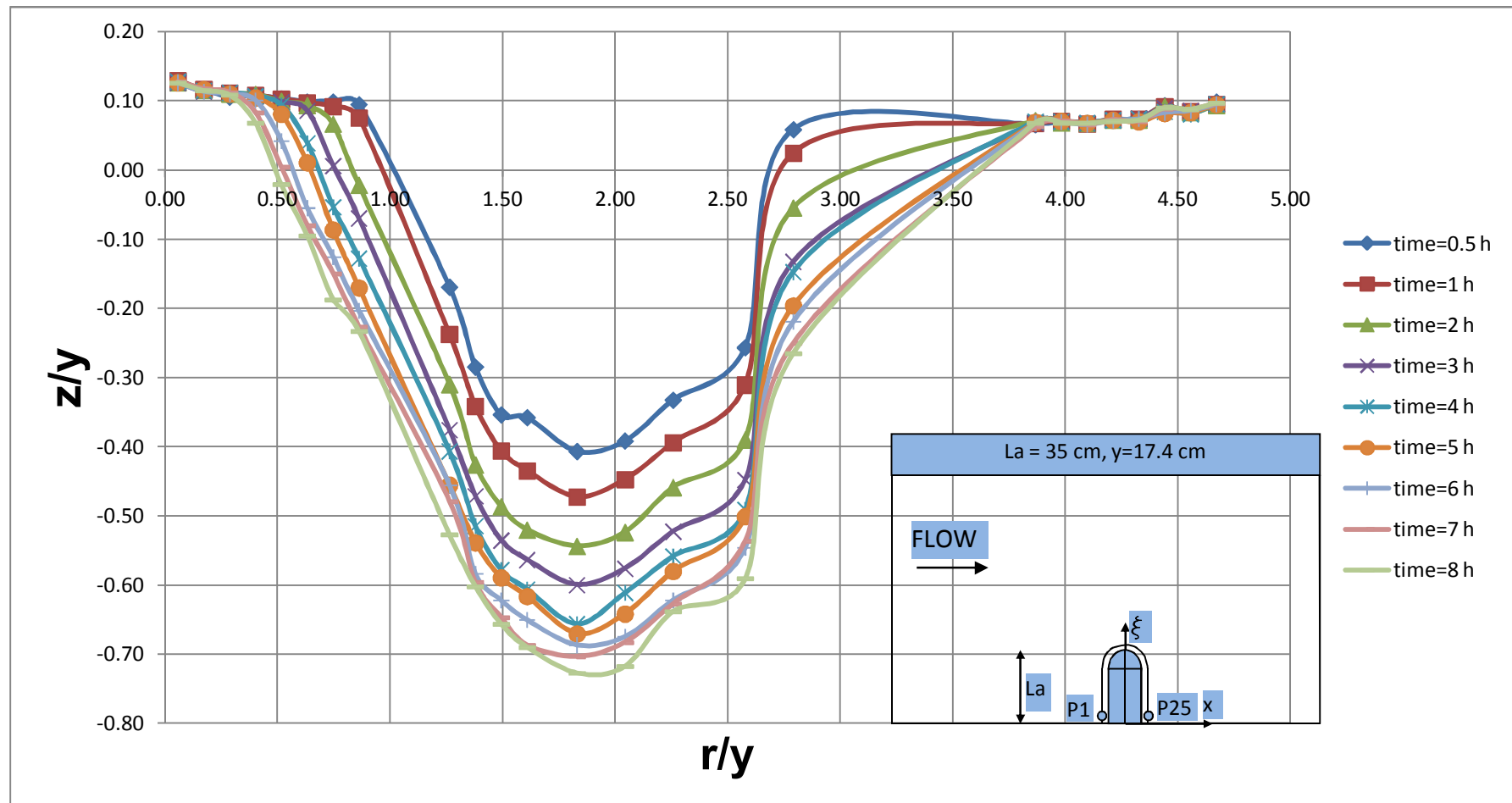


Figure 5.24 Time development of local scour around the abutment model of  $L_a=35$  cm at section 5

## CHAPTER 6

### CONCLUSIONS AND RECOMMENDATIONS

#### 6.1 CONCLUSIONS

In the laboratory flume, experimental investigations were performed in order to investigate the effects of flow depth and collars, attached to the semi-circular end abutment models, on the development of local scour around bridge abutments. Also, the effects of flow depth and abutment length on the time development of local scour were studied using two different abutment models without a collar. The results of the experimental investigations have been presented and the following conclusions can be drawn:

- Collars were found to be effective in reducing the development of local scour around semi-circular end bridge abutments.
- The scour reduction performances of collars increase as the collar width,  $B_c$  increases (Figure 4.2).
- The dimensionless maximum scour depth corresponding to the optimum collar size,  $(d_s)_{\max,c} / y$ , increase as the dimensionless abutment length,  $L_a/B$  increases for a given collar size, both for the two different flow depths similar to the previous result of Daşkın (2011), (Figure 4.4).

- Similar trends were observed for the variation of  $(d_s)_{\max,c} / y$  with  $\sqrt{\theta(L_a/B_c)}$  both for semi-circular end and rectangular abutments, (Figure 4.6). The dimensionless maximum scour depth corresponding to the optimum collar size increases with the increase in  $\sqrt{\theta(L_a/B_c)}$  value.
- The optimum location of collars  $[Z_c/y]_{\text{opt}}$ , is obtained at the sand bed level for the flow intensity of  $U/U_c=0.70$  for all  $L_a/B_c$  values; whereas for the value of  $U/U_c=0.80$ , the optimum location of collars are obtained at  $[Z_c/y]_{\text{opt}}=-0.25$  for  $L_a/B_c \leq 3.0$ , and at  $[Z_c/y]_{\text{opt}}=-0.50$  for the values of  $L_a/B_c > 3$ .
- At the upstream of the abutment, the depth of the local scour increases rapidly within the duration of first three hours of the experiment for the different flow depths, and the rate of development of scour hole decreases after this time period as a general trend.
- As the abutment length increases, the maximum scour depth increases.
- As the flow depth increases, the maximum scour depth decreases.
- Throughout the scour process, the deposition hill forming at the downstream of the abutment moves both in the streamwise and lateral direction towards the channel sidewall on which the abutment model is attached.

## 6.2 RECOMMENDATIONS

Abutment scour has been a major concern to ensure the safety of the bridge, and therefore further studies are still required to prevent or mitigate the scour phenomenon in an effective manner to protect the bridges from the imminent danger of scour failure (Khwairakpam and Mazumdar, 2009).



Hence, recommendations regarding future works in relation to the current study are given as follows:

- Although the present study is confined to two different  $U/U_c$  ratios in order to investigate the effect of flow depth on the scour reduction performances of collars, it would be useful to perform more experiments at different  $U/U_c$  ratios so that the interaction between the flow depth and scour reduction efficiency of collars may further give valuable results to the behaviour of collar under these circumstances.
- The use of collars as a countermeasure for local scour may be tested with bridge abutments and piers of various sizes together by placing the collars at different elevations on both structures in order to investigate the efficiency of collars associated with the abutment pier interaction.
- It may be useful to perform experiments with and without collars under live-bed scour conditions concerning the temporal development of local scour phenomenon.
- In the present study and the previous investigations, the collars are tested using a physical hydraulic model in the laboratory. The efficiency of the collars may be tested in the field conditions by performing prototype studies for the scour-critical bridges.
- Collars may be tested on different types of abutments, like spill through or wing wall abutments.

## REFERENCES

- Abou-Seida M. M., Elsaeed G. H., Mostafa T. M. S. and Elzahry E. F. M. (2009). Experimental investigation of abutment scour in sandy soil. Journal of Applied Sciences Research, 5(1): 57-65, 2009.
- Ahmad, M. (1953). Experiments on design and behaviour of spur-dikes. Proc. Int. Hydraul. Convention.: 145-159.
- Alabi, P. D. (2006). Time Development Of Local Scour At A Bridge Pier Fitted With A Collar. Thesis Submitted to the College of Graduate Studies and Research in Partial Fulfillment of the Requirements for the Degree of Master of Science in the Department of Civil and Geological Engineering.
- Baker, R. E. (1986). Local scour at bridge piers in non-uniform sediment. Rep. No. 402, School of Engineering, University of Auckland, Auckland, New Zealand.
- Ballio, F. and Orsi, E. (2000). Time Evolution of Scour Around Bridge Abutments. Water Eng. Res. 2: 243-259.
- Barbhuiya, A. K. and Dey, S. (2004). Local Scour at Abutments: A Review. Sadhana. Vol.29, Part 5, 449-476.
- Blench, T. (1957). Regime Behavior of Canals and Rivers. Butterworths Scientific Publications, London.
- Borghei, S. M., Vatannia, Z., Ghodsian, M., Jalili, M. R. and Nalder, G. (2004). Discussion: Oblique rectangular sharp-crested weir. Water Management, Vol. 157, No. 4.

- Breusers, H. N. C., Nicollet, G. and Shen, H. W. (1977). Local scour around cylindrical piers. Journal of Hydraulic Research, 15(3): 211-252.
- Breusers, H. N. C. And Raudkivi, A. J. (1991). Scouring-hydraulic Structures Design Manual. IAHR, A. A. Balkema, Rotterdam.
- Cardoso, A. H. and Bettess, R. (1999). Effects of time and channel geometry on scour at bridge abutments. ASCE Journal of Hydraulic Engineering, Vol. 125: 388-399.
- Chabert, J. and Engeldinger, P. (1956). Etude des affouillements autour des piles de points (Study of scour at bridge piers). Bureau Central d'Etudes les Equipement d'Outre-Mer, Laboratoire National d'Hydraulique, France.
- Cheremisinoff, P. N., Cheremisinoff, N. P. and Cheng, S. L. (1987). Hydraulic Mechanics 2. Civil Engineering Practice, Technomic Publishing Company, Inc., Lancaster, Pennsylvania, U.S.A. 780 p.
- Chiew, Y. M. (1984). Local scour at bridge piers. Ph.D Thesis, University of Auckland, Auckland, New Zealand.
- Chiew, Y. M. (1992). Scour protection at bridge piers. J. Hydr. Eng. ASCE, 118: 1260-1269.
- Coleman, S. E., Lauchlan, C. S. and Melville, B. W. (2003). Clear-water scour development at bridge abutments. J. Hydraul. Res. 41: 521-531.
- Cunha, L. V. (1975). Time evolution of local scour. Proc. 16th Conf. Int. Assoc. Hydraulic Research (Delft: IAHR) pp 285-299.
- Dargahi, B. (1990). Controlling mechanism of local scouring. ASCE Journal of Hydraulic Engineering, Vol. 116: 1197-1214.

- Daşkın, S. (2011). Effects Of Collars On Local Scour Around Semi-Circular End Bridge Abutments. Thesis presented to Middle East Technical University, Ankara, Turkey, in partial fulfillment of the requirements for the degree of Master of Science in Civil Engineering.
- Deng, L. and Cai C. S. (2010). Bridge scour: Prediction, Modeling, Monitoring, and Countermeasures- Review. ASCE Practice Periodical on Structural Design and Construction, Vol. 15, No. 2, 125-134.
- Dey, S. and Barbhuiya, A. K. (2005). Turbulent flow field in a scour hole at a semicircular abutment. Canadian Journal of Civil Eng. Vol.32, 213-232.
- Doğan, A. E. (2008). Effects Of Collars On Scour Reduction At Bridge Abutments. Thesis presented to Middle East Technical University, Ankara, Turkey, in partial fulfillment of the requirements for the degree of Master of Science in Civil Engineering.
- Dongol, D. M. S. (1994). Local scour at bridge abutments. Rep. No. 544, School of Engineering, University of Auckland, Auckland, New Zealand.
- Ettema, R. (1980). Scour at bridge piers. Rep. No. 216, School of Engineering, University of Auckland, Auckland, New Zealand.
- Ettema, R., Nakato, T. and Muste, M. (2010). Estimation of Scour Depth at Bridge Abutments. Final Report, NCHRP 24-20, Transportation Research Board, Washington, DC.
- Field, W. G. (1971). Flood protection at highway bridge openings. University of Newcastle, N. S. W., Engineering Bulletin CE3.

- Fotherby, L. M. and Jones, J. S. (1993). The influence of exposed footings on pier scour depths. Proc. Hydraulic Engineering Conf. ASCE, Reston, Va., 922-927.
- Garde, R. J., Subramanya, K. and Nambudripad, K. D. (1961). Study of scour around spur dikes. ASCE Journal of the Hydraulics Division, 87(HY6), 23-37.
- Gill, M. A. (1970). Bed erosion around obstructions in rivers. PhD Thesis, The University of London (Imperial College of Science and Technology).
- Gill, M. A. (1972). Erosion of sand beds around spur-dikes. ASCE Journal of Hydraulic Engineering, Vol. 98: 1587-1602.
- Husain, D., Quraishi, A. A. and Ibrahim, A. (1998). Local Scour at Bridge Abutments. JKAU: Eng. Sci., Vol. 10, No. 1, 141-153.
- Izzard, C. F. and Bradley, J. N. (1958). Field Verification of Model Tests on Flow Through Highway Bridges and Culverts. State University of Iowa, Studies in Engineering, Bulletin No. 39.
- Kandasamy, J. K. (1985). Local scour at skewed abutments. Rep. No. 375, School of Engineering, University of Auckland, Auckland, New Zealand.
- Kandasamy, J. K. (1989). Abutment scour. Rep. No. 458, School of Engineering, University of Auckland, New Zealand.
- Kapoor, B. S. and Keana, C. M. (1994). Experimental overview to mechanism of scour around a round nosed pier and effect of delta wing like device on scour pattern around it. Modelling, Measurement & Control C: Energetics, Chemistry, Earth, Environmental & Biomedical Problems, Vol. 46, No. 3, AMSE Press, Tassin-la-Demi-Lune, France.

- Kayatürk, Ş. Y. (2005). Scour And Scour Protection At Bridge Abutments. Thesis presented to Middle East Technical University, Ankara, Turkey, in partial fulfillment of the requirements for the degree of Doctor of Philosophy.
- Khwairakpam, P. and Mazumdar, A. (2009). Local scour around hydraulic structures. International Journal of Recent Trends in Engineering, Vol. 1, No.6, 59-61.
- Köken, M. and Constantinescu, G. (2008a). An investigation of the flow and scour mechanisms around isolated spur dikes in a shallow open channel. Part I. Conditions corresponding to the initiation of the erosion and deposition process. Water Resources Research, 44, W08406, doi: 10.1029/2007WR006489.
- Köken, M. and Constantinescu, G. (2008b). An investigation of the flow and scour mechanisms around isolated spur dikes in a shallow open channel. Part II. Conditions corresponding to the final stages of the erosion and deposition process. Water Resources Research, 44, W08407, doi: 10.1029/2007WR006491.
- Köken, M. and Constantinescu, G. (2009). An investigation of the dynamics of coherent structures in a turbulent channel flow with a vertical sidewall obstruction. American Institute of Physics, 21, 085104, doi: 10.1063/1.3207859.
- Köken, M. and Constantinescu, G. (2011). Flow and turbulence structure around a spur dike in a channel with a large scour hole. Water Resources Research, Vol. 47, W12511, doi: 10.1029/2011WR010710.
- Kumar, V., Ranga Raju, K. G. and Vittal, N. (1999). Reduction of local scour around bridge piers using slots and collars. Journal of Hydraulic Engineering, ASCE, 125(12): 1302-1305.

- Kumcu Ş. Y., Göğüş, M. and Kökpınar, M. A. (2007). Temporal scour development at bridge abutments with a collar. Can. J. Civ. Eng. Vol.34: 549-556.
- Kwan, F. (1984). Study of Abutment Scour. Report No. 328, University of Auckland, School of T. Engineering, Department of Civil Engineering Private Bag. Auckland, New Zealand.
- Kwan, F. (1987). A study of abutment scour. PhD Thesis, University of Auckland.
- Kwan, T. F. (1988). Study of Abutment Scour. Report No. 451, University of Auckland, School of T. Engineering, Department of Civil Engineering Private Bag, Auckland, New Zealand.
- Kwan, T. F. and Melville, B. W. (1994). Local scour and flow measurements at bridge abutments. J. Hydraul. Res. 32: 661-673.
- Lagasse, P. F., Zevenbergen, L. W., Schall, J. D. and Clopper, P. E. (2001). Bridge Scour and Stream Instability Countermeasures – Experience, Selection, and Design Guidelines. National Highway Institute, FHWA NHI 01-003, HEC No. 23, Washington, D. C.
- Laursen, E. M. and Toch, A. (1956). Scour around bridge piers and abutments. Bull. No. 4, Iowa Highways Research Board, Ames, Iowa.
- Laursen, E. M. (1958). Scour at bridge crossings. Iowa Highway Research Board Bulletin, No. 8.
- Laursen, E. M. (1960). Scour at bridge crossings. J. Hydraul. Div., Am. Soc. Civ. Eng. 86: 39-54.

- Laursen, E. M. (1962). Scour at bridge crossings. ASCE Transactions, Vol. 127, Part I, 166-180.
- Li, H., Kuhnle, R. A. and Barkdoll, B. D. (2006). Countermeasures Against Scour At Abutments. National Sedimentation Laboratory, Research Report No. 49, U.S.
- Lim, S. Y. (1997). Equilibrium clear-water scour around an abutment. J. Hydraul. Eng., Am. Soc. Civ. Eng. 123: 237-243.
- Liu, H. K., Chang, F. M. and Skinner, M. M. (1961). Effect of bridge construction on scour and backwater. CER 60 HKL 22, Colorado State University, Civil Engineering Section, Fort Collins, Colorado.
- Mashair, M. B. and Zarrati, A. R. (2002). Effect of collar on time development of scouring around rectangular bridge piers. 5th International Conference on Hydrosience and Engineering, Warsaw, Poland, 9 p.
- Masjedi, A., Bejestan, M. S. and Esfandi, A. (2010). Reduction of Local Scour at a Bridge Pier using Collar in a 180 Degree Flume Bend. Journal of Applied Sciences, Vol. 10, 124-131.
- Melville, B. W. (1992). Local scour at bridge abutments. ASCE Journal of Hydraulic Engineering, Vol. 118: 615-631.
- Melville, B. W. (1997). Pier and abutment scour: integrated approach. ASCE Journal of Hydraulic Engineering, Vol. 123: 125-136.
- Melville, B. W. and Chiew, Y. M. (1999). Time Scale for Local Scour at Bridge Piers. J. Hydr. Eng. Vol. 125, No. 1, 59-65.



- Melville, B. W. and Coleman, S. E. (2000). Bridge Scour. Water Resources Publications, LLC, Colorado, USA.
- Menzies, J. B. (1997). Bridge failures, hazards and societal risk. Safety of Bridges. The Inst. of Civil Eng. and the Highways Agency, London, 36-41, 36 p.
- Morris, J. L. and Pagan-Ortiz, J. E. (1999). Bridge scour evaluation program in the United States. Stream Stability and Scour at Highway Bridges, E. V. Richardson and P. F. Lagasse, eds., ASCE, 61-70.
- National Cooperative Highway Research Program, (2007). Countermeasures to Protect Bridge Abutments from Scour. NCHRP Report 587. Washington, D.C.
- Oliveto, G. and Hager, W. H. (2002). Temporal evolution of clear-water pier and abutment scour. ASCE Journal of Hydraulic Engineering, Vol. 128: 811-820.
- Parola, A. C., Hagerty, D. J. and Kamojjala, S. (1998). Highway infrastructure damage caused by the 1993 upper Mississippi River basin flooding. NCHRP Report 417, Transportation Research Board, Washington, DC.
- Rajaratnam, N. and Nwachukwu, B. A. (1983). Flow near groin-like structures. ASCE Journal of Hydraulic Engineering, Vol. 109: 463-480.
- Ramu, K. L. V. (1964). Effect of sediment size on scour. PhD Thesis, University of Roorkee, Roorkee, India.

- Raudkivi, A. J. and Ettema, R. (1983). Clear-water scour at cylindrical piers. ASCE Journal of Hydraulic Engineering, Vol. 109: 338-350.
- Richardson, E. V. and Davis, S. R. (2001). Evaluating scour at bridges. HEC18 FHWA NHI-001. Federal Highway Administration, US Department of Transportation, Washington, DC.
- Sastry, C. L. N. (1962). Effect of spur-dike inclination on scour characteristics. M. E. Thesis, University of Roorkee, Roorkee.
- Shen, H. W. and Schneider, V. R. (1969). Local scour around bridge piers. Journal of the Hydraulics Division, Proceedings of the American Society of Civil Engineers, 95(6): 1919-1941.
- Shen, H. W. (1971). Scour near piers. River Mechanics. (H. W. Shen Ed.) Colorado State University Fort Collins, Colorado, Vol. 2, Chap. 23, 25 p.
- Singh, C. P., Setia, B. and Verma, D. V. S. (2001). Collar-sleeve combination as a scour protection device around a circular pier. Proceedings of Theme D, 29th Congress on Hydraulics of River, Water Works and Machinery, Chinese Hydraulic Engineering Society, Beijing, China, 202-209.
- Tanaka, S. and Yano, M. (1967). Local scour around a circular cylinder. Proc., 12th Congress, IAHR, Vol. 3, Delft, The Netherlands, 193-201.
- Tey, C. B. (1984). Local scour at bridge abutments. Rep. No. 329, School of Engineering, University of Auckland, New Zealand.
- Wong, W. H. (1982). Scour at bridge abutments. Rep. No. 275, School of Engineering, University of Auckland, New Zealand.

- Zaghloul, N. A. and McCorquodale, J. A. (1975). A stable numerical model for local scour. J. Hydraul. Res. 13: 425-444.
- Zaghloul, N. A. (1983). Local scour around spur-dikes. J. Hydrol. 60: 123-140.